Charles University in Prague
Faculty of Science, Department of Biochemistry

Karel Müller

Regulation of phospho*enol*pyruvate carboxylase in tobacco plants during potyviral infection

Ph. D. thesis

Supervisor: RNDr. Helena Ryšlavá, CSc.

Prague 2008

Acknowledgments

First, I am very grateful to my supervisor Dr. Helena Ryšlavá for her patient guidance during my study. I am also grateful to Dr. Noemi Čeřovská, Dr. Helena Štorchová, Dr. Helena Synková and stuff of IEB CAS for all their support and valuable help and advice. My thanks belong to Veronika Doubnerová and other dear colleagues from laboratory, where I spent most of the work.

Whole study could never been done without never-ending support of my parents and my wife. In addition, I owe a lot to many different people, who made my life easier and more beautiful.

Declaration

I hereby declare that the work presented in this thesis is my own and was carried out entirely with help of literature and aid cited in the manuscript. I also declare that this presented thesis is submitted only to Charles University, Faculty of Natural Sciences, Department of Biochemistry.

Prague, Czech Republic

March, 2008

List of abbreviations

3-PGA	3-phosphoglycerate
ABA	abscisis acid
C_3 plants	plants producing 3-phosphoglycerate as the first product of CO_2 assimilation
C_4 plants	plants producing oxaloacetate as the first product of CO_2 assimilation
CAM	crassulacean acid metabolism
cDNA	complementary DNA
CK	cytokinin
Cp	crossing point
DAG	diacylglycerol
DEAE	diethylaminoethyl
DHAP	dihydroxyaceton phosphate
dNTPs	nucleotide triphoshpate mix
dsRNA	double stranded DNA
DTT	dithiothreitol
EDTA	ethylenediaminetetraacetic acid
glucose-6-P	D-glucose-6-phosphate
GOGAT	glutamate-α-ketoglutarate amino transferase (EC 1.4.1.13)
GS	glutamine synthetase (EC 6.3.1.2)
HEPES	4-(2-hydroxyethyl)-1-piperazineethanesulfonic acid
HR	hypersensitive reaction
HSP	heat-shock protein
InsP3	inositol-1,4,5-trisphosphate
JA	jasmonic acid
MALDI	matrix-assisted laser desorption/ionization
MAPK	mitogen-activated protein kinase
MDH	malate dehydrogenase (EC 1.1.1.37)
Mr	relative molecular weight
NADP-ME	NADP-dependent malate dehydrogenase (decarboxylating) (EC 1.1.1.40)
NBT-BCIP	nitroblue tetrazolium, 5-bromo-4-chloro-3-indolyl phosphate
OAA	oxaloacetate
PAGE	polyacrylamid gel electrophoresis
PCR	polymerase chain reaction
PEP	phosphoenolpyruvate

PEPC	phosphoenolpyruvate carboxylase (EC 4.1.1.31)
PEPCk	phosphoenolpyruvate carboxylase kinase
PI-PLC	phospholipase C
PK	pyruvate kinase
PPDK	pyruvate, phosphate dikinase (EC 2.7.9.1)
PR	pathogenesis related
PUFA	Polyunsaturated fatty acids
PVA	Potato virus A
PVY^{NTN}	Potato virus Y, Strain NTN
qRT PCR	quantitative real time PCR
ROS	reactive oxygen species
Rubisco	ribulose 1,5-bisphosphate carboxylase/oxygenase (EC 4.1.1.39)
SA	salicylic acid
SAR	systemic acquired resistance
SDS	sodium dodecyl sulphate
TCA	tricaboxylic acid
TRIS	2-amino-2-hydroxymethyl-1,3-propanediol

Table of content

1. Introduction

1.1. Phospho*enol*pyruvate carboxylase

Phospho*enol*pyruvate carboxylase (PEPC; EC 4.1.1.31) was revealed by Bandurski and Greiner in 1953. The formation of oxaloacetate from phospho*enol*pyruvate and CO_2 was demonstrated in a spinach-leaf extract. The reaction scheme proposed by Bandurski and Greiner was subsequently slightly modified when the bicarbonate ion, rather than CO_2, was shown to be the true substrate for the enzyme. More than 50 years later over 1000 publications can be found in database, most of them being published in last 15 years.

1.1.1. General description

Phospho*enol*pyruvate carboxylase is one of the CO_2-fixing enzymes, which yields oxaloacetate from phospho*enol*pyruvate (PEP) and bicarbonate (HCO_3^-), liberating Pi at the presence of Mg^{2+}. PEPC is a cytosolic enzyme, widespread not only in all photosynthetic organisms such as plants, algae, cyanobacteria and photosynthetic bacteria, but also in most non-photosynthetic bacteria and protozoa. The enzyme is apparently absent in animals, fungi and yeasts (O'Leary, 1982; Latzko and Kelly, 1983; Andreo et al., 1987; Stiborova 1988; Lepiniec et al., 1994; Chollet et al., 1996; Izui et al., 2004).

1.1.1.1. Primary structure of PEPC

Prokaryotes contain a single PEPC gene. By contrast, plants contain a small gene family for PEPC (Izui et al., 2004). Most studies on PEPC gene family have been carried out in C_4 and CAM plants. In these plants the gene family is composed of a house-keeping gene, which is widely expressed in most plant organs and is probably involved in the anaplerotic function, whereas the other members of the family show tissue-specific expression and are involved in more specialised functions. Recently, Sanchez and Cejudo (2003) reported that the PEPC family of *Arabidopsis thaliana* is formed by four genes (Sanchez, 2003). Three of these genes encode PEPC isoforms highly homologous to each other (84-91%) as well as to other plant PEPCs. One PEPC gene was identified, which shows higher similarity to bacterial than to plant PEPCs. It also lacks the phosphorylation motif near the N terminus, which resembles a bacterial-type PEPC. A gene encoding a bacterial-type PEPC was also identified in rice (*Oryza sativa*) (Sanchez and Cejudo, 2003). Both bacterial-type PEPC genes have an unusually high number of introns, suggesting a different evolutionary origin from other known plant PEPC genes.

The primary structure of the PEPC monomer was first deduced from *E. coli* in 1984 (Fujita et al., 1984). Since then, more than 100 molecular species of PEPC have been identified to date from the deduced primary structures, including three isoforms for *Zea mays*, *Sorghum vulgaris*, *Flaveria trinerva* and *Oryza sativa* (Toh et al., 1994, Dong et al., 1998, Lepiniec et al, 1994, Blasing et al., 2002, Sanchez and Cejudo, 2003, Izui et al., 2004). The alignment of all deduced amino acids sequences and the construction of phylogenetic trees showed that these various PEPCs had evolved from the same ancestral origin and that the amino acid identities and similarities between various pairs of enzyme forms were more than 31 and 52%, respectively. For pairs of higher plant enzymes, the identities were more than 71% (Lepiniec et al., 1994, Nakamura et al., 1995, Blasing et al., 2002).

1.1.1.2. Structure of PEPC

PEPC is usually composed of four identical subunits with M_r of about 95-110 kDa. First three-dimensional structures were resolved for PEPCs from *Escherichia coli* and *Zea mays* (Kai et al., 1999, Matsumura et al, 2002). Figure 1 shows the quarternary structure of maize C_4-PEPC viewed from three axes. The maize C_4-PEPC monomer consists of eight-stranded β–barrel and 42 α–helices. The secondary structural features show that α helices comprise 65% of the polypeptide, whereas β strands comprise only 5%. The secondary structures of maize C_4-PEPC remain essentially the same as those of *E. coli* PEPC.

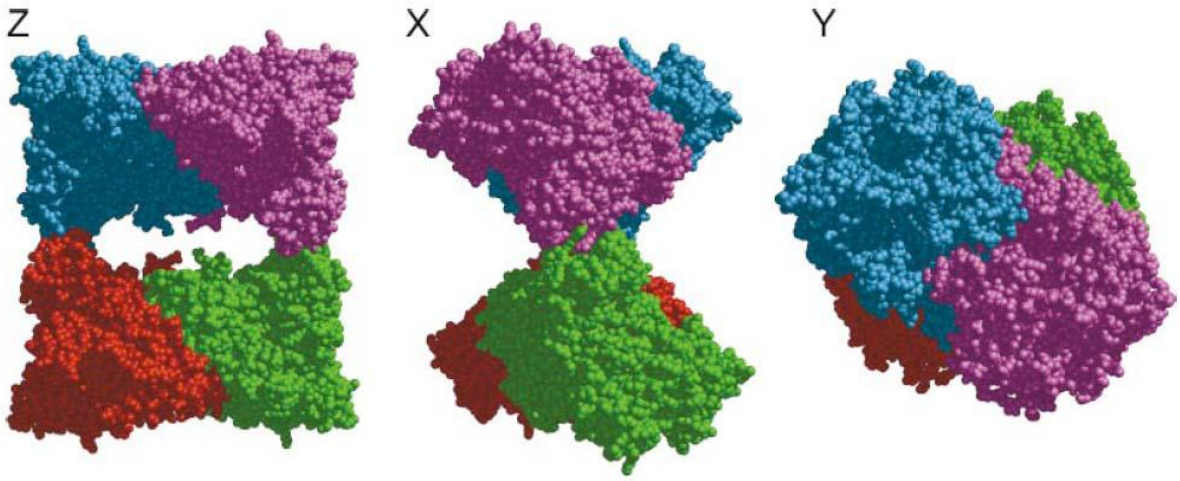

Figure 1: Space-filling model of the maize C_4-PEPC, in which the four identical subunits are colored in blue, purple red and green. The models are rotated 90° along the X (*horizontal*), Y (*vertical*), and Z (*perpendicular to the screen*) axes (Izui et al., 2004).

The PEPC catalytic site is located at the C-terminal region of the β barrel. Histidine, glutamate, aspartate and arginine residues play a crucial role in the active centre. The structure of Mn^{2+} binding site is surprisingly similar to those in other PEP utilizing enzymes, such as pyruvate kinase and pyruvate orthophosphate dikinase, despite the lack of amino acid sequence similarity (Matsumura et al., 1999). The binding site for asparagine was found about 20 A from the catalytic site on *E. coli*. Site-directed mutagenesis caused marked desensitization to both inhibitors, confirming involvement of at least two amino acids in inhibitor binding in plant PEPC (Izui et al., 2004). Four positively charged residues, which are strictly conserved in all plant PEPCs, were found in the maize C_4-PEPC. A hydrophobic pocket is found near these residues and this space is large enough to accommodate a glucosyl moiety. Therefore, this site may be the binding site for D-glucose-6-phosphate, an allosteric activator of plant PEPC. In fact, replacement of each residue caused almost complete desensitization to D-glucose-6-phosphate (Izui et al., 2004).

Due to high PEPC sequence identity, the three-dimensional structures of PEPC from various sources can be assumed to be highly similar to each another.

1.1.1.3. Mechanism of reaction catalyzed by PEPC

A variety of PEP analogs have been examined for PEPC as substrates. Isotopic studies and several stereochemical probes have been used to define PEPC catalysis. More structure information has been obtained from site-directed mutagenesis (Chollet et al., 1996). Recently, the three-dimensional structures were resolved for PEPCs from *Escherichia coli* and *Zea mays* (Izui et al., 2004). These advances in PEPC research provided the information of the molecular mechanisms of catalysis and allosteric regulation, which have been studied for long time.

The PEPC reaction is highly exergonic and is strictly irreversible. Bicarbonate, but not the carbon dioxide, is the true substrate. The “three-step reaction mechanism” is currently most plausible (Figure 2). In this mechanism carboxyphosphate and enolate anion of pyruvate are postulated as intermediates, with the subsequent formation of CO_2 within the catalytic cavity (Chollet et al., 1996).

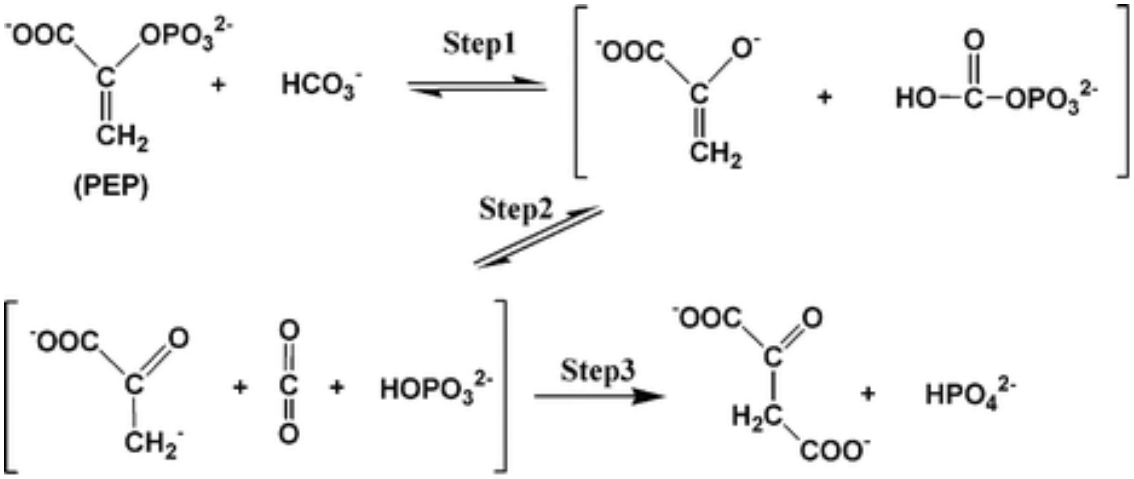

Figure 2: The chemical representation of the three-step reaction mechanism. Step 1: Enolate anion of pyruvate and carboxyphosphate are formed from PEP and bicarbonate by reversible partial reaction. Step 2: Enolate anion isomerizes and carboxyphosphate cleaves into carbon dioxide and Pi inside the catalytic site. Step 3: Carbon dioxide makes electrophilic attack on the enolate anion to form oxaloacetate and liberate Pi irreversibly (Izui et al., 2004).

1.1.2. Functions of PEPC

PEPC has many physiological roles in plants, which are distributed among several isoforms with different catalytic and regulatory properties. These include important roles in the photosynthesis of C_4 and Crassulacean acid metabolism (CAM) plants, supplying carbon to N_2-fixing root nodules and maintaining cellular pH (Latzko and Kelly, 1983).

1.1.2.1. Bacteria and *Archaea*

PEPC plays an important role in heterotrophic bacteria via replenishement of C_4-dicarboxylic acid into tricarboxylic acid (TCA) cycle. As such, PEPC performs a central role by maintaining the continuity of the TCA cycle carbon fluxes, connecting glycolysis to the TCA cycle.

For some methanogenic species of *Archaea*, a partial TCA cycle has been found to operate in a reductive direction from OAA to α-ketoglutarate. In contrast, methanogens from the order *Methanosarcinales* make use a partial TCA cycle that operates in the oxidative direction from OAA to α-ketoglutarate (Simpson and Withman, 1993). Therefore, it is obvious that OAA biosynthetic pathways play a central role in methanogenic archaeal species (Figure 3). The identification of the archaeal PEPC gene reveals OAA formation for *Methanopyrus kandleri* (Slesarev et al., 2002).

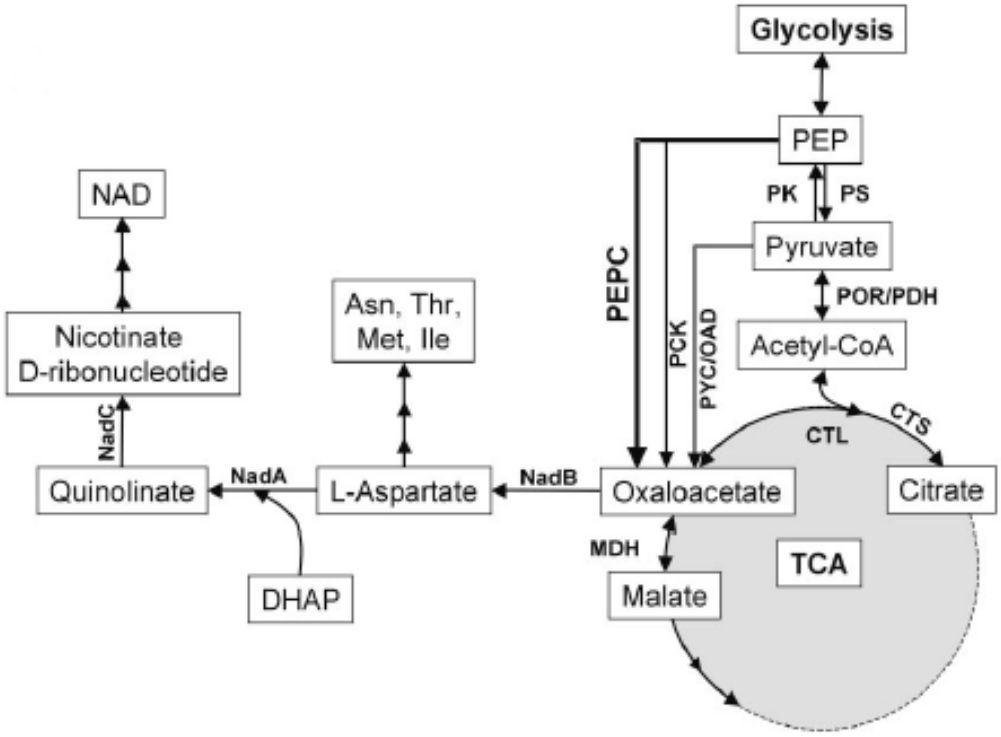

Figure 3: Overview of oxaloacetate biosynthetic and metabolic pathways in *Archeae*. Abbreviations: PYC, pyruvate carboxylase, OAD, oxaloacetate carboxylase; MDH, malate dehydrogenase; PCK, phosphoenolpyruvate carboxykinase (ATP/GTP dependent); PK, pyruvate kinase; PS, phosphoenolpyruvate synthase; CTS, citrate synthase; CTL, ATP:citrate lyase; POR, pyruvate oxido-reductase; PDH, pyruvate dehydrogenase; NadA, quinolinate synthase; NadB, L-aspartate oxidase; NadC, nicotinate-nucleotide pyrophosphorylase (carboxylating); DHAP, dihydroxy-acetone-phosphate (Ettema et al. 2004).

1.1.2.2. C_3 plants

PEPC fulfills a variety of physiological roles in C_3 plant leaves. In the anaplerotic pathway, which also occurs in C_4 and CAM plants, the enzyme contributes to the replenishment of Krebs cycle intermediates when organic acids are directed towards other metabolic pathways such as amino acid (via glutamine synthetase/glutamate-α-ketoglutarate amino transferase cycle) and protein synthese (Figure 4) (Stitt, 1999; Champigny and Foyer,1992). In this respect, PEPC reaction can be considered as a branch of the glycolytic pathway. In relation to the anaplerotic function, PEPC activity also contributes to the homeostasis of cell cytosolic pH (Sakano, 1998) and the chloroplastic OAA/malate shuttle that provides the cytosol with reducing power required by nitrate reductase (Oaks, 1994).

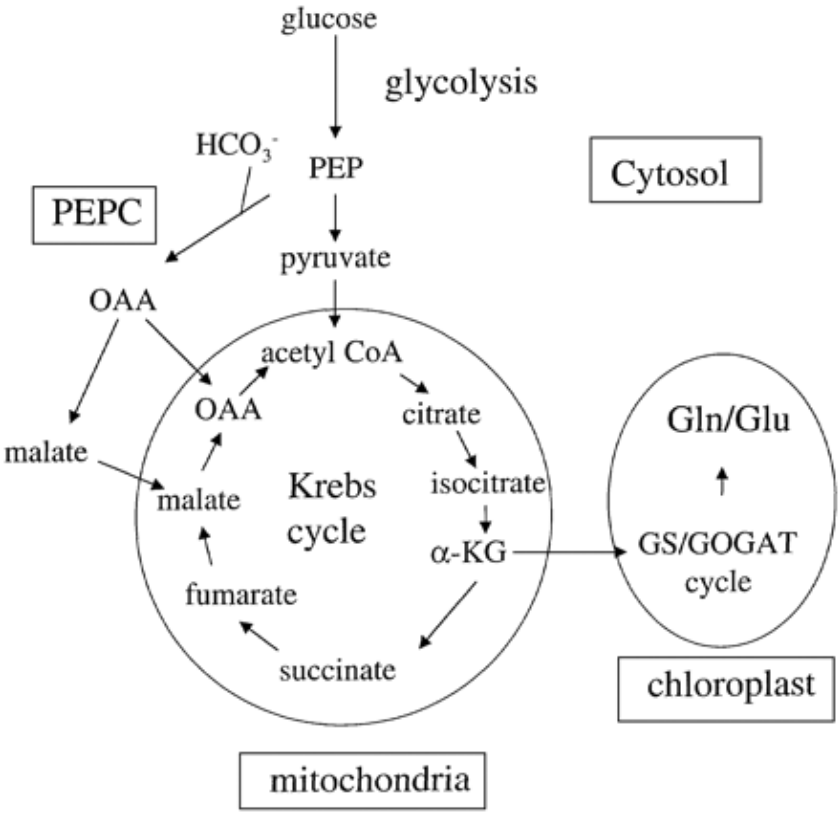

Figure 4: The anaplerotic pathway leading to amino acid synthesis. PEPC replenishes the Krebs cycle intermediates that are depleted when α-ketoglutarate is used for amino acid synthesis in the chloroplasts via the glutamine synthetase (GS)/glutamate-α-ketoglutarate amino transferase (GOGAT) cycle. (Jeanneau et al., 2002)

Organ-, tissue- and cell-specific PEPCs fulfil many other various roles in C_3 plant species. Guillet et al. (2002) reported 2 PEPC genes (*LYCes;Ppc1* and *LYCes;Ppc2*) regulated in different way which were involved in development of the tomato fruit. While *LYCes;Ppc1* was expressed at a low and constant level in almost all tomato tissues, *LYCes;Ppc2* was strongly and specifically expressed in fruit and may therefore fulfill a specialised role in tomato fruit development. Accumulation of malate and citrate was indeed associated with increase in PEPC protein level and activity. Apart from increasing fruit acidity, the accumulation of organic acids in the vacuole may further serve to sustain fruit growth. Evidence for the involvement of PEPC and organic acids in cell growth has been presented in the case of cotton fibers (trichome cells), which grow up to 2 mm per day in length and accumulate potassium malate (Smart et al. 1998). Additional function of PEPC during early development of tomato fruit may be recapture of CO_2 and thereby to reduce CO_2 losses that may reach up to 25% of the carbon imported into the fruit during the rapid growth phase (Ho, 1996).

Kopka et al. (1997) described potential PEPC role in stomatal opening. The transcript level of PEPC was found to be regulated in guard cells specifically as compared with whole leaves. Previous research has shown that accumulation and loss of potassium ions regulate guard cell turgor (MacRobbie, 1987). In addition to inorganic ions, carbohydrates are thought to play an important role. Malate, which results from PEPC activity, may serve as counter-ion to potassium during stomatal opening.

Furthermore, in lipid-rich seeds, malate has been reported to be the best precursor for fatty acid synthesis in leucoplasts and a high PEPC activity coincides with the seed maturation (Smith et al., 1992).

1.1.2.3. C_4 and CAM plants

In C_4 and CAM plants, a specific isoform of PEPC is highly expressed and catalyzes the initial CO_2 fixation during C_4 and CAM photosynthesis.

C_4 plants usually display a concentric organization of photosynthetic leaf tissues (mesophyll and bundle sheath) in which enzymes of the photosynthetic pathway, C_4 cycle and Benson-Calvin cycle, are distributed. This is so called Kranz anatomy. The role of photosynthetic PEPC is fixation of atmospheric CO_2 into C_4 acids. This is accomplished through the use of the PEP generated in chloroplasts by pyruvate orthophosphate dikinase (PPDK). C_4 compounds in the form of malate or aspartate are transported to bundle sheath cells where they are decarboxylated by specific enzyme (NADP-malic enzyme, NAD-malic enzyme or phosphoenolpyruvate carboxykinase), and CO_2 is recaptured by Rubisco in the chloroplasts (Slack and Hatch, 1967). Figure 5 shows scheme of metabolic pathways of C_4 photosynthesis in malate formers.

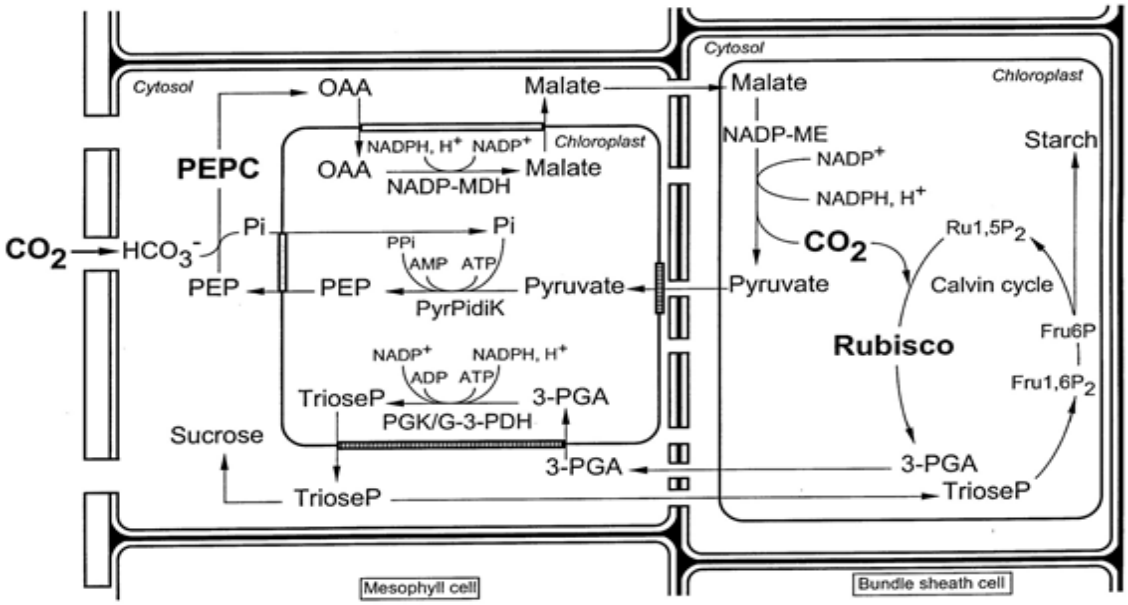

Figure 5: The pathway of C_4 photosynthesis in malate formers. The enzymes of the C_4 cycle (PEPC, phosphoenolpyruvate carboxylase; NADP-MDH, NADP-malate dehydrogenase; PyrPidiK, pyruvate-Pi-dikinase; NADP-malic enzyme) provide CO_2 to the ribulose-bisphosphate carboxylase in the bundle sheath cell chloroplasts. In addition, 3-phosphoglycerate (3-PGA) moves to the mesophyll chloroplasts for reduction to triose-P (PGK, phosphoglycerate kinase; G-3-PDH, NADP-glyceraldehyde phosphate dehydrogenase) (Jeanneau et al., 2002).

Recently, new variants of C_4 photosynthesis were described. Several species in the Chenopodiaceae family were found to have a unique mechanism of C_4 photosynthesis, which occurs within individual photosynthetic cells. There are currently two types of single-cell C_4 systems. One is monomorphic (one chloroplast type that contains Rubisco, the C_3 cycle and C_4 acid decarboxylase). The other is dimorphic (two chloroplast types with spatial compartmentation within the cell analogous to that in Kranz-type anatomy) as found in the single-cell C_4 chenopods (Voznesenskaya et al. 2003; Edwards et al., 2004; Akhani et al., 2005).

Function of PEPC in CAM plants is similar to C_4. In contrary to C_4 photosynthesis, PEPC is in CAM plants active during the night. During the nocturnal phase, phospho*enol*pyruvate carboxylase assimilates atmospheric and respiratory CO_2 into oxaloacetate by carboxylating phospho*enol*pyruvate derived from glycolysis. OAA is then reduced to malate by cytosolic and/or mitochondrial NAD(P)-malate dehydrogenase and stored in the vacuole. During most of the day, when stomata are closed, malate decarboxylation commences as the released CO_2 is refixed by Rubisco (Cushman and Bohnert, 1999).

1.1.3. Regulation of PEPC

Most PEPCs are allosteric enzymes with a wide variety of allosteric effectors depending on the species. Furthermore, vascular plant PEPCs are regulated by reversible phosphorylation at the conserved serine residue located near N terminus (Vidal and Chollet, 1997; Nimmo, 2000).

1.1.3.1. Bacteria and *Archaea*

Most bacterial PEPCs are sensitive to various metabolite effectors. For example, PEPC of *E. coli* is activated by acetyl-CoA, fructose-1,6-bisphosphate, long-chain fatty acids and guanosine 3',5'-bisphosphate, it is inhibited by C_4-dicarboxylic acids, especially aspartate and malate (Sauer and Eikmanns, 2005).

PEPCs from *Archaea* represent unique set with molecular weight of subunit of 60 kDa. These smaller molecules are missing certain regulatory domains; allosteric activators (glucose-6-phosphate, fructose-1,6-bisphosphate and acetyl-CoA) do not affect their activity. Purified PEPC from archaeal methanogen *Methanothermus sociabilis* has been reported to be insensitive to aspartate, as well as to all other known PEPC effectors, including malate. (Ettema et al., 2004; Patel et al., 2004). However, PEPC from *Sulfolobus solfataricus* is inhibited by malate and aspartate. Taking into account the absence of known allosteric domains this sensitivity is surprising (Ettema et al., 2004).

1.1.3.2. Plants with C_4 and CAM photosynthesis

Regulation of plant PEPC is a complex, coordinated mechanism, which includes regulation of many enzymes and transporters, including signalling networks and metabolites. Regulation of C_4 PEPC activity in mesophyll cell cytosol involves availability of PEP, photosynthesis-related metabolite effectors like glucose-6-phosphate (activator) and malate (feedback inhibitor) and a highly complex, light-dependent reversible phosphorylation process (Chollet et al., 1996). Also pH plays an important role in regulation of photosynthetic PEPC, not only affecting the activity but also the sensitivity of PEPC to effectors and substrate. However, the research over past decade has focused primarily on the reversible phosphorylation of the enzyme. This modification changes the functional properties of C_4 PEPC, increasing maximal reaction rate and activation constant for glucose-6-P, and decreasing its sensitivity to malate. It has been suggested that the phosphorylated N-terminus of the enzyme is moved closer to the entry of the inhibitor site thus impeding access of

malate (Kai at el., 1999). Moreover, a study of the enzyme chimera between C_4 and C_3 PEPC isoforms from *Flaveria* species and site-directed mutagenesis have revealed a crucial role of the residue at position 774 (serine in C_4 and alanine in C_3 enzymes) as a major determinant for the specific properties of each enzyme form (Bläsing et al., 2000).

In vitro, C_4 PEPC activity, phosphorylation and metabolic control are highly sensitive to pH (Echevarria et al., 1994; Gao and Woo, 1996). The increase in pH that has been proposed to occur in the mesophyll cell cytosol upon illumination of the C_4 leaf (between 7.0 and 7.5) is expected to activate the C_4 PEPC and, partially, to promote desensitization of the enzyme towards the effectors, notably, L-malate. Therefore most of the interactive players, which act in the regulation of PEPC (i.e. pH, glucose-6-P and phosphorylation), are opposed to the negative feedback exerted by malate.

The phosphorylation of PEPC is in plants catalyzed by highly specific phosphoenolpyruvate carboxylase kinase (PEPCk). This unique Ser/Thr protein kinase exhibits several interesting features. It is the smallest protein kinase known so far with a predicted molecular mass around 31 kDa. It is made up of a catalytic domain with minimal or no additions. Although it belongs to the Ca^{2+}/calmodulin-regulated group of protein kinases, it lacks the regulatory auto-inhibitory region and the EF-hands. It displays a pH optimum around 8 and it specifically phosphorylates the N-terminal regulatory serine of the target PEPC. Its activity is not modulated directly by second messengers (such as Ca^{2+}/calmodulin or cyclic nucleotides) or by phosphorylation/dephosphorylation processes, but rather through rapid changes in its turnover rate (Jeanneau et al., 2002).

The light-transduction chain leading to C_4 PEPC phosphorylation by PEPCk has been studied and a model of the spatio-temporal organization of the cascade in the C_4 leaf is shown in Figure 6. In this scenario, 3-phosphoglyceric acid, generated in bundle sheath cell chloroplast represents the intercellular metabolic messenger that diffuses into mesophyll cells. In these cells, its subsequent transport into the chloroplasts under the protonated form is expected to cause alkalization of pH of this organelle. This early cascade event is followed by activation of a mesophyll cell phospholipase C (PI-PLC) and transient production of the second messenger ($InsP_3$) (Coursol et al., 2000). $InsP_3$ modulates tonoplast calcium channels, thereby increasing the flux of calcium into the cytosol. This results in the activation of a calcium-dependent protein kinase. The ultimate step in the cascade implicates the nucleus and the up-regulation of a PEPC kinase gene. This highly complex, light-dependent cascade involves the contribution of various components (pH, ion channels and signalling enzymes),

cell types (bundle sheath and mesophyll) and subcellular compartments (chloroplasts, vacuole and nucleus) (Jeanneau et al., 2002).

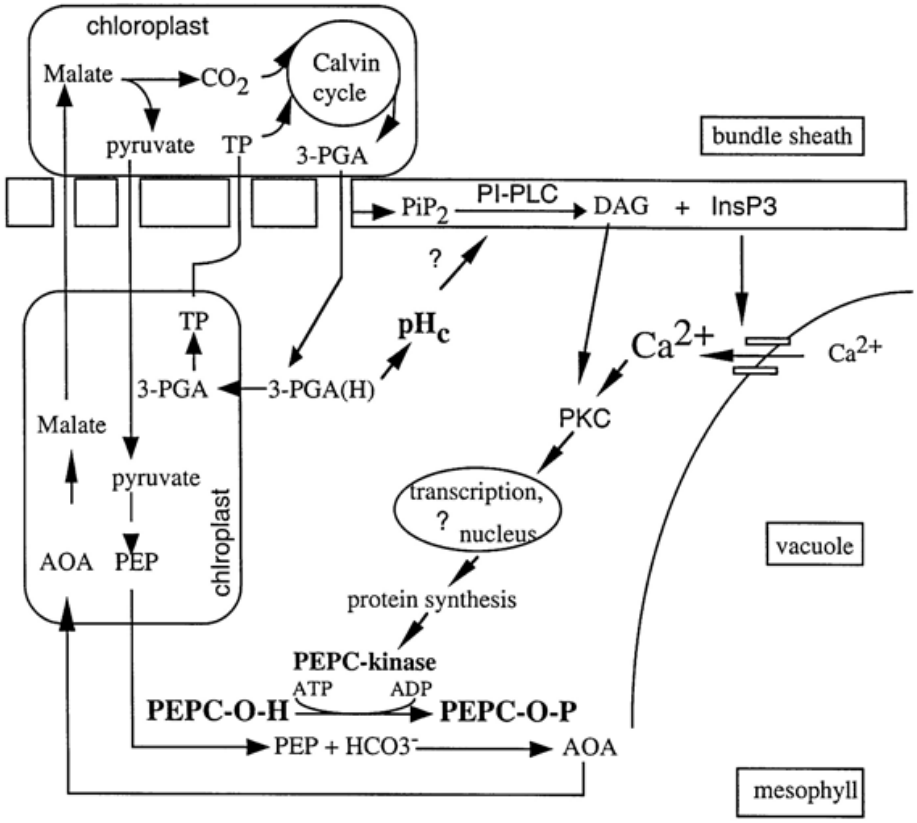

Figure 6: Schematic model for the spatio-temporal organization of the transduction cascade in the C_4 leaf. An increase in 3-phosphoglyceric (3-PGA) acid ensures the intercellular coupling via pHc changes in the mesophyll cell cytosol. This is followed by activation of mesophyll cell phospholipase C (PI-PLC) and transient production of the second messenger inositol-1,4,5-trisphosphate ($InsP_3$) and diacylglycerol (DAG). $InsP_3$ causes tonoplast calcium channels to open and efflux of calcium into the cytosol while DAG and calcium activate a PKC-like activity. The rapid synthesis of the calcium-independent PEPC kinase leads to the phosphorylation of C_4 PEPC. Questionmarks indicate the steps that remain to be elucidated (Jeanneau et al., 2002).

In CAM plants, up-regulation of PEPC kinase and PEPC phosphorylation occurs during the night and is dependent on a circadian oscillator (Nimmo, 2000). In the CAM species *Mesembryanthemum crystallinum*, it has been shown that a cascade similar to that found in C_4 plants operates in mesophyll cells during the night (Bakrim et al., 2001).

Two other mechanisms have been proposed for the regulation of CAM PEPC activity and/or sensitivity to L-malate based wholly on *in vitro* observations. The Wedding et al. found that CAM PEPC purified from day- and night-adapted *Crassula argentea* leaves exists

as kinetically distinct but interconvertible oligomers (Wu and Wedding, 1985). The day enzyme was mainly a malate-sensitive homodimer ($\alpha 2$) and the night form a malate-"insensitive" homotetramer ($\alpha 4$), with about a two-fold higher inhibition constant. On the contrary, several reports document that the phospho- and dephospho- C_4 and CAM enzyme forms are isolated in the same aggregation state while retaining the characteristic differential sensitivity to L-malate (Nimmo et al., 1986; Willeford and Wedding, 1992). Significance of regulation of photosynthetic PEPC in vivo by changes in its aggregation state is still not known.

Even more speculative is the regulation of C_4 PEPC under the control of the redox state of certain critical cysteines (Chardot and Wedding, 1992).

1.1.3.3. Plants with C_3 photosynthesis

In contrary to C_4 plants, there have not been many studies describing effects of metabolites on PEPC activity. General presumption is that C_3 PEPC shows similar reaction to metabolites like C_4 isoform, however at much lower extent. Inhibitory effect of malate on tobacco PEPC has been reported (Wang and Chollet, 1993). Schuller at el. (1990) reported activation of soybean PEPC by glucose-6-phosphate, fructose-6-phosphate, glucose-1-phosphate and dihydroxyacetone phosphate, while malate, aspartate, glutamate, citrate and 2-oxoglutarate were potent inhibitors.

Intuitively, the concept that PEPC must be protected against malate (via phosphorylation process) as proposed in C_4 and CAM plant photosynthesis, should apply to any system in which the concentration of this metabolite increases, such as anaplerotic carbon flow and its interaction with nitrogen metabolism. Regulatory phosphorylation of C_3 PEPC is supported by a number of facts. 1) The presence of N-terminal phosphorylation domain in all plant PEPCs sequenced so far, whatever the physiological type. 2) The presence of a Ca^{2+}-independent PEPCk in leaves of C_3 plants (Schuller and Werner, 1993; Wang and Chollet, 1993) and the isolation of C_3-plant PEPCk cDNAs and genes (Taybi et al., 2003; Nimmo 2000). Similarity of this kinase to the C_4 and CAM enzymes has been demonstrated (Wang and Chollet, 1993; Duff and Chollet, 1995). 3) The induction of PEPCk activity in illuminated C_3 leaves and protoplasts, that is blocked by cykloheximide, like the corresponding C_4 and CAM enzyme, indicates that protein turnover is involved in the up-regulation of the PEPCk in C_3 plants (Vidal and Chollet, 1997).

Collectively, these data support the hypothesis that up-regulation of PEPCk in C_3-plant context is via a transduction cascade similar to that operating in C_4 plants and CAM plants. However, whether the upstream signalling elements identified in C_4 mesophyll cells are also key players in the C_3 cascade remains to be fully elucidated.

1.2. Response of plants to stress conditions

Plants frequently encounter stresses, external conditions that adversely affect growth, development, or productivity. Stresses can be biotic, imposed by other organisms, or abiotic, arising from an excess or deficit in the physical or chemical environment. Environmental conditions causing damage include water-logging, drought, high or low temperatures, excessive soil salinity, inadequate mineral nutrients in the soil, and too much or too little illumination. Phytotoxic compounds such as ozone can also damage plant tissues.

Stresses trigger a wide range of plant responses, which result in altered gene expression and modulation of cellular metabolism as well as in changes of growth rates and crop yields. The duration, severity and rate at which a stress is imposed all influence how a plant responds. Several adverse conditions in combination may elicit a response different from that for a single type of stress. The simplified view of complexity of plant stress reactions but also parallelism of reactions caused by different stress factors is shown in Figure 7. Features of the plant, including organ or tissue identity, developmental age, and genotype, also influence plant responses to stress (Bray et al., 2000).

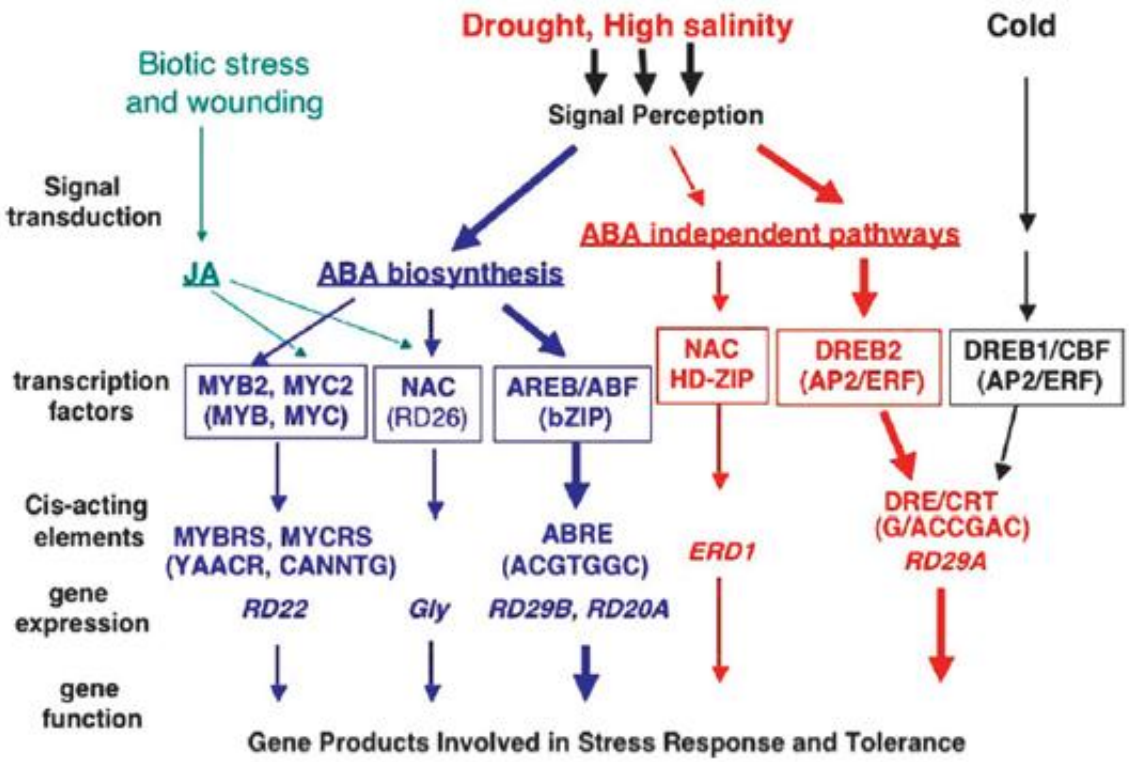

Figure 7: The complex transcriptional regulatory networks of abiotic and some biotic stress signals and gene expression. At least six signal transduction pathways exist in drought, high salinity, and cold-stress responses: three are ABA dependent and three are ABA independent. In the ABA-dependent pathway, ABRE functions as a major ABA-responsive element. AREB/ABFs are AP2 transcription factors involved in this process. MYB2 and MYC2 function in ABA-inducible gene expression of the RD22 gene. MYC2 also functions in JA-inducible gene expression. The RD26 NAC transcription factor is involved in ABA- and JA-responsive gene expression in stress responses. These MYC2 and NAC transcription factors may function in cross-talk during abiotic-stress and wound-stress responses. In one of the ABA-independent pathways, DRE is mainly involved in the regulation of genes not only by drought and salt but also by cold stress. DREB1/CBFs are involved in cold-responsive gene expression. DREB2s are important transcription factors in dehydration and high salinity stress-responsive gene expression. Another ABA-independent pathway is controlled by drought and salt, but not by cold. The NAC and HD-ZIP transcription factors are involved in ERD1 gene expression (Shinozaki and Yamaguchi-Shinozaki, 2007).

1.2.1. Oxidative stress

Oxidative stress may arise from any abiotic or biotic stress that causes formation of reactive oxygen species (ROS), such as hydrogen peroxide, superoxide anion and hydroxyl radical, or perhydroxyl radical. Non-enzymatic one electron O_2 reduction can occur at about 10^{-4} M and higher oxygen concentrations (Skuchalev, 1997).

Mechanisms for generation of reactive oxygen species in biological systems are represented by both non-enzymatic and enzymatic reactions. Among enzymatic sources of ROS, xanthine oxidase, an enzyme responsible for the initial activation of dioxygen should be mentioned. Xanthine oxidase can use as electron donors xanthine, hypoxanthine or acetaldehyde (Bolwell and Wojtazsek, 1997). The next enzymatic step is dismutation of the superoxide anion by superoxide dismutase to yield H_2O_2. Due to its relative stability the level of H_2O_2 is regulated enzymatically by a set of catalases and peroxidases localized in almost all compartments of the plant cell. Peroxidases, besides their main function in H_2O_2 elimination, can also catalyze $O_2^{\cdot -}$ and H_2O_2 formation by a complex reaction in which NADH is oxidized using trace amounts of H_2O_2 first produced by non-enzymatic breakdown of NADH. Next, the $NAD^{\cdot}$ radical formed reduces O_2 to $O_2^{\cdot -}$, some of which dismutates to H_2O_2 and O_2 (Lamb and Dixon, 1997). Thus, peroxidases and catalases play an important role in the fine regulation of ROS concentration in the cell through activation and deactivation of H_2O_2 (Blokhina et al., 2002).

ROS can also be formed as by-products in the electron transport chains of chloroplasts (Asada, 1999), mitochondria and plasma membrane (cytochrome b-mediated electron transfer). Plant mitochondrial electron transport chain, with its redox-active electron carriers, is considered as the most probable candidate for intracellular ROS formation. Generation of hydrogen peroxide by higher plant mitochondria and its regulation by uncoupling of electron transport chain and oxidative phosphorylation have been demonstrated by Braidot et al. (1999).

Lipoxygenase reaction is another possible source of ROS. It catalyzes the hydroperoxidation of poly-unsaturated fatty acids (Rosahl, 1996). The hydroperoxyderivatives of poly-unsaturated fatty acids can undergo autocatalytic degradation, producing radicals and thus initiating the chain reaction of lipid peroxidation.

Several apoplastic enzymes may also lead to ROS production. Other oxidases, responsible for the two-electron transfer to dioxygen (amino acid oxidases and glucose

oxidase) can contribute to H_2O_2 accumulation. Also an extracellular germin-like oxaloacetate oxidase catalyzes the formation of H_2O_2 and CO_2 from oxalate in the presence of oxygen (Bolwell and Wojtaszek, 1997).

To control the level of ROS and to protect cells under oxidative stress conditions, plant tissues contain several enzymes scavenging ROS (Table 1) and a network of low molecular mass antioxidants (ascorbate, glutathione, phenolic compounds and tocopherols). In addition, a whole set of enzymes is needed for the regeneration of the active forms of the antioxidants (monodehydroascorbate reductase, dehydroascorbate reductase and glutathione reductase) (Blokhina et al., 2003).

Table 1: Enzymes scavenging and detoxifying reactive oxygen species (Blokhina et al., 2003). PUFA ... Polyunsaturated fatty acids; DHA.... Dehydroascorbate; AA... Ascorbic acid; MDHA.... Monodehydroascorbate; GSH... Glutathione.

Enzyme	EC number	Reaction catalyzed
Superoxide dismutase	1.15.1.1	$O_2^{\cdot -} + O_2^{\cdot -} + 2H^+ \Leftrightarrow H_2O_2 + O_2$
Catalase	1.11.1.6	$2H_2O_2 \Leftrightarrow O_2 + 2H_2O$
Glutathione peroxidase	1.11.1.12	$2GSH + PUFA–OOH \Leftrightarrow GSSG + PUFA + 2H_2O$
Glutathione S-transferases	2.5.1.18	$RX + GSH \Leftrightarrow HX + R\text{-}S\text{-}GSH^*$
Phospholipid-hydroperoxide glutathione peroxidase	1.11.1.9	$2GSH + PUFA\text{-}OOH\ (H_2O_2) \Leftrightarrow GSSG + 2H_2O$
Ascorbate peroxidase	1.11.1.11	$AA + H_2O_2 \Leftrightarrow DHA + 2H_2O$
Guaiacol type peroxidase	1.11.1.7	$Donor + H_2O_2 \Leftrightarrow oxidized\ donor + 2H_2O$
Monodehydroascorbate reductase	1.6.5.4	$NADH + 2MDHA \Leftrightarrow NAD^+ + 2AA$
Dehydroascorbate reductase	1.8.5.1	$2GSH + DHA \Leftrightarrow GSSG + AA$
Glutathione reductase	1.6.4.2	$NADPH + GSSG \Leftrightarrow NADP^+ + 2GSH$

Plant peroxidases, which have been mentioned for their function in the formation and scavenging of H_2O_2, may also function in oxidation of various substrates (which leads to catabolism or the polymerization of substrates). This can lead to cross-linking of cell wall compounds in response to different stimuli such as wounding, pathogen interactions and climatic aggressions (Passardi et al., 2005).

1.2.2. Abiotic stress

1.2.2.1. Drought

Dehydration is one of the most important abiotic stresses affecting crop yields. Plants suffer from dehydration under the conditions of drought, high salinity, and low–temperatures, all of which cause hyper-osmotic stress characterized by a decrease of turgor pressure and water loss (Munns et al., 2005; Shao et al., 2007). Dehydration triggers the biosynthesis of the phytohormone abscisic acid (ABA), which in turn causes stomatal closure and induces expression of stress-related genes. Several drought-inducible genes are induced by exogenous ABA treatment, whereas others are not affected. Existence of both ABA-independent and ABA dependent regulatory systems was proved (Yamaguchi-Shinozaki and Shinozaki, 2005). The products of the drought-inducible genes identified through the recent microarray analyses in *Arabidopsis* can be classified into two groups (Shinozaki et al., 2003). The first group includes proteins that most probably function in abiotic stress tolerance. These includes molecules such as chaperones, late embryogenesis abundant proteins, osmotin, antifreeze proteins, mRNA-binding proteins, key enzymes for osmolyte biosynthesis, water channel proteins, sugar and proline transporters, detoxification enzymes and various proteases. The second group is comprised of regulatory proteins, i.e. protein factors involved in further regulation of signal transduction and stress-responsive gene expression. These include various transcription factors, protein kinases, protein phosphatases, enzymes involved in phospholipid metabolism and other signalling molecules such as calmodulin-binding protein (Shinozaki and Yamaguchi-Shinozaki, 2007). Osmotic stress also induces oxidative damage (Chen et al., 2004; Sarowar et al., 2005).

1.2.2.2. Flooding

Plants can be damaged not only by the absence of water but also by its excess, which blocks entry of O_2 into the soil so that roots and other organs cannot carry out respiration. The ability to tolerate flooding varies greatly among species and can be altered by acclimation processes which involve exposure to hypoxic conditions (Bray et al., 2000; Perata and Alpi, 1993). During short-term acclimation to anoxic conditions, plants generate ATP through glycolysis and fermentation. This shift from aerobic metabolism to anaerobic glycolytic fermentation involves changes in gene expression (Sachs et al., 1996). The plant hormone ethylene promotes long-term acclimation responses, including formation of

aerenchyma and stem elongation. Some wetland genotypes are adapted to long-tem flooding (Voesenek et al., 2006).

1.2.2.3. Heat stress

Plants exposed to excess heat exhibit a characteristic set of cellular and metabolic responses, many of which are conserved in all organisms. The signature response to heat stress is a decrease in the synthesis of normal proteins, accompanied by an accelerated transcription and translation of a new set of proteins known as heat shock proteins (HSPs) (Lee at al., 1995). The five major classes of HSPs, defined according to their size, are conserved among different organisms. In general, the high molecular weight HSPs function as chaperones to promote proper folding of proteins (Bray et al., 2000). Thus the function of these heat shock proteins is not applied only during heat stress, but other stress factors can also promote their expression.

1.2.3. Biotic stress

Plants must continuously defend themselves against attack from bacteria, viruses, fungi, invertebrates, and even other plants. Because their immobility precludes escape, each plant cell possesses both preformed and inducible defence mechanisms (Hammond-Kosack and Jones, 2000).

1.2.3.1. Pathogenesis-related proteins

Plant responses to attack by pathogenic microorganisms are complex and involve induction of the expression of a large array of genes encoding diverse proteins, many of which are believed to have a role in defence. One of the crucial components in the inducible repertoire of the plant's self-defence mechanism is the production/accumulation of pathogenesis-related (PR) proteins in response to invading pathogen and /or related stress situations (Jwa et al., 2006). The PR proteins were initially classified into 5 families based upon molecular mass, isoelectric point, localization and biological activity (Van Loon, 1985). The latest proposition divides the currently known PR proteins into 14 families based on sequence or predicted sequence of amino acids, serological relationships and biological activity (Van Loon, 1999).

The PR proteins have been widely studied in dicots. The most attention has been focused on the PR class 1, a dominant group commonly used as a marker for systemic acquired resistance (SAR) (Linthorst, 1992). Their regulation is rather complex. Two *OsPR1* (PR class 1 genes from *Oryza sativa*) were shown to be differentially regulated by diverge signals, such as wounding by cut, jasmonic acid, salicylic acid, abscisic acid, ethylene, hydrogen peroxide and few others (Agrawal et al, 2001).

The family of PR class 2 proteins, β-1,3-glucanases, are able to catalyze hydrolytic cleavage of the 1,3-β-D-glucosidic linkages in β-1,3-glucans. Reduction of the plant susceptibility to infection by certain fungi was observed in plants expressing β-1,3-glucanases transgenes alone or in combination with chitinase transgenes (Lusso and Kuc, 1996).

Outstanding among the PR proteins are chitinases, which catalyze the hydrolysis of chitin. Chitinases belong to the PR3, 4, 8 and 11 families. A major natural role for chitinases in defence seems to be based on their ability to inhibit the growth of many fungi in vitro, and to accumulate fungal hyphae material in planta (Broglie et al., 1991; Collinge et al., 1993).

Proteinase inhibitors belong to the PR class 6 family and are widely distributed in the plant kingdom. They appear to be an essential part of plant's natural defence against pathogens (Ryan, 1990). Among the proteinase inhibitors, serine-protease inhibitors have been studied in detail (Ryan, 1973). The other examples are Bowman-Birk- and Kunitz-type inhibitors, cysteine-, aspartyl-, and metallo-proteinase inhibitors classes (Ryan, 1990). Duan et al. reported that incorporation of potato proteinase inhibitor II gene into rice increased significantly resistance against insect (Duan et al., 1996).

Thionins, present in monocot and dicot species, are of particular interest because of their antimicrobial activity in plants. These proteins are present in cell walls, vacuoles and protein bodies. They and have been isolated as 5 kDa mature proteins. Thionins have been grouped into four major classes based on the number of cystein residues and the pattern of disulphide bridges. Recently, over-expression of oat thionin in rice was shown to result in resistance to infection by two major seed-transmitted soil borne bacteria (Iwai et al., 2002).

1.2.3.2. Hypersensitive reaction

The process, which occurs prior (and/or in parallel) to the transcriptional activation of the PR genes, is the generation of ROS (Figure 8). This oxidative burst has a high impact on pathogen and also plant cells directly at the site of pathogen attack or close to it. This defence response is also called hypersensitive reaction (HR) (Grant and Loake, 2000). H_2O_2 (a stable

and less reactive oxygen compound), which originates in this oxidative burst, plays a central role in the expression of HR. In addition, nitric oxide (NO), a key signal molecule in animal cells, has also been shown to accumulate during HR formation (Grant and Loake, 2000). In order to minimize the damage from oxidative injuries, plants have developed enzymatic systems for scavenging these highly reactive forms of oxygen (as mentioned in 1.3.4).

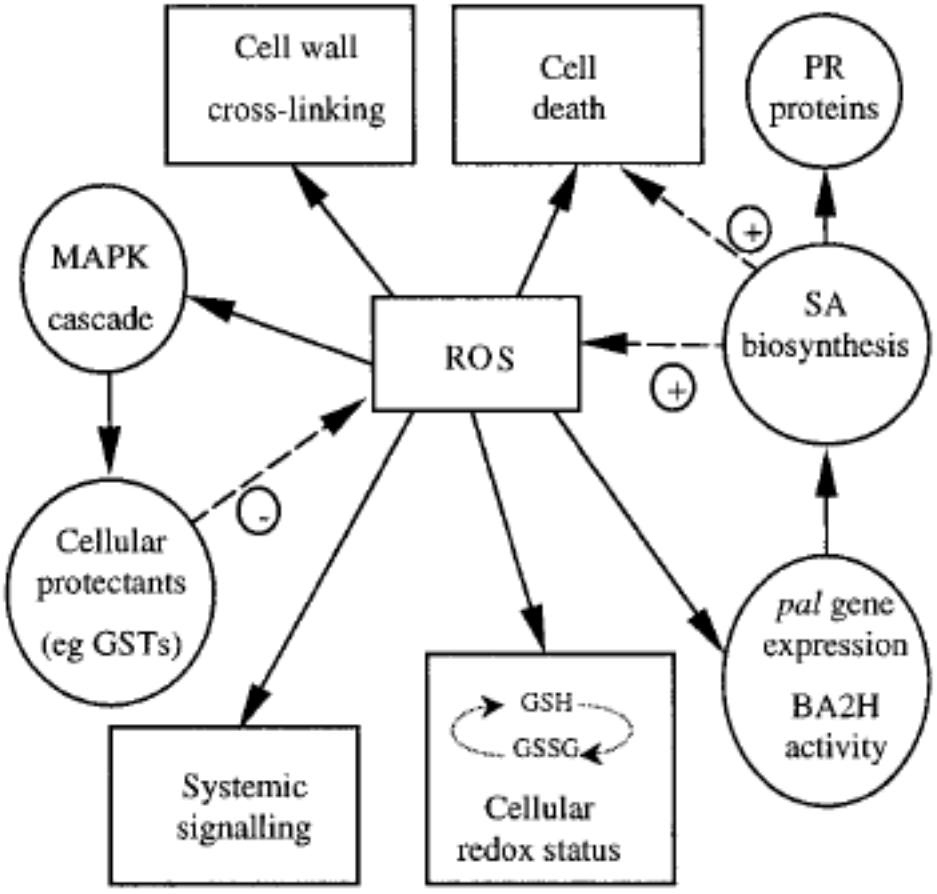

Figure 8: Functional integration of defence responses by reactive oxygen species during the establishment of plant disease resistance. ROS accumulation may integrate a plenty of local and systemic defence responses. BA2H, benzoic acid 2-hydroxylase; pal, phenylalanin ammonia lyase; GSH/GSSG, reduced and oxidized forms of glutathione, respectively; SA, salicylic acid; MAPK, mitogen activated protein kinase (Grant and Loake, 2000).

1.2.3.3. Phytoalexins

Apart from the production of PRs during the defence/stress response(s), plants accumulate a variety of low molecular mass natural products, known as secondary metabolites. Secondary metabolites, derived from isoprenoid, phenylpropanoid, alkaloid or fatty acid/polyketide pathways, differ from the components of primary metabolism, being

generally non-essential for the basic metabolic processes of the plant (Dixon, 2001). The antimicrobial secondary metabolites ("phytoalexins") contribute to the self-defence systems in plants, due to their high antifungal activity and accumulation around infection sites soon after pathogen attack (Grayer and Kokubun, 2001). Virtually, all the enzymes of flavonoid and isoflavonoid biosynthesis leading to the phytoalexin production have now been isolated and functionally characterized (Dixon, 2001).

1.2.3.4. Gene silencing

Gene silencing was perceived initially as an unpredictable and inconvenient side effect of introduction of transgenes into plants. Now it seems to be a consequence of accidental triggering of the plant adaptive defence mechanisms against viruses and transposable elements. This defence mechanism has a number of parallels with the immune system of mammals. The plant defence system generates agents (short dsRNAs) with the specifity to recognize sequences in the invading viral RNA genomes and guide destruction complexes (nucleases) to them. Viruses have responded by evolving mechanisms to circumvent the reaction. The silencing can also be enhanced by prior "vaccination" with virus components (Waterhouse et al., 2001).

1.2.4. Potato viruses

Aphid-transmitted potyviruses (genus *Potyvirus*) are the largest group of plant viruses. *Potyvirus* genome is formed by a single stranded molecule of RNA. It is translated into one protein molecule. Individual functional proteins are released from that large polypeptide by three different viral proteases. Potyviruses induce *in vivo* formation of cytoplasmic and nuclear inclusions in host cells containing aggregates of viral proteins (Shukla et al., 1994).

Potato virus Y (PVY) is one of the most damaging plant viruses particularly, due to the economical importance of its plant host species. Generally, PVY potato strains are divided into three main groups, i.e. PVY^{o}, PVY^{c}, and PVY^{N}. However during the last few decades, new strain variants have been reported, such as the tuber necrosis strain (PVY^{NTN}). Isolates of PVY^{NTN} are associated with potato tuber necrotic ringspot disease (Beczner et al., 1984). The disease is characterised by a superficial necrosis on tubers, which occurs at harvest, and often develops during storage. Most of PVY isolates inducing necrosis on tubers belong to the PVY^{N} subgroup according to their reaction on *Nicotiana tabacum*.

Potato virus A (PVA) is one of the potyviruses discovered earlier. It occurs world-wide, infects many potato cultivars, and can cause about 40% yield losses. The isolates of PVY^{NTN} and PVA have the capacity to infect tobacco plants systemically. The main difference between both viruses is in symptom occurrence. PVY^{NTN} causes the vein necrosis, but in some isolates of tobacco it also induces leaf distortion and stem necrosis (e.g. Lebanon isolate). The symptoms of PVA infection are very mild diffuse mottle and vein clearing (Shukla et al, 1994).

1.3. Phosphoenolpyruvate carboxylase in plants during stress

Influence of stress on plant basal metabolism and photosynthesis has been described in various reports. Environmental stresses have also been shown to induce PEPC activity. PEPC activity increases in *Phaseolus vulgaris* grown at toxic concentrations of zinc (Vangrosveld and Clijsters, 1994) and in *Cucumis sativus* under iron deficiency (De Nisi and Zocchi, 2000). Higher activity of PEPC was detected in phosphorus-deficient roots of *Lupinus albus* (Johnson et al., 1994).

Induction of PEPC expression by salt stress was documented in facultative CAM plant *Mesembryanthemum crystallinum*; being a part of the switch from C_3 to CAM photosynthesis (Thomas et al., 1992; Cushman and Bohnert 1999). LiCl and NaCl induced expression of the PEPC in roots of wheat (Gonzales et al., 2003). The synthesis of malate and PEPC activity was affected by osmotic stress caused by mannitol (Asai et al., 2000). Other stresses affecting water balance such as drought and cold had also a positive effect on the level of PEPC in various plants (Fedina and Popova, 1996; Thind and Malik, 1988).

Low oxygen stress induced an increase of PEPC activity in roots and etiolated leaves in rice seedlings (Moons et al., 1998). In rice under photo-oxidative stress, PEPC activity was stimulated (DeMao et al., 1995). Exposure to ozone caused increase of PEPC activity in *Pinus sylvestris, Picea abies* and *Pinus halepensis* (Sehmer et al., 1998; Fontaine et al., 1999; Fontaine et al., 2003). The same result was obtained in leaves of *Betula pendula* subjected to ozone exposure and low nutrition (Saurer et al., 1995).

Most of the studies were performed either on protein or mRNA level, by measuring activity, determination of the amount of PEPC protein using specific antibodies or by transcription quantification by reverse transcription followed by real-time PCR. Induction of PEPC phosphorylation in wheat leaves treated by light and nitrate by stimulated PEPC-

kinase activity was reported by Duff and Chollet (1995). Similarly elevation of PEPC phosphorylation under ozone stress was reported in *Pinus halepensis* (Fontaine et al., 2003).

1.4. Cytokinins

Plant hormones cytokinins (CK) were discovered during the search for the factors that could promote division of plant cells in culture (Skoog and Miller, 1957). In their classical reports they revealed that undifferentiated callus cultures would form into roots or shoots depending on the relative amount of cytokinins and auxin in medium; the ratio rather than absolute amount of these two hormones was critical. A balanced ratio keeps the cells in an undifferentiated state, while high cytokinin to auxin ratios promote shoot and low ratios promote root development.

Naturally occurring cytokinins are N^6-substituted adenine derivatives that generally contain an isoprenoid or aromatic side chain. These hormones influence numerous aspects of plant development and physiology, including germination, de-etiolation, chloroplast differentiation, branching, plant-pathogen interactions, flower and fruit development and delay of leaf senescence. These processes are also influenced by various other stimuli (e.g. light and other phytohormones), and the physiological and developmental outcomes reflect a highly integrated response to these multiple stimuli (Haberer and Kieber, 2002).

Cytokinins occur in a bound form in the tRNAs of most organisms, including plants, but plants also possess significant amounts of free cytokinins, which function as plant hormones. Isoprenoid-type cytokinins are the most abundant, but several plant species contain adenine derivatives with aromatic substituents. In addition, there are synthetic cytokinins derived from diphenylurea that are structurally unrelated to the adenine-type cytokinins (Haberer and Kieber, 2002).

1.4.1. Biosynthesis, metabolism and degradation of cytokinins

Due to the presence of CKs in several tRNAs, the breakdown of these molecules was originally suggested as a possible mechanism for CK synthesis (Vremarr et al., 1972). Soon it became evident, that the tRNAs could not be the sole source of CKs. Enzymatic activity catalyzing the transfer of isopentenyl moiety from dimethylallyl-diphosphate to AMP to form the active cytokinin isopentenyladenosine-5'-monophosphate was first demonstrated in *Dictyostelium discoiedum* by Taya et al (1978). The CK biosynthetic enzyme (isopentenyl transferase) was identified in the gall-forming bacterium *Agrobacterium tumefaciens*

(Akiyoshi et al., 1984). Since that time bacterial ipt gene has been numerously used to increase the level of CKs in plants (Klee and Romano, 1994)). The completion of *Arabidopsis* genomic sequences enabled Takei et al. (2001) and Kakimoto (2001) in independent studies to identify a total of nine *ipt*-homologs in *Arabidopsis*. An alternative cytokinin biosynthesis pathway, using transfer of hydroxylated isopentenyl moiety to AMP/ATP, was suggested by Astot et al. (2000).

Cytokinins are present in plants as physiologically active free bases and the corresponding nucleosides and nucleotides. The interconversions among these forms are very fast (Mok and Mok, 2001). O-Glucosyl-conjugates of the hydroxylated N^6-side chain are a common modification in all plants. In addition, O-xylosyl-conjugates have been reported in *Phaseolus* (Mok and Mok, 2001). O-glycosylated cytokinins are resistant to the cleavage of the N^6-side chain by cytokinin oxidases/dehydrogenases. As these forms can be easily converted into active cytokinins by β-glucosidases (Brzobohatý et al, 1993), it is believed that O-glycosylated cytokinins are inactive, stable storage forms that play an important role in balancing cytokinin levels.

Free cytokinin bases and nucleosides with an unsaturated N^6-side chain are irreversibly degraded by cleavage of the side-chain by cytokinin oxidases/dehydrogenases. These enzymes have been found in many plant species. They represent a class of highly diverse proteins (Jones and Schreiber, 1997).

1.4.2. Transport and signal transduction

Primary site of CK biosynthesis are root tips. Cytokinins are transported from the roots via xylem the aerial parts of plants. When CK concentrations reach certain threshold levels in competent tissues, their own CK biosynthesis may be initiated (e.g. in developing meristems, Kamínek et al. 1997). A purine transporter has been isolated in Arabidopsis (Gillissen et al., 2000). Feeding roots of nitrogen-depleted maize with nitrate caused cytokinin accumulation first in the roots, subsequently in the xylem sap, and finally in leaves (Takei et al., 2001). Thus, cytokinin may represent a long-distance signal for nitrogen availability from the root to the shoot, presumably to coordinate shoot and root development.

Cytokinin perception and signalling is mediated by His-Asp systems; also known as two-component systems (Figure 9) (Ferreira and Kieber, 2005). The signalling cascade consists of three functional modules: a sensory His-protein kinases (HK, i.e. CK receptors), a His-containing phosphotransfer proteins (HP), and response regulators (RR). There are two

types of CK response regulators, type-B regulators (positive) transmit the CK signal and stimulate the expression of CK-responsive genes, type-A regulators (negative) are induced by CKs and "switch off" the CK signal.

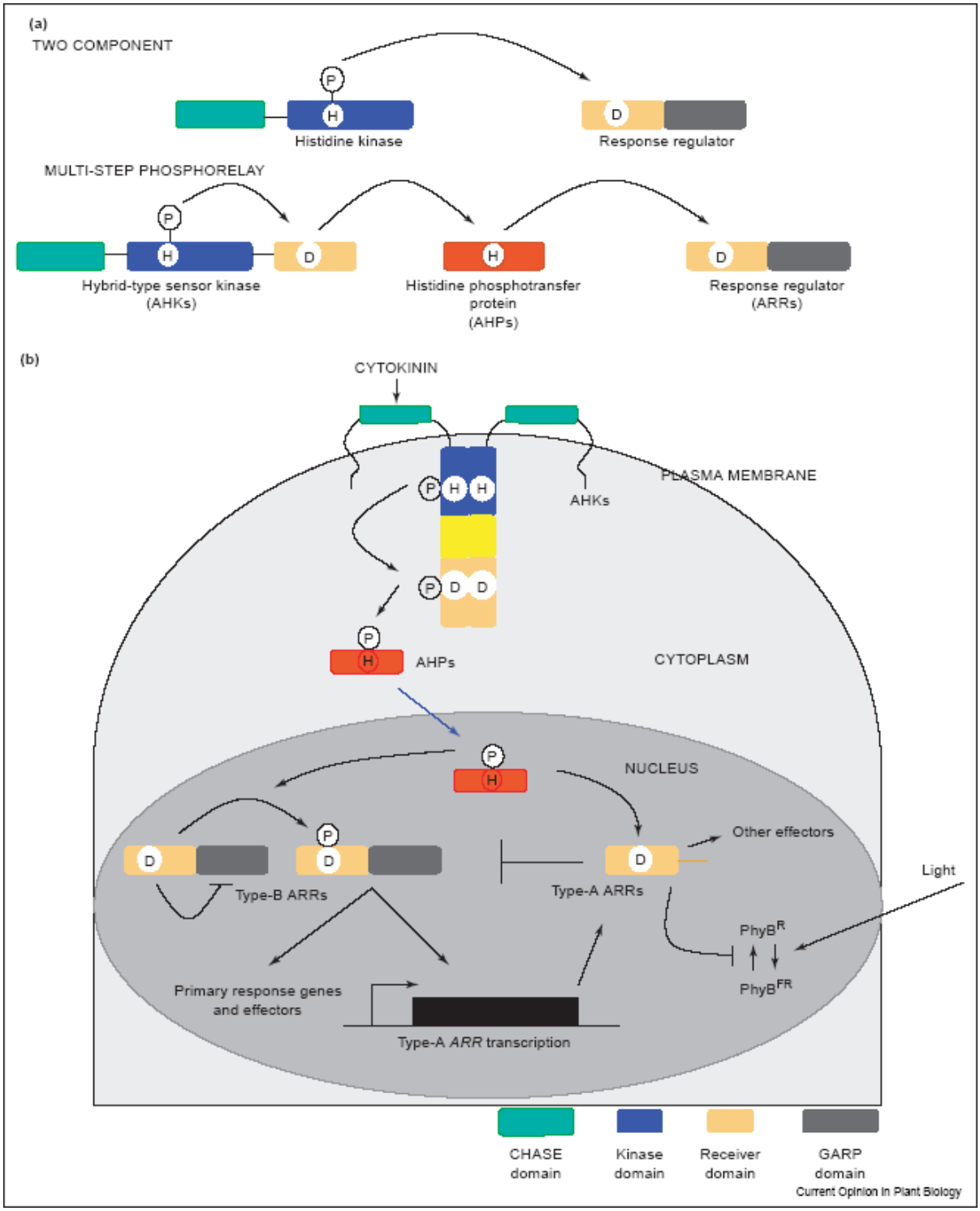

Figure 9: Cytokinin signaling. (a) Two-component signaling. Simple two-component signaling systems are comprised of a receptor kinase and a response regulator. The kinase auto-phosphorylates in response to an environmental stimulus. The phosphoryl group is subsequently transferred to a conserved Asp residue within the receiver domain of the response regulator. Multi-step phosphorelay

systems are comprised of sensor kinase receptors that have both a kinase and a receiver domain, histidine phosphotransfer proteins and response regulators. Ligand binding alters the auto-phosphorylation activity of the sensor kinase. The phosphoryl group is transferred from the auto-phosphorylated His to an Asp residue within the fused receiver domain, then to a His residue in a His-phosphotransfer protein, and ultimately to an Asp residue in a response regulator. The phosphotransfers always occur between histidine and aspartate residues. The Arabidopsis cytokinin-signaling proteins are in parentheses. (b) General model of cytokinin signalling in Arabidopsis. Cytokinin is perceived at the plasma membrane where the hybrid sensor auto-phosphorylates at a conserved His residue that is contained in the kinase domain. The phosphoryl group is then transferred to an Asp residue in the receiver domain of the sensor. There is then an inter-molecular transfer of the phosphoryl group to a His residue in an AHP protein. Activated AHP then translocates to the nucleus and transfers the phosphoryl group to an Asp residue in a response regulator. The type-B ARR receiver domain negatively regulates its own transcriptional activation domain. Upon phosphorylation, this repression is relieved, allowing type-B ARRs to induce the expression type-A ARRs and other primary response genes. Type-A ARRs are negative regulators of cytokinin responses and restrict their own transcription. ARR4 accumulates in the light where it negatively regulates the dark reversion of activated PhyB (Ferreira and Kieber, 2005).

1.4.3. Function of cytokinins in plant-pathogen interactions

Clark et al. (1999) found that 3 days following inoculation with *White clover mosaic potexvirus*, when the virus content began to increase, the contents of CK free bases and ribosides declined. Contrary, 10 days after inoculation total CK content was similar as in control plants. This could indicate that the decline in active CKs is needed prior to virus replication. Further studies proved that supplementing the xylem stream with low concentration of CKs inhibited virus replication at the dsRNA level (Clarke et al., 2000), and also prevented virus-induced decline in several enzymes involved in the scavenging of free radicals (Clarke et al., 1996). Higher level of CKs prior the virus attack could help alleviate the infection impact and retard the virus replication and the symptom development (Dermastia and Ravnikar, 1995). Sano et al. (1996) found that CKs interfered with the signal transduction mechanism participating in PR protein synthesis by controlling endogenous levels of salicylic and jasmonic acids.

1.5. Aim of the work

Phospho*enol*pyruvate carboxylase belongs to important plant enzymes. Its importance was originally attributed to its CO_2 fixation role in C_4 and CAM plants. Recently, variety of anaplerotic functions in all plants is becoming the centre of PEPC studies.

Plant stress response has acquired attention of many scientists due to its high economical significance, especially in agriculture area. Namely biotic stress has caused high losses in agronomic production. Most studies examine mechanisms of plant defence reactions. Effect of pathogens on plant primary metabolism is less explored field.

Presented thesis covers both subjects; enzyme phospho*enol*pyruvate carboxylase and the biotic stress in C_3 plant *Nicotiana tabacum* L. Following aims were set to characterise and evaluate the role and regulation of PEPC in tobacco during biotic stress caused by potyviral infection:

- Isolation and characterisation of PEPC from tobacco leaves.
- Study of phosphorylation of tobacco leaf PEPC and the effect of phosphorylation on kinetic parameters.
- Study of the role of PEPC and related enzymes during potyviral infection in tobacco plants.
- Regulation of PEPC on transcriptional, translational and post-translational level.
- Study of the effect of enhanced level of endogenous cytokinins in tobacco plants under biotic stress.

2. Materials and methods

2.1. Chemicals

Acrylamide ... Sigma, USA

Anti-phosphoamino acids (specific for phosphoserine, phosphothreonine and phosphotyrosine) … Zymed, USA

Bradford Reagent ... Sigma, USA

CDP-Star, substrate for alkaline phosphatase … Roche, Germany

DEAE-cellulose ... Whatman, USA

Deoxynucleotide mix ... Sigma, USA

DNase I ... Qiagen, USA

Enzymes for measurements of metabolites concentration (glucose-6-P dehydrogenase, hexokinase, aspartate transaminase) ... Sigma, USA

FastStart DNA Master SYBR Green Plus kit ... Roche Diagnostics, Germany

M-MLV reverse transkriptase ... Promega, USA

Malate dehydrogenase, from bovine heart ... Sigma, USA

Phosphatase, Alkaline from bovine intestinal mucosa ... Sigma, USA

Phosphatase Inhibitor Cocktail ... Sigma, USA

- Sodium orthovanadate
- Sodium molybdate
- Sodium tartrate
- Imidazole

Phosphoprotein Phosphate Estimation Assay kit … Pierce, USA

Protease Inhibitor Cocktail (for plant cell and tissue exctracts) ... Sigma, USA

- AEBSF – [4-(2-Aminoethyl)benzenesulfonyl fluoride hydrochloride]
- Bestatin hydrochloride
- E-64 – [N-(trans-Epoxysuccinyl)-L-leucine 4-guanidinobutylamide]
- Leupeptin hemisulfate
- Pepstatin A
- 1,10-Phenanthroline

Protein Kinase A Catalytic Subunit, from bovine heart ... Promega, USA

Protein Standard Marker ... Serva, Germany

RNAse Out ... Invitrogen, USA

RNeasy Plant Mini Kit ... Qiagen, USA

Sephadex G-200 ... Sigma, USA

Sodium bicarbonate – ^{14}C (2-10 mCi/mmol) ... Sigma, USA

Substrates (L-malate, phosphoenolpyruvate, pyruvate, glucose-6-P) ... Sigma, USA

Other various chemicals ... Sigma, USA; Lachema, Czech Republic

2.2. Instruments

Centrifuge Hettich Universal 32R ... Hettich, Germany

Electrophoretic device Multigel G-44 ... Biometra, Germany

Fastblot B33 ... Biometra, Germany

Homogenizer Turrax DI18... IKA, Germany

LightCycler 1.2 ... Roche Diagnostics, Germany

LightCycler software v. 3.5 ... Roche Diagnostics, Germany

Liquid scintillation counter LS 600 SE … Beckman, USA

Spectrophotometer Helios α ... Thermo Spectronic, USA

Spectrophotometer Ultrospec 2100 ... Amersham, UK

2.3. Plant materials

Tobacco plants (*Nicotiana tabacum L.* cv. Petit Havana SR1) were grown in a greenhouse under 22/18^{o}C day/night temperatures. Day irradiance [overall integrated mid-values were ca. 500 μmol(quantum) $m^{-2}s^{-1}$] was prolonged by the additional irradiation [PPFD ca. 200 μmol(quantum) $m^{-2}s^{-1}$] to 16 hours. Seeds were sown in pots with sand. Plantlets were transferred to soil after 3 weeks. For PEPC isolation leaves of 8-10 weeks old plants were collected, frozen in liquid nitrogen and stored at -80^{o}C.

Five-week old plants were mechanically inoculated with PVA or PVY^{NTN} on the adaxial surface of the bottom mature leaves. Virus isolates of PVA and PVY^{NTN} (Lebanon) were provided by Dr. P. Dědič (Potato Research Institute, Havlíčkův Brod, Czech Republic). Three independent experiments of virus infection were performed in presented work. Each experiment consisted of 10-15 control plants and 20-30 infected by the virus. Results from each experiment are described separately in the result section. Mixed samples of leaves above the inoculated ones (systemically infected leaves) were collected at regular intervals or at the maximal symptoms of viral infection, frozen in liquid nitrogen and stored at -80^{o}C. Sampling was always made ante meridiem.

Tobacco samples for cytokinin related experiments were kindly provided by Dr. H. Synková (Institute of Experimental Botany, Prague, Czech Republic). This experiment involved control rooted tobacco (SR1), plants grafted onto control rootstock (SRG), transgenic tobacco containing a supplementary *ipt*-gene under a control of promoter for the small subunit of Rubisco grown as shoots grafted onto control rootstock (G), and autogamic progeny of the transgenic grafts (SE). Gene *ipt* codes for isopentenyl transferase, the key enzyme of cytokinin synthetic pathway.

2.4. Methods

2.4.1. PEPC, NADP-ME, PPDK and Rubisco activity assays in physiological experiments

Leaf samples (0.5 g of fresh weight) were homogenized in 1.5 ml of extraction buffer containing 100 mM Tris-HCl (pH 7.5), 1 mM dithiothreitol, 1 mM EDTA, 5% glycerol and 5 mM $MgCl_2$ (buffer A). The homogenate was centrifuged at 20,000 g at 4^oC for 15 min. The supernatant was immediately used for enzyme activity measurements.

The PEPC assay mixture contained 100 mM Tris-HCl buffer (pH 8.1), 5 mM $NaHCO_3$, 2 mM $MgCl_2$, 2 mM PEP and 0.2 mM NADH in total volume of 1 ml. The NADP-ME assay mixture contained 100 mM MOPS (pH 7.4), 10 mM malate, 2 mM $MgCl_2$ and 0.2 mM NADP in total volume of 1 ml. The PPDK assay mixture contained 100 mM Tris-HCl (pH 7.4), 10 mM $MgCl_2$, 5 mM $NaHCO_3$, 2 mM pyruvate, 2 mM K_2HPO_4, 1 mM ATP, and 0.2 mM NADH in a total volume of 1 ml. Reactions were initiated by addition of 50 μl of crude extract. PEPC, NADP-ME and PPDK activities were monitored for 5 minutes as absorbance changes at 340 nm at 25^oC and activities were calculated as units per gram of fresh weight. One unit is defined as conversion of 1 μmol of substrate converted per minute.

Rubisco activity was measured in crude extracts as ^{14}C fixed into the acid stable reaction product in a toluene scintillation cocktail in a LS 600 SE liquid scintillation counter (Beckman). The assay mixture contained 100 mM Tris-HCl (pH 8.1), 1 mM EDTA, 30 mM $MgCl_2$, 5 mM DTT and 5 mM $NaHCO_3$ and 50 μl of crude extract. After 10 minutes preincubation at 23^oC, 1 mM ribulose-bisphosphate and 1 mM $Na_2{}^{14}CO_3$ were added. The reaction was stopped after 5 min by adding 0.5 ml 6 M HCl.

2.4.2. Protein amount determination

Soluble proteins were determined according to Bradford (1976). 50 μl of sample was mixed with 1.5 ml Bradford solution and incubated for 15 minutes at room temperature. Absorbance at 595 nm was measured and protein concentrations were calculated from calibration equation. Calibration curve was obtained using concentrations of bovine serum albumin as standard.

2.4.3. Measurement of free phosphate concentration

Concentration of free phosphate was determined using Phosphoprotein Phosphate Estimation Assay kit (Pierce) according to manufacturer instructions. In this method, malachite green reacted with phosphate in solution to form a green complex. The intensity developed proportional to the phosphate concentration and could be determined spectrophotometrically. Calibration curve was obtained using 2.5, 5, 10, 15 μg/ml of phosvitin. Modified method was performed to measure concentration of free phosphate in crude extracts of tobacco leaves; alkaline hydrolysis of phosphate groups was skipped and replaced by treatment with alkaline phosphatase (2.4.8).

2.4.4. Metabolite measurements

Tobacco leaf samples were homogenized in 1 M $HClO_4$ and centrifuged at 20,000g for 15 min. The supernatant was neutralized using 5 M K_2CO_3 to approx. pH 7. Precipitated $KClO_4$ was removed by centrifugation. Metabolite extracts were stored at -30^{o}C.

Metabolite contents were measured enzymatically based on methods described by Stitt et al. (1989). For the determination of glucose and glucose-6-phosphate, the reaction mixture contained 100 mM Tris–HCl (pH 8.1), 5 mM $MgCl_2$, 1 mM ATP and 0.8 mM NADP in a total volume of 1 ml. The reaction was started adding 0.1 U of glucose-6-phosphate dehydrogenase and 0.1 U hexokinase. Increasing absorbance at 340 nm was monitored spectrophotometrically. Glucose-6-phoshpate was determined through the same reaction lacking the hexokinase and ATP.

For the determination of malate, the reaction mixture contained 100 mM Tris-HCl (pH 8.1), 0.2 mM NAD, 0.05 U of malate dehydrogenase, 5 U aspartate transaminase and 2 mM aspartate. Increasing absorbance at 340 nm was monitored spectrophotometrically.

Concentrations of metabolites in samples were calculated from calibration curves using known concentrations of corresponding metabolite.

2.4.5. Native electrophoresis

Native electrophoresis was performed according to Lee and Lee (2000). Approximately 1 mU of PEPC in 10% sucrose was loaded on 6% polyacrylamide gel. After electrophoretic separation, activity of PEPC was detected in gel according to Rivoal et al. (2002). Staining solution contained 10 mM $MgCl_2$, 2.5 mM $NaHCO_3$ 5 mM DTT, 15% (v/v) glycerol, 0.15 mM NADH, 2 U/ml MDH and 1.5 mM PEP in 100 mM Tris-HCl buffer (pH 8.1). After 60 minutes of incubation at 25^{o}C staining solution is removed and presence of PEPC is

visualized on a UV transilluminator. Activity bands (sites of NADH oxidation in gel) appeared as dark bands over a fluorescent background.

2.4.6. SDS electrophoresis

SDS polyacrylamide gel was prepared according to Laemmli (1970). 10% resolving and 5% stacking gels were used. Separation was carried out using electrophoretic system Multigel Biometra in SDS electrophoretic buffer (25 mM Tris-HCl buffer pH 8.3, 250 mM glycine, 3.5 mM SDS) with the voltage control 70 V for the stacking gel and 140 V for the resolving one. Gel was stained using staining solution contained: 2 g Coomassie Brilliant Blue R 250, 0.5 g Coomassie brilliant blue G 250, 425 ml ethanol, 100 ml acetic acid, 50 ml methanol and 425 ml H_2O. Destaining solution contained ethanol, acetic acid and H_2O in ratio 25 : 10 : 65.

2.4.7. Isolation of phosphoenolpyruvate carboxylase

2.4.7.1. Extraction and ammonium-sulphate fractionation

30 g of tobacco leaves were homogenized in 100 ml of 100 mM Tris-HCl (pH 7.5), 1 mM dithiothretitol, 1% (v/v) proteinase inhibitor cocktail (Sigma, USA; contains: 4-(2-aminoethyl)benzenesulfonyl fluoride hydrochloride, bestatin hydrochloride, N-(trans-epoxysuccinyl)-L-leucine 4-guanidinobutylamide, leupeptin hemisulfate, pepstatin A, 1,10-phenanthroline), 1 mM EDTA, 5% glycerol and 5 mM $MgCl_2$ (buffer A) by homogenizer Turrax DI18. After filtration through cheesecloth the filtrate was centrifuged at 10,000g for 30 min at 4^{o}C. The extract was fractionated with ammonium sulphate (30% to 55% saturation), the precipitate was dissolved in 10 ml of 50 mM Tris-HCl (pH 7.8), 5 mM $MgCl_2$, 1 mM EDTA, proteinase inhibitor cocktail mix, 5% glycerol and 0.5 mM dithiothreitol (buffer B) and dialyzed against buffer B at 4^{o}C overnight.

2.4.7.2. DEAE-cellulose chromatography

Dialyzed sample was applied to a DEAE-cellulose column (1.5 x 15 cm) equilibrated with buffer B. After washing with buffer B elution was performed with a linear NaCl gradient (0-300 mM) in buffer B at flow rate 1 ml/min. PEPC activity was eluted as a single peak at 250 mM NaCl. Fractions containing the highest PEPC activity were pooled, precipitated with 80% saturation of ammonium sulphate and centrifuged at 10,000g for 15 min.

2.4.7.3. Gel and hydroxyapatite chromatography

The pellet was dissolved in 1 ml of buffer B and applied to Sephadex G-200 column (1.5 cm x 30 cm). Elution was performed with buffer B. Fractions with PEPC activity were collected and applied to hydroxyapatite column (1.5 cm x 15 cm) previously equilibrated with 20 mM potassium orthophosphate (pH 7.0), 5 mM $MgCl_2$, 1 mM EDTA, 5% glycerol and 0.5 mM dithiothreitol (buffer C). After washing the column with buffer C the protein was eluted with stepwise increases in the phosphate concentration of the buffer: 50 ml of each 40 mM, 100 mM and 200 mM phosphate buffer pH 7.0. The PEPC was eluted in the peak at 100 mM phosphate buffer pH 7.0.

2.4.7.4. Purification of PEPC from maize seeds

Isolation of PEPC from maize seeds was performed similarly to that from tobacco leaves with minor modifications. 100 g of freshly homogenized maize seeds were used as starting material for each isolation process. Ammonium sulphate fractionation, ionex, gel and hydroxylapatite chromatography were performed according to 2.4.7.1, 2.4.7.2 and 2.4.7.3. In addition, the hydroxylapatite chromatography was followed by ionex chromatography carried out similarly to 2.4.7.2 with a modification; the column was equilibrated with buffer B containing 200 mM NaCl and the elution was performed with a linear 200-400 mM gradient of NaCl. Fractions with PEPC activity were collected and dialyzed against PBS and adjusted to desired final volume.

2.4.8. Phosphatase treatment

Dephosphorylation assay was performed using 50 U of alkaline phosphatase (Sigma) per milligram of total protein and desalted enzyme in 50 mM Tris buffer (pH 7.5). The reaction was incubated at 37^{o}C. PEPC activity was measured in aliquots in regular intervals. Reaction with 1% (v/v) phosphatase inhibitor cocktail (Sigma, USA; contains: sodium orthovanadate, sodium molybdate, sodium tartrate, imidazole) was used as negative control.

2.4.9. Protein kinase treatment

Phosphorylation assay contained 100 u (1 u is defined by manufacturer as the amount of enzyme required to incorporate 1 pmol of phosphate into casein in one minute at 30°C) of protein kinase A (Sigma) per milligram of protein in desalted PEPC sample, 2 mM ATP, phosphatase inhibitor cocktail (1:100 dilution) and 20 mM $MgCl_2$ in presence of 100 mM HEPES-KOH buffer (pH 7.3). Reaction was incubated for 3 hours at 30^{o}C. PEPC activity

was measured in aliquots in regular intervals. Reaction with distilled water instead of kinase was used as negative control.

2.4.10. Kinetic studies of tobacco PEPC

Measurements of initial velocity were performed at 25°C in a final volume of 1 ml of 100 mM HEPES-KOH buffer (pH 7.3 or 8.1), 5 mM $NaHCO_3$, 2 mM $MgCl_2$, 0.2 mM NADH and 4 units malate dehydrogenase with concentrations of PEP, malate, glucose-6-phosphate, glycine or aspartate as described in each experiment. Assays were initiated by the addition of 10 μg PEPC. The progress of the reaction was followed during first 180 s at 340 nm spectrophotometrically. Activities were calculated as units per milligram of protein. One unit [U] is defined as conversion of 1 μmol of substrate converted per minute. All measurements were repeated 3-times from independent enzyme isolations.

2.4.10.1. Data analysis of kinetic studies

PEPC kinetic data were analyzed by nonlinear regression calculations using MS Excell software. Kinetic data, which were dependent upon varied concentration of substrate, were fitted to the Michaelis-Menten equation 1, or in case of inhibitor present in the reaction to the equation for mixed inhibition (equation 2),

1 ... $$v = \frac{V_{\max}.[S]}{K_m + [S]}$$

2 ... $$v = \frac{V_{\max}.[S]}{K_m.(1 + \frac{[I]}{K_{IC}}) + [S].(1 + \frac{[I]}{K_{IU}})}$$

where v is experimentally determined initial reaction rate, V_{max} the maximum reaction rate, *[S]* is the concentration of the substrate, *[I]* is the concentration of inhibitor, K_m is the Michaelis constant, K_{IC} and K_{IU} refer to the competitive and uncompetitive components of mixed-type inhibition.

When concentration of activator varied at a constant concentration of substrates, the experimental data were fitted to equation 3 for data confirming to hyperbolic character,

3 ... $$v = V_0 + \frac{(V_{a\max} - V_0).[A]}{A_{0.5} + [A]}$$

where V_o is maximal reaction rate at absence of activator, [A] is concentration of activator, V_{amax} is the highest reaction rate obtained at saturating activator concentrations and $A_{0.5}$ is the

concentration of the activator that gives half-maximum activation at fixed concentrations of substrates.

The points in the figures are the experimentally determined values, whereas the curves are calculated from fits of these data by the appropriate equation. The best fits were determined by the relative fit error and other relevant variables such as observed reaction rates, substrate concentration and data number.

Studies of inhibition were supplied with linear plots of Lineweaver-Burk and Dixon. Measured data were interlaced with linear curve obtained by linear regression. These plots give the advantage of secondary control of the type of inhibition (Dixon, 1953).

2.4.11. Rabbit immunization with PEPC from maize seeds

Two rabbit were used for anti-PEPC antibody preparation. Total 2 mg of PEPC protein isolated from maize seeds were used for immunization of each rabbit. The scheme of antigen dosage is shown in table 4. Blood serum was collected 10 days after the last antigen injection.

Table 2: Scheme of antigen dosing.

Day	Amount of antigen [mg]	Adjuvans
1	0.150	Freund complete
21	0.225	Freund incomplete
42	0.300	Freund incomplete
63	0.625	Pure antigen in PBS
84	0.625	Pure antigen in PBS

IgG fraction was purified from serum adding 0.04 M sodium acetate and 2% caprylic acid (Steinbuc and Audran, 1969). After the centrifugation, the supernatant was dialysed against PBS. IgG fraction was then stored at 4^{o}C.

2.4.12. Detection of PEPC by Western blot

Equal amounts of total proteins were subjected to SDS-polyacrylamide gel electrophoresis (PAGE) (Laemmli, 1970) on 10% polyacrylamide gels. After electrophoresis proteins were transferred from the gel to nitrocellulose membrane by electroblotting using a semi-dry system [Fastblot B31, Biometra].

The immunochemical detection of PEPC was carried out using polyclonal rabbit antiserum (diluted 1:200) raised against maize seed PEPC. Bound antibodies were visualized using alkaline phosphatase conjugate mouse antirabbit IgG (diluted 1:30,000). NBT-BCIP (nitroblue tetrazolium, 5-bromo-4-chloro-3-indolyl phosphate) was used as substrate for alkaline phosphatase. The linearity of signal was tested using various quantities of PEPC protein.

The immunochemical detection of phosphoproteins was carried out using commercial rabbit antibodies specific for phosphoserine, phosphothreonine and phosphotyrosine (diluted 1:1,000). Bound antibodies were visualized using alkaline phosphatase conjugate mouse antirabbit IgG (diluted 1:30,000). CDP-Star (1:100 in 0.1 M Tris-HCl, 0.1 M NaCl, pH 9.5) was used as substrate for alkaline phosphatase, luminescence was detected on X-ray film.

2.4.13. Isolation of total RNA

Total RNA was isolated from 100 mg of leaf sample using Plant RNeasy kit (Qiagen). Any contaminated genomic DNA was removed by on column treatment with DNaseI (Qiagen). The quantity of the mRNA was determined spectrophotometrically as absorbance at 260 nm and the level of intact RNA was determined by agarose gel electrophoresis. Approximately 1 μg of RNA was mixed with 2.5% SDS and loading buffer, heated at 75^{o}C for 2 minutes and loaded on 0.8% agarose gel. After electrophoretic separation RNA was visualized by ethidium bromide staining.

2.4.14. Reverse transcription

RNA was transcribed using oligo-dT primer. 5 μg of RNA was mixed with 0.5 μg Oligo(dT)$_{12-18}$ primer and heated for 5 minutes at 65^{o}C. 100 units M-MLV reverse transcriptase (Promega), 1 mM dNTPs, 20 units of RNAse Out (Invitrogen) and reaction buffer were added on ice and cDNA synthesis was carried out at 42^{o}C for 55 minutes. Heating for 10 minutes at 75^{o}C inactivated the reaction.

2.4.15. Quantification of PEPC mRNA

The real-time quantitative PCR was performed on LighCycler 1.2 (Roche) using DNA Master SYBR Green Plus kit and glass reaction capillaries. Specific PEPC primers were designed by Tib Molbiol (Germany) according to genomic sequence X59016 (GI:22588). Sequence of PEPC primers were:

PEPC-se, ATT GCT GGA CAC AAG GAT CTT

PEPC-as, GCT TGA GAG TGT AGG CTT GC

Tobacco *Actin9* was used as standard (reference) gene, primers were kindly provided by Dr. H. Štorchová (IEB CAS, Prague, Czech Republic). The PCR contained 2.5 μl of cDNA, 0.3 μM PEPC or Actin9 primers and 2 μl of Master mix (component 1 of the reaction kit) in total volume of 10 μl.

Conditions for the amplification of PEPC transcripts were: 10 min polymerase activation at 95°C and 50 cycles, each cycle at 95°C for 10s, 58°C for 6s and 72°C for 10s. PCR of Actin9 involved 10 min polymerase activation at 95°C and 50 cycles, each cycle at 95°C for 10s, 60°C for 6s and 72°C for 10s. Second derivative maximum (as implemented in LightCycler software v. 3.5) was used to determine crossing point (CP).

2.4.15.1. Data analysis of real-time PCR

The ratio corresponding to the difference in PEPC transcription between healthy and infected plants was calculated according to equations 4:

4 ... $$ratio = \frac{e_{PEPC}^{CP_{PEPC}}}{e_{Actin9}^{CP_{Actin9}}}$$

Values e_{PEPC} and e_{Actin9} represent PCR amplification efficiency of both products and *CP* represents the crossing point of each sample reaction. PCR efficiency was estimated from equation 5 describing the calibration curve of cDNA serial dilutions.

5 ... $$e = 10^{\frac{1}{|slope|}}$$

Slope value was obtained from LightCycler software v. 3.5.

2.4.16. Virus detection

2.4.16.1. Immunochemical detection

The extent of viral infection was determined by TAS ELISA (Clarks and Adams, 1997) in homogenates of the leaves of infected plants using polyclonal or monoclonal antibodies raised against the respective pathogens (Čeřovská, 1998). Bound antibodies were visualized by anti-rabbit mouse antibodies conjugated with alkaline phosphatase. *P*-nitrophenylphosphate was used as enzyme substrate (1 mg/ml in 10% diethanolamine, pH 9.8) and absorbance at 405 nm corresponds to virus content.

2.4.16.2. Real-time PCR detection

The real-time quantitative PCR was performed on LighCycler 1.2 (Roche) using DNA Master SYBR Green Plus kit and glass reaction capillaries. Specific PVY^{NTN} primers were kindly provided by Dr. T. Moravec (IEB CAS, Prague, Czech Republic) (Moravec et al., 2003). *Actin9* was used as standard gene. The PCR contained 2.5 μl of cDNA, 0.5 μM PVY^{NTN} primers (0.3 μM Actin9 primers) and 2 μl of Master mix (component 1 of the reaction kit) in total volume of 10 μl.

Conditions for the amplification of PVY^{NTN} transcripts were: 10 min polymerase activation at 95°C and 50 cycles, each cycle at 95°C for 10s, 58°C for 6s and 72°C for 10s. Actin9 PCR involved 10 min polymerase activation at 95°C and 50 cycles, each cycle at 95°C for 10s, 60°C for 6s and 72°C for 10s. Second derivative maximum (as implemented in LightCycler software v. 3.5) was used to determine crossing point (CP).

Data analysis of quantification of PVY^{NTN} RNA was performed similarly to PEPC mRNA quantification (2.4.15.1).

3. Results

3.1. Characterization of tobacco PEPC

3.1.1. Isolation of PEPC from *Nicotiana tabacum* L.

Phosphoenolpyruvate carboxylase was partially purified from tobacco leaves collected from 8-10 weeks old plants. To ensure minimal enzyme degradation, the whole isolation procedure was performed in 2 days and protease inhibitors were added to all isolation buffers. The enzyme was purified to final specific activity 0.81 U/mg from 30 g of leaf material. Ammonium sulphate fractionation, ionex chromatography on DEAE cellulose, gel chromatography on Sephadex G200 and hydroxyapatite chromatography were the main steps of isolation. The whole procedure is summarized in Table 3. Typical result of ionex chromatography is shown in Figure 10, linear gradient of sodium chloride was used for protein elution. The PEPC eluted as a single peak at 0.25 mM NaCl. Typical result of gel chromatography is shown in Figure 11. The PEPC eluted as a single peak at Ve 20-25 ml.

Typical result of hydroxyapatite chromatography is shown in Figure 12. The PEPC was eluted by step-wise concentration gradient of phosphate buffer. The majority of PEPC protein was eluted at 100 mM phosphate.

Table 3: Summary of purification of phosphoenolpyruvate carboxylase from tobacco leaves (30g).

purification step	volume [ml]	total PEPC activity [U]	total protein [mg]	specific PEPC activity [U/mg]
crude extract	110	5.7	264	0.02
$(NH_4)_2SO_4$ precipitation	7	5.0	111	0.04
ionex chrom.(DEAE cellulose)	35	2.8	18	0.16
gel chrom. (Seph G200)	8	2.1	10	0.21
hydroxyapatite chrom.	10	1.6	2	0.81

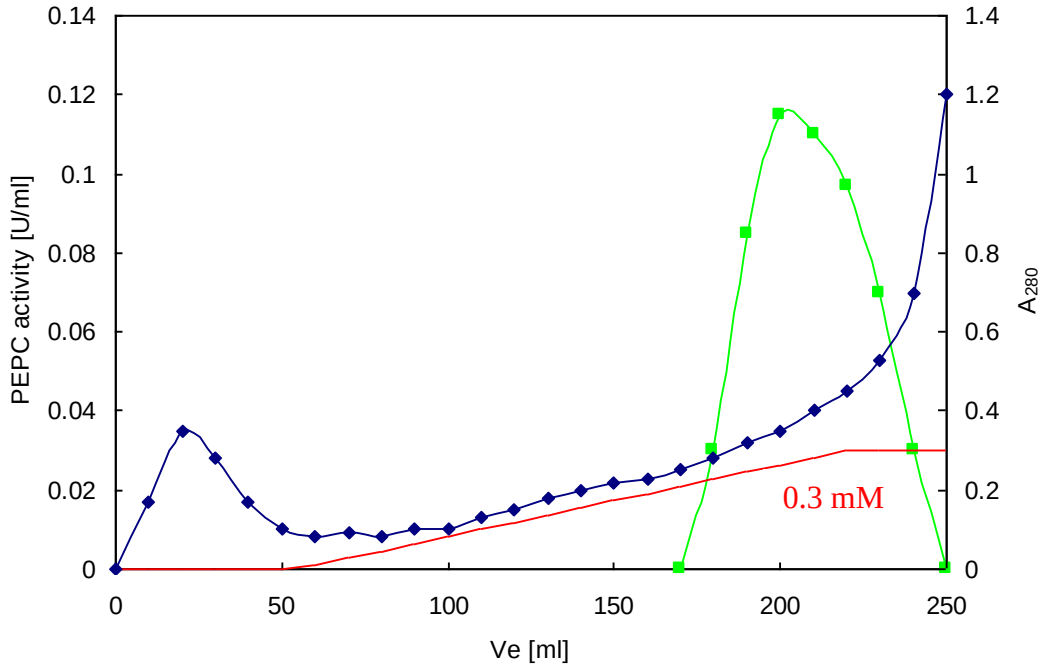

Figure 10: Ionex chromatography of PEPC from tobacco leaves on DEAE-cellulose. Elution was performed by linear gradient of NaCl (0 - 0.3 mM; red line). The blue line indicates the protein level measured as absorbance at 280 nm. The green data show activity of PEPC in fractions.

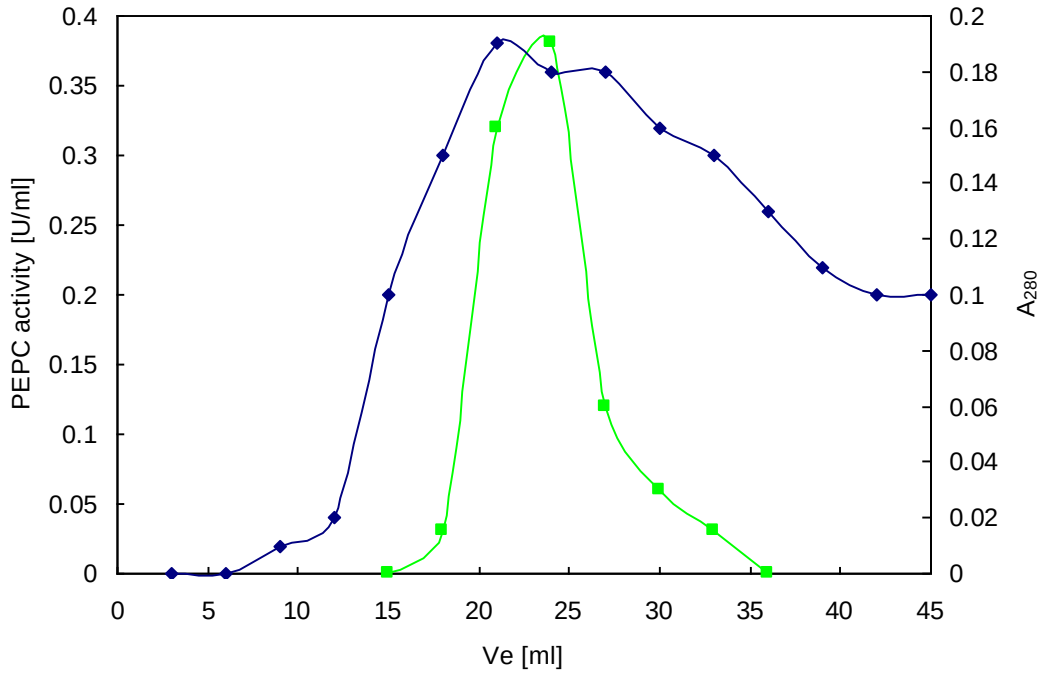

Figure 11: Gel chromatography of PEPC from tobacco leaves on Sephadex G200 column. The blue line shows protein level measured as absorbance at 280 nm. The green data shows activity of PEPC in fractions.

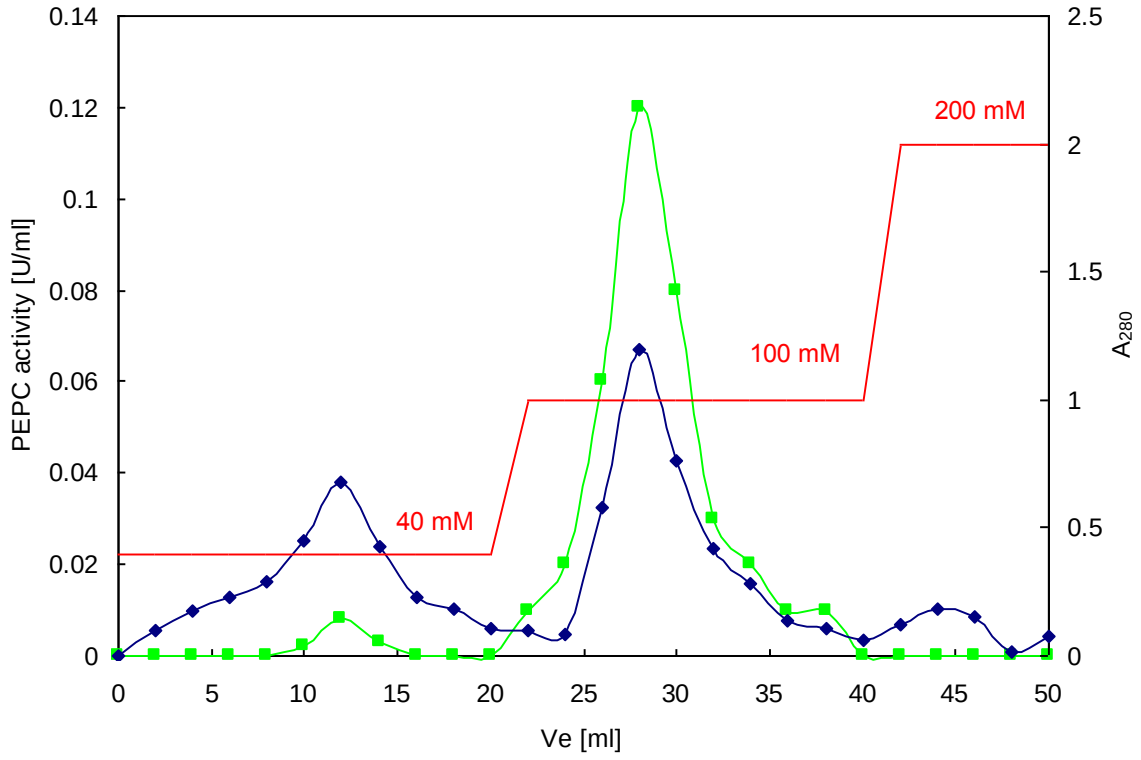

Figure 12: Chromatography of PEPC from tobacco leaves on hydroxylapatite column. Elution was performed by step-wise gradient of phosphate buffer (40 mM, 100 mM and 200 mM; red line). The blue line shows protein level measured as absorbance at 280 nm. The green data shows activity of PEPC in fractions.

3.1.2. Study of affinity of tobacco PEPC to phosphoenolpyruvate

Availability of the substrate can be one of many possible ways to regulate PEPC activity *in vivo*. The PEPC affinity to substrate is also an attribute that discriminates photosynthetic and non-photosynthetic PEPC isoforms. The C_3 and non-photosynthetic forms generally embody higher affinity to PEP than C_4 and CAM photosynthetic forms.

The kinetics of saturation of the PEPC isolated from tobacco leaves by PEP was studied. All measurements were done at 5 mM bicarbonate, 2 mM $MgCl_2$ and 25°C. Effect of pH on PEPC substrate affinity is shown in Figure 13. The measurements were carried out at optimal pH 8.1 and sub-optimal pH 7.3. In both cases reaction indicated classical hyperbolic character described by equation 1 (Figure 13).

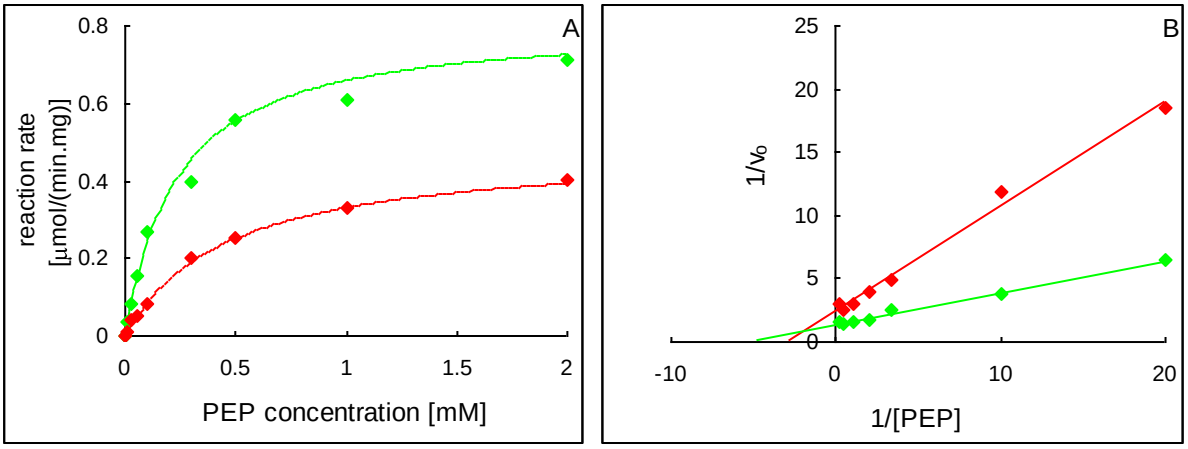

Figure 13: Standard (A) and Lineweaver-Burke (B) plot of affinity of PEPC to substrate [PEP] at optimal pH 8.1 (green data) and suboptimal pH 7.3 (red data). The points represent experimental data. The lines are the result of the best fit of the experimental data to equation 1 (A) or result of linear regression of the double-reciprocal plot (B).

Maximal reaction rate was 0.8 µmol/(min.mg) and 0.5 µmol/(min.mg) at pH 8.1 and 7.3, respectively. PEPC showed higher affinity to substrate at pH 8.1; Michaelis constant (K_m) was 0.25 mM at pH 8.1 and 0.45 mM at pH 7.3.

3.1.3. Role of potential effectors in regulation of tobacco PEPC

The potential effectors of PEPC, activators such as D-glucose-6-phosphate and glycine and inhibitors such as L-malate and L-aspartate were studied to confirm or deny their effects on tobacco leaf PEPC.

3.1.3.1. Effect of L-malate on PEPC activity

Effect of L-malate on activity of PEPC isolated from tobacco leaves was studied. All measurements were done at 25°C, 5 mM $NaHCO_3$ and 2 mM $MgCl_2$. The sensitivity to malate was affected by pH and concentration of total PEP. L-malate caused decrease of tobacco PEPC activity at both optimal and sub-optimal pH conditions; however, the higher effect was monitored at pH 7.3. Figure 14 shows inhibition of PEPC by malate at pH 8.1 and 7.3 at concentrations of PEP 2 mM and 0.5 mM. The PEPC was more sensitive to inhibition at lower pH, the $I_{0.5}$ was about 5- to 10-fold lower at pH 7.3 compared to pH 8.1 depending on final concentration of PEP.

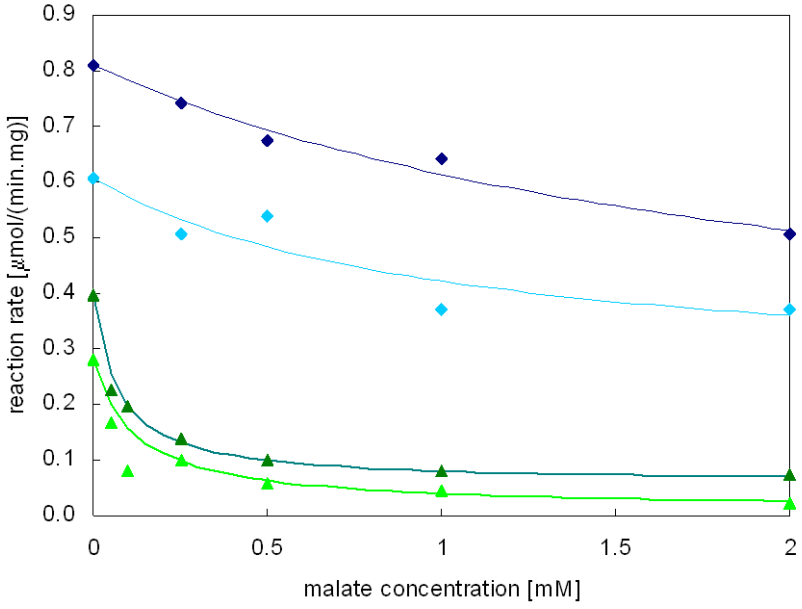

Figure 14: Effect of L-malate on PEPC reaction rate at optimal (blue lines) and sub-optimal (green lines) pH. Dark color lines describe measurement at PEP saturation (2 mM) while light color ones describe lower PEP concentration (0.5 mM). The points are experimental data, the lines are the result of the best fit of experimental data to equation 3.

Figure 15 shows effect of malate on reaction rate of PEPC at PEP range 0-2 mM. Malate has effect on both maximal reaction rate (V_{max}) and Michaelis constant (K_m). V_{max} is decreased and K_m is increased at higher malate concentration. Inhibition constants obtained by non-linear regression from equation 2 were 0.2 mM (K_{IC}, competitive inhibition constant)

and 1.3 mM (K_{IU}, uncompetitive inhibition constant). This result indicates mixed type of inhibition. Dixon plot (Figure 16) and also Lineweaver-Burke plot (result not shown) display the mixed type of inhibition. K_{IC} obtained from Dixon plot was 0.3 mM, which is well corresponds to the value obtained by non-linear regression.

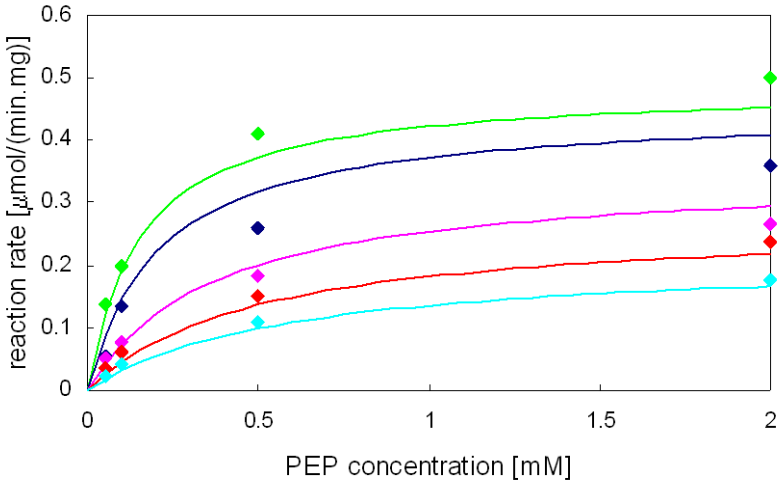

Figure 15: Effect of malate on reaction rate of tobacco leaf PEPC at varied concentration of PEP. Concentrations of malate were 0 mM, 0.1 mM, 0.5 mM 1 mM and 2 mM. The concentration of bicarbonate in the assay was 5 mM and 2 mM $MgCl_2$, the measurements were done at 25°C and pH 7.3. The points represent experimental data. The lines are the result of the best fit of experimental data to equation 2.

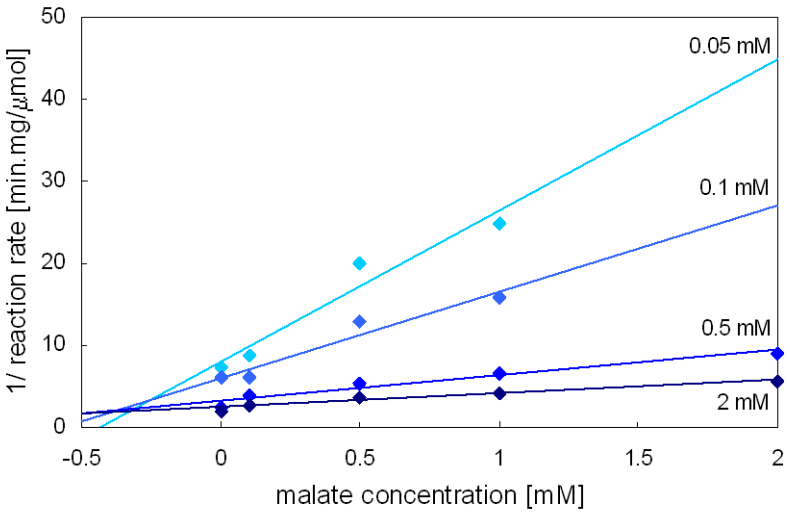

Figure 16: Effect of malate on PEPC reaction rate in Dixon plot at various concentrations of PEP (inset values). The concentrations of bicarbonate and $MgCl_2$ in the assay were 5 mM and 2 mM, respectively. All measurements were done at 25°C and pH 7.3. The lines are linear regression of experimental data (points).

3.1.3.2. Effect of L-aspartate on PEPC activity

Effect of L-aspartate on PEPC activity was studied at pH 7.3, 25°C and two concentration values of total PEP (Figure 17). The concentrations of bicarbonate and $MgCl_2$ in all assays were 5 mM and 2mM, respectively. Very weak inhibition was monitored; 2 mM aspartate caused 10% decrease of PEPC reaction rate at 0.5 mM concentration of PEP. Inhibition constants calculated by non-linear regression from equation 2 indicated, that the inhibition corresponds mostly to competitive one (K_{IC} = 3, K_{IU} > 10^5). K_{IC} can be determined also from Dixon plot (Figure 17) as abscissa of intercept of linear regressions. This method confirms high value of competitive inhibition constant (K_{IC} > 3).

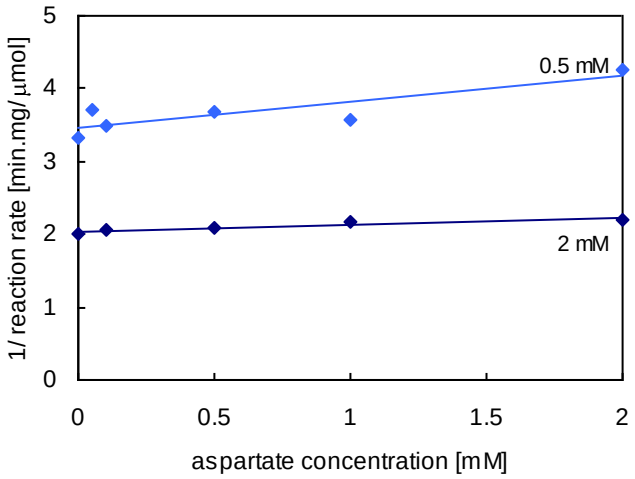

Figure 17: Dixon plot of effect of L-aspartate on PEPC reaction rate measured at pH 7.3 at 2 mM and 0.5 mM PEP (inset values). The concentrations of bicarbonate and $MgCl_2$ in the assay were 5 mM and 2 mM, respectively. All measurements were done at 25°C. The points are experimental data. The lines are linear regression of experimental data.

3.1.3.3. Effect of D-glucose-6-phosphate on PEPC activity

The activity of PEPC isolated from tobacco leaves was studied at the presence of D-glucose-6-phosphate. Figure 18 shows 20% increase of PEPC reaction rate at pH 7.3, 25°C, 2 mM PEP and 1 mM glucose-6-P. The activation was much higher at 0.5 mM PEP; 1 mM concentration of glucose-6-P caused nearly 100% increase of PEPC reaction rate. The effect of glucose-6-P on PEPC activity was much lower at pH 8.1 (result not shown). 1 mM glucose-6-P caused only 10% increase of PEPC reaction rate at 0.5 mM and 2 mM concentrations of PEP.

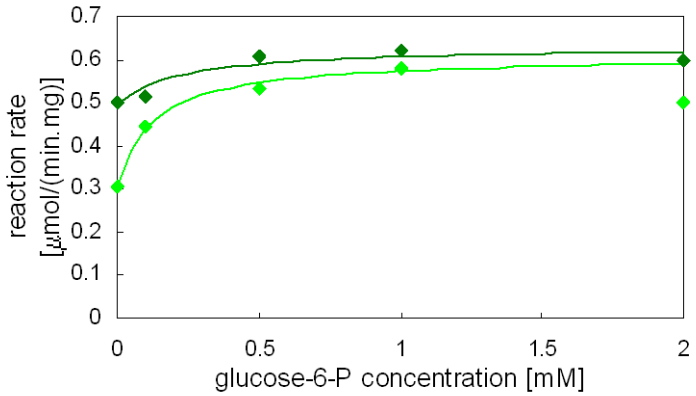

Figure 18: Effect of D-glucose-6-phosphate on PEPC reaction rate at pH 7.3 and 25°C. Dark green line describes measurement at PEP saturation (2 mM) while light green line describes measurement at 0.5 mM PEP. The points represent experimental data, the lines are the result of the best fit of experimental data to equation 3.

3.1.3.4. Effect of glycine and 3-P-glycerate on PEPC activity

The activity of PEPC was studied at the presence of glycine and 3-P-glycerate. No effect on PEPC reaction rate was monitored under any conditions used. Table 4 shows the PEPC reaction rate at pH 7.3, 25°C and 0.5 mM PEP. PEPC reaction rate remained similar at all glycine and 3-phosphogylcerate concentrations to that with no effector added.

Table 4: PEPC reaction rate at the presence of glycine and 3-phosphoglycerate measured at pH 7.3 and 25°C. Concentration of PEP in the reaction was 0.5 mM. Values of reaction rate are in μmol/(min.mg).

	concentration of effector				
effector	0 mM	0.05 mM	0.1 mM	1 mM	2 mM
glycine	0.3	0.36	0.27	0.24	0.33
3-phosphoglycerate	0.39	0.27	0.45	0.33	0.36

3.1.4. Study of PEPC phosphorylation

Phosphorylation of serine residue near N terminus of plant type PEPC plays an important role in activity regulation. *In vivo* PEPC is phosphorylated by specific PEPC kinase and dephosphorylated by a protein phosphatase type 2A.

3.1.4.1. In vitro dephosphorylation of native PEPC

PEPC was isolated from tobacco leaves and treated with alkaline phosphatase. 200 U of alkaline phosphatase was added per 4 mg of total protein. Reaction was incubated for 4 hours at 37°C. PEPC activity was measured at optimal conditions (pH 8.1, 2 mM PEP) in aliquots collected in regular intervals. Reaction with phosphatase inhibitors was used as control. Figure 19 shows the progress of PEPC activity during the dephosphorylating reaction. While no change in PEPC activity was estimated in the control reaction, dephosphorylation caused 40% decrease of PEPC activity after 4 hours. There was no difference in PEPC activity after 2-4 hours of treatment, thus the enzyme becomes probably completely dephosphorylated.

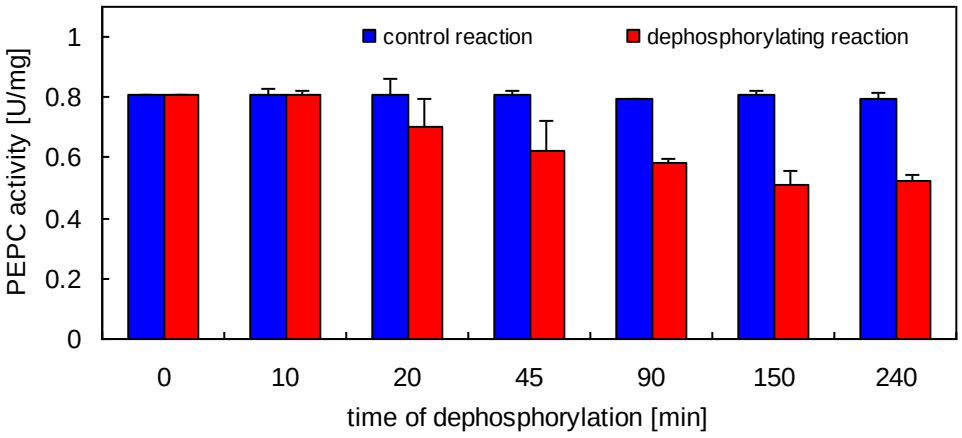

Figure 19: Effect of phosphatase on activity of tobacco PEPC. PEPC was incubated with alkaline phosphatase at 37°C for 4 hours. Red columns show decreasing PEPC activity during reaction. Blue columns show PEPC activity (measured at pH 8.1) in control reaction containing phosphatases inhibitors.

3.1.4.2. PEPC in vitro rephosphorylation and phosphorylation of native PEPC

PEPC isolated from tobacco leaves was incubated with protein kinase A at the presence of 1 mM ATP at room temperature and pH 7.3 for 3 hours. PEPC activity was measured at optimal conditions (pH 8.1, 2 mM PEP) in aliquots collected in regular intervals. Reaction without protein kinase was used as a negative control. Inhibitors of phosphatases were added to both reactions.

Figure 20 shows effect of protein kinase A on PEPC activity. Both control and protein kinase treated samples embodied similar progress; no change in PEPC activity was visible during the whole experiment.

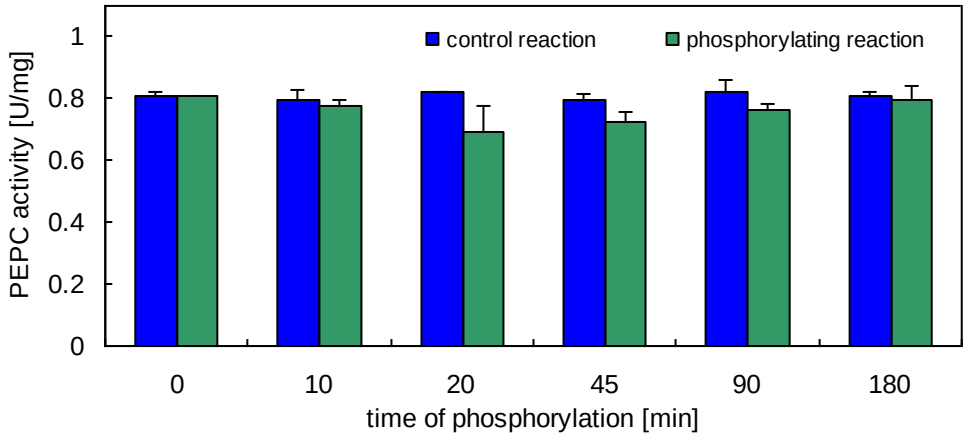

Figure 20: Effect of protein kinase A on activity of tobacco PEPC. PEPC was incubated with protein kinase A at room temperature for 3 hours (green columns). Blue columns show PEPC activity (measured at pH 8.1) of control reaction with no kinase.

In the next step, PEPC previously dephosphorylated by alkaline phosphatase was incubated with protein kinase A at presence of 1 mM ATP. The activity of PEPC did not change during the whole experiment (result not shown).

3.1.4.3. Study of substrate affinity of dephosphorylated PEPC

Kinetics of saturation of dephosphorylated tobacco leaf PEPC by PEP was studied. All measurements were done at 5 mM bicarbonate, 2 mM $MgCl_2$ and at 25^{o}C. Effect of pH on PEPC substrate affinity is shown in Figure 21. The measurements were carried out at optimal pH 8.1 and sub-optimal pH 7.3. In both cases reaction indicated classical hyperbolic character described by equation 1 (Figure 21).

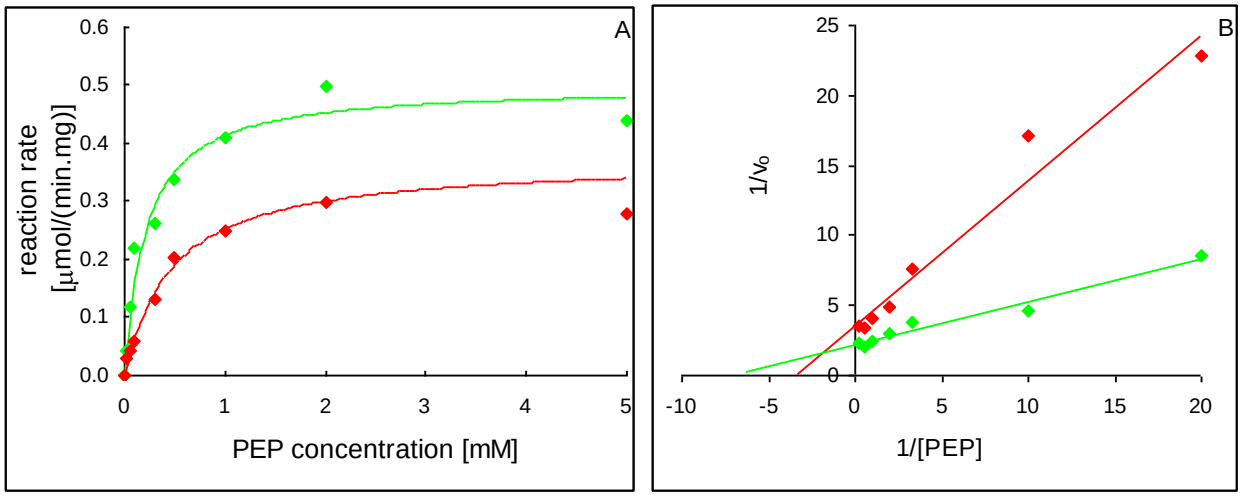

Figure 21: Standard (A) and Lineweaver-Burke (B) plot of affinity of PEPC to substrate [PEP] at optimal pH 8.1 (green data) and suboptimal pH 7.3 (red data). The points represent experimental data. The lines are the result of the best fit of the experimental data to equation 1 (A) or result of linear regression of the double-reciprocal plot (B).

Maximal reaction rate was 75% at sup-optimal pH conditions compared to that at pH 8.1. Values of V_{max} and K_m were obtained by non-linear regression of equation 1. The maximal reaction rate at pH 8.1 was 0.45 μmol/(min.mg) and 0.37 μmol/(min.mg) at pH 7.3. Dephosphorylated PEPC showed higher affinity to substrate at pH 8.1; Michaelis constant (K_m) was 0.21 mM at pH 8.1 and 0.47 mM at pH 7.3.

3.1.4.4. Effect of malate and aspartate on activity of dephosphorylated PEPC

Effect of L-malate on reaction rate of dephosphorylated tobacco leaf PEPC was studied. L-malate caused decrease of tobacco PEPC activity at both optimal and-sub optimal pH conditions; however the more severe effect was monitored at pH 7.3 (result not shown).

Figure 22 shows effect of malate on reaction rate of dephosphorylated PEPC at varied concentration of PEP. Malate has effect on both maximal reaction rate (V_{max}) and Michaelis constant (K_m). V_{max} is decreased and K_m is increased at higher malate concentration. Inhibition constants obtained by non-linear regression from equation 2 were 0.5 mM (K_{IC}, competitive inhibition constant) and 1.7 mM (K_{IU}, uncompetitive inhibition constant). This result indicates mixed type of inhibition. Dixon plot (Figure 23) and also Lineweaver-Burke plot (result not shown) display the mixed type of inhibition. K_{IC} obtained from Dixon plot was 0.6 mM, which corresponds well to the value obtained by non-linear regression.

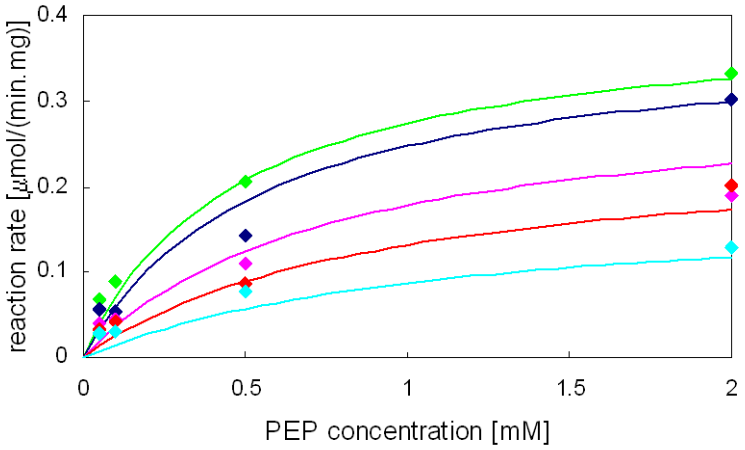

Figure 22: Effect of malate on reaction rate of dephosphorylated PEPC at varied concentration of PEP. Concentrations of malate were 0 mM, 0.1 mM, 0.5 mM 1 mM and 2 mM. The concentration of bicarbonate in the assay was 5 mM and 2 mM$MgCl_2$, the measurement were done at pH 7.3 and 25°C. The points represent experimental data. The lines are the result of the best fit of experimental data to equation 2.

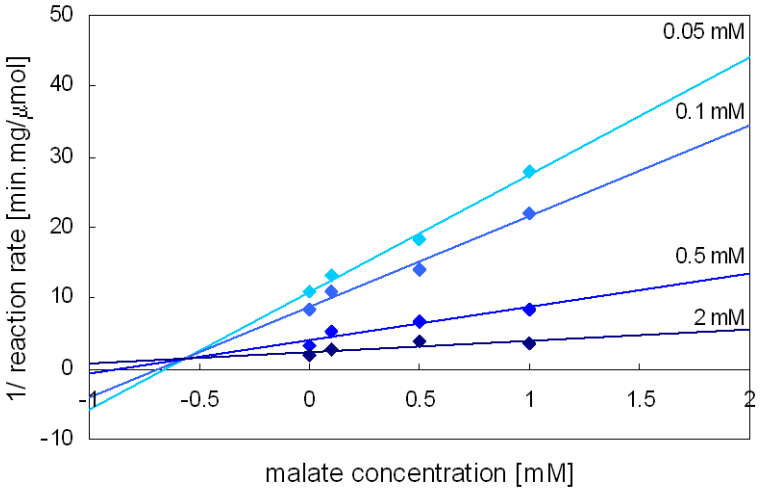

Figure 23: Effect of malate on dephosphorylated tobacco leaf PEPC reaction rate in Dixon plot at varied concentration of PEP (inset values). The concentrations of bicarbonate and $MgCl_2$ in the assay were 5 mM and 2 mM, respectively. The measurements were done at 25°C and pH 7.3. The lines are linear regression of experimental data (points).

Effect of L-aspartate on reaction rate of dephosphorylated PEPC was studied at 25°C, pH 7.3 and at two concentrations of total PEP. Very weak inhibition was observed at both PEP concentrations (Figure 24). 2 mM aspartate caused 5% decrease of PEPC reaction rate at 0.5 mM concentration of PEP. Inhibition constants calculated by non-linear regression from equation 2 indicated, that the inhibition corresponds mostly to competitive one (K_{IC} = 10, K_{IU} > 10^5). Dixon plot (Figure 24) confirms high value of competitive inhibition constant (K_{IC} > 10).

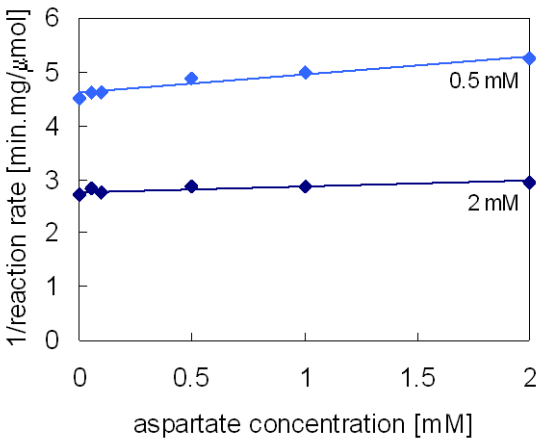

Figure 24: Dixon plot of effect of aspartate on dephosphorylated PEPC reaction rate measured at 2 mM and 0.5 mM PEP (inset values). The concentrations of bicarbonate and $MgCl_2$ in the assay were 5 mM and 2 mM, respectively. The measurements were done at 25°C and pH 7.3. The lines are linear regression of experimental data (points). The points are experimental data. The lines are linear regression of experimental data.

3.1.4.5. Effect of D-glucose-6-phosphate on activity of dephosphorylated PEPC

Effect of D-glucose-6-phosphate on reaction rate of dephosphorylated tobacco leaf PEPC was studied at 25°C, pH 7.3 and two different concentration of total PEP. Figure 25 shows 10% increase of PEPC reaction rate at 2 mM PEP caused by 1-2 mM glucose-6-P. The sensitivity of the enzyme to glucose-6-P at 0.5 mM PEP was higher; 1 mM concentration of glucose-6-P caused 40% increase of PEPC reaction rate.

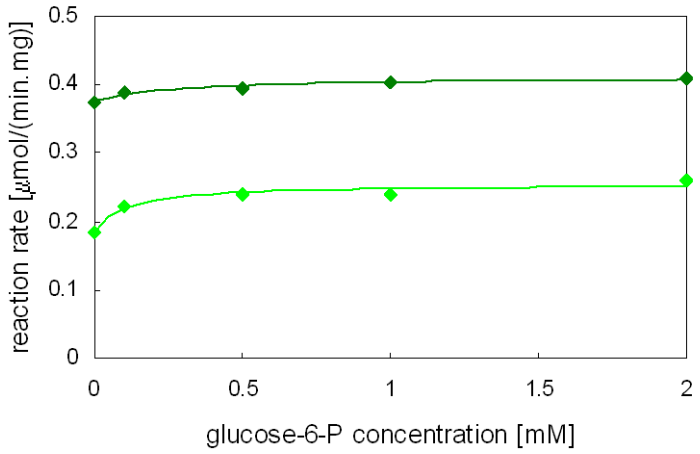

Figure 25: Effect of D-glucose-6-phosphate on reaction rate of dephosphorylated PEPC at pH 7.3 and 25°C. Dark green line describes measurement at PEP saturation (2 mM) while light green line describes measurement at 0.5 mM PEP. The points represent experimental data, the lines are the result of the best fit of experimental data to equation 3.

3.2. Preparation of PEPC antibodies

3.2.1. Isolation of PEPC from maize seeds

Phosphoenolpyruvate carboxylase was purified from maize seeds to homogeneity. The isolation procedure included ammonium sulphate fractionation, ionex chromatography on DEAE cellulose, gel chromatography on Sephadex G200 and chromatography on hydroxylapatite column. Phosphatases and proteinases inhibitors were added to all isolation buffers. The whole procedure is summarized in Table 5.

About 1 mg of protein was isolated from 100 g of maize seeds. The PEPC specific activity in final extract was 3 U/mg. The homogeneity of isolated PEPC was checked using polyacrylamide gel electrophoresis under denaturating conditions (Figure 26), which showed a single band corresponding to 105 kDa. The protein was identified also by mass spectrometry; the tryptic digestion of isolated PEPC shared very high similarity with maize root PEPC isoform.

Table 5: Isolation of PEPC from maize seeds (100g). All purification steps were carried out according to material and methods.

purification step	volume (ml)	total PEPC activity [U]	total protein [mg]	specific PEPC activity[U/mg]
crude extract	216	50.9	1015.2	0.05
$(NH_4)_2SO_4$ precipitation	8	40.0	337.6	0.12
dialysis	10	35.8	293	0.12
ionex chrom. (DEAE cellulose)	44	30.1	52.8	0.57
gel chrom. (Sephadex G-200)	10	17.1	12	1.42
hydroxyapatite chrom.	52	6.7	3.4	1.97
ionex chrom. (DEAE cellulose)	17	3.0	1.02	2.96

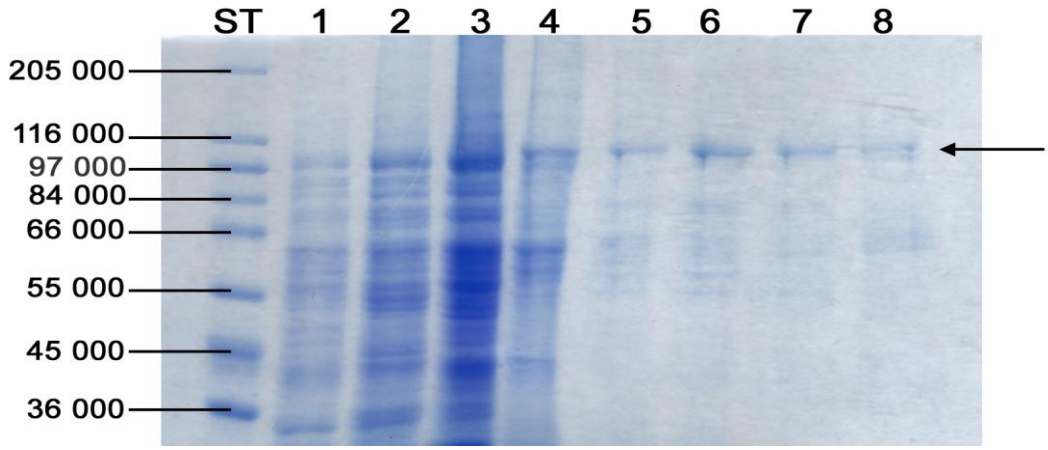

Figure 26: Electrophoretic separation (SDS) of PEPC isolated from maize seeds. 10 μg of protein was loaded in each line. 1… crude extract; 2… dialysis; 3… DEAE cellulose; 4… Sephadex G-200; 5-8… hydroxyapatite (20, 40, 50 and 60 mM phosphate buffer). Arrow indicates the band corresponding to PEPC subunit.

3.2.2. Verification of PEPC antibodies

The blood serum was collected from immunized rabbits (cca 50 ml from each rabbit) 10 days after the final antigen injection. Immunoglobulin fractions were isolated and tested by ELISA and Western Blot. The PEPC purified from tobacco leaves and maize seeds used as homological antigens were subjected to ELISA. Bound antibodies were visualized using alkaline phosphatase conjugate mouse antirabbit IgG (result not shown).

The PEPC isolated from tobacco leaves was separated by SDS PAGE and transferred to nitrocellulose membrane. 5, 10, 15 and 20 μg of protein were loaded in each line. The PEPC was detected using the rabbit serum. Bound antibodies were visualized using alkaline phosphatase conjugated mouse antirabbit IgG (Figure 27). NBT-BCIP (nitroblue tetrazolium, 5-bromo-4-chloro-3-indolyl phosphate) was used as substrate for alkaline phosphatase.

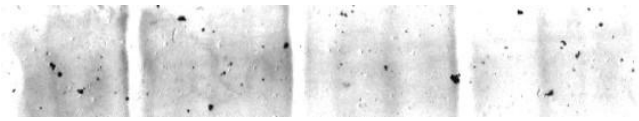

Figure 27: Western blot analysis of PEPC protein. 20 μg, 15 μg, 10 μg and 5 μg of total proteins of tobacco crude extract were separated by electrophoresis and detected immunochemically using polyclonal rabbit antiserum raised against maize seed PEPC. Bound antibodies were visualized using alkaline phosphatase conjugated mouse antirabbit IgG.

3.3. Regulation of tobacco PEPC during stress

Several independent experiments were done to study PEPC activity, its regulation and activity of enzymes functionally related to PEPC during biotic stress in tobacco plants. The first experiment shows changes in PEPC, NADP-ME and PPDK activities in tobacco leaves during infection by PVY^{NTN} and PVA. In next experiments we followed the induced PEPC activity during PVY^{NTN} infection and focused also on detection of the source of the increased PEPC activity. We studied changes in tobacco *PEPC* gene transcription and PEPC protein amount together with changes in phosphorylation level of PEPC in leaves at maximal symptoms of PVY^{NTN} infection.

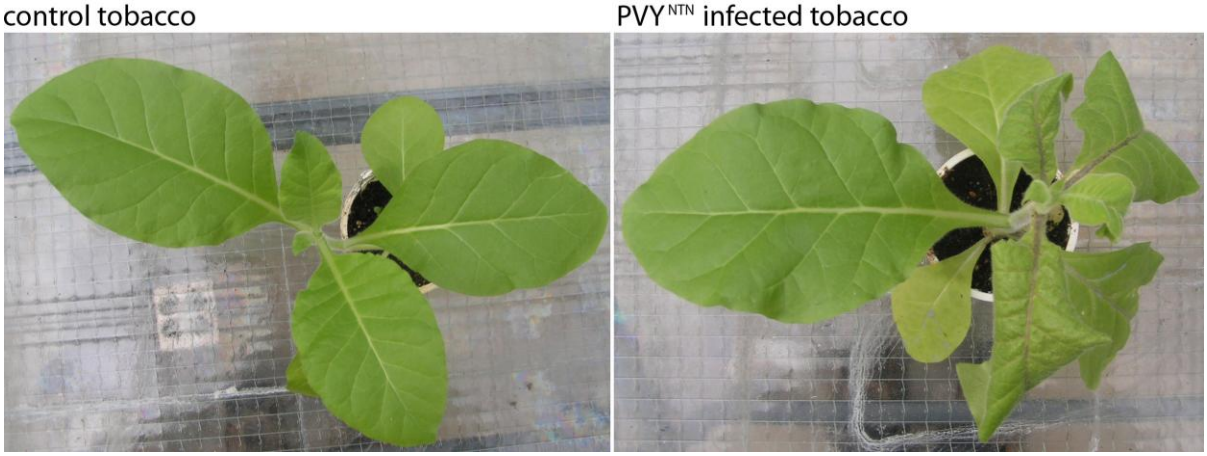

3.3.1. Detection of virus presence in infected tobacco plants

The time course of viral infection of tobacco plants was monitored by immunochemical semi-quantitative method (ELISA) and by relative quantification of viral RNA in infected tobacco leaves. Polyclonal or monoclonal antibodies were used to detect presence of PVY^{NTN} and PVA virus in the first experiment. The maximal content of both viruses were found 6 days after inoculation and was more-or-less constant further on (Figure 28). The severity of symptoms and accumulation of viruses was much stronger in PVY^{NTN} infected plants.

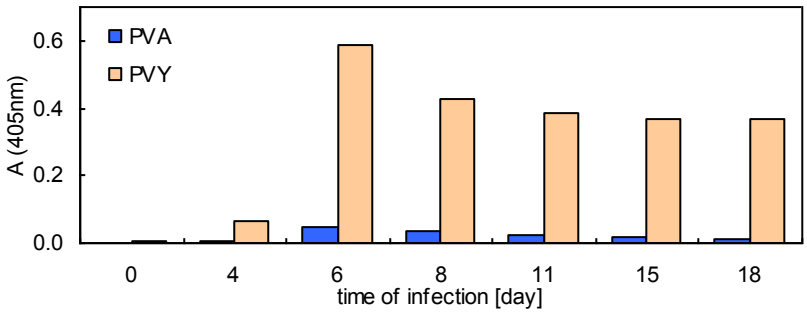

Figure 28: Time course of PVY^{NTN} and PVA infection in tobacco plants. The relative content of virus was determined by DAS-ELISA with *p*-nitrophenylphosphate as enzyme substrate. Absorbance at 405 nm corresponds to virus content.

Presence of viral RNA was monitored by real-time PCR method using specific PVY^{NTN} primers and *actin9* was chosen as a reference gene. The results are shown as ratio of amount of PVY^{NTN} RNA to actin9 transcript. In the second experiment, the presence of PVY^{NTN} RNA was found 10 days after inoculation and the amount was 100-600 times higher than actin9 mRNA (Figure 29). No PVY^{NTN} RNA was found in control healthy tobacco leaves.

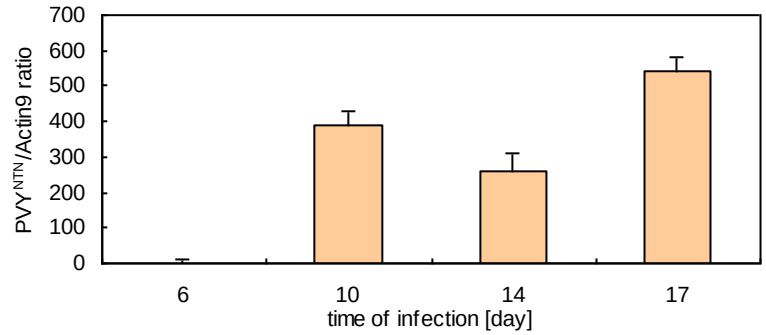

Figure 29: Amount of PVY^{NTN} RNA in infected tobacco leaves during the infection measured by real-time PCR. Results are shown as ratio of PVY^{NTN} RNA to actin9 transcript.

In next experiment, presence of PVY^{NTN} was proved by both ELISA and real-time PCR method. The PVY^{NTN} / actin9 ratio was approximately 1,000 in tobacco leaves 17 days after PVY^{NTN} inoculation (data not shown).

3.3.2. Activity of PEPC, NADP-ME and PPDK during potyviral infection

The activities of PEPC and its biochemically related enzymes (PPDK and NADP-ME) were studied in tobacco leaves during PVY^{NTN} and PVA infection.

The time courses of PEPC, NADP-ME and PPDK activities showed significant differences in PVY^{NTN} and PVA infected tobacco plants (Figure 30 and Figure 31). PVY^{NTN} infection caused an increase in activity of all three enzymes; the most sensitive was NADP-ME with 6-fold higher activity compared to healthy control. The activities of both PEPC and PPDK were 2-3-fold elevated.

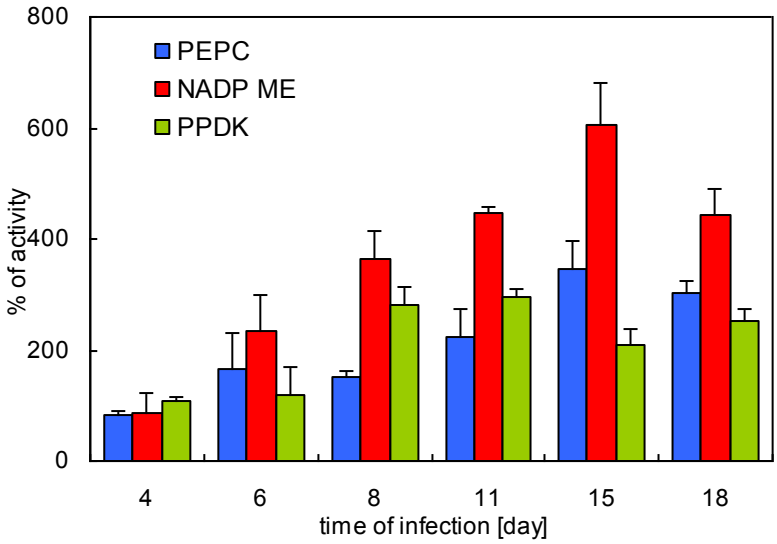

Figure 30: Activities of PEPC, NADP-ME, and PPDK in tobacco leaves 4–18 days after inoculation by PVY^{NTN} calculated per fresh weight. The activity of each sample is calculated as percentage of the non-infected control. Graph shows means ± S.E. in each repetition of the experiment, the activity was measured in triplicate.

In contrast to PVY^{NTN}, PVA infection affected enzymes activities insignificantly. Although a moderate increase in activities was observed, the changes were not statistically significant (Figure 31).

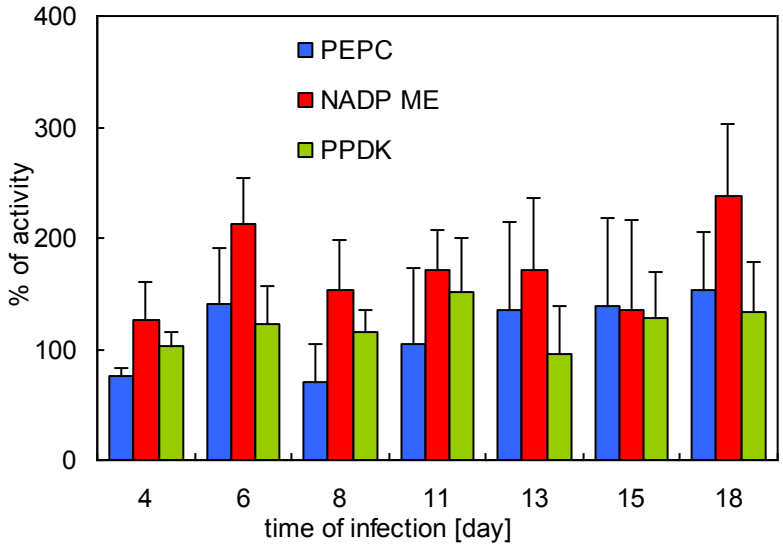

Figure 31: Activities of PEPC, NADP-ME, and PPDK in tobacco leaves 4–18 days after inoculation by PVA calculated per fresh weight. The activity of each sample is calculated as percentage of the non-infected control. Graph shows means ± S.E. in each repetition of the experiment, the activity was measured in triplicate.

In another set of experiments, samples were collected 17 days after PVY^{NTN} inoculation at maximal symptoms of infection. Increased PEPC activity was confirmed in leaves of infected tobacco plants and the activity was 3.5-fold higher compared to healthy control (Figure 32).

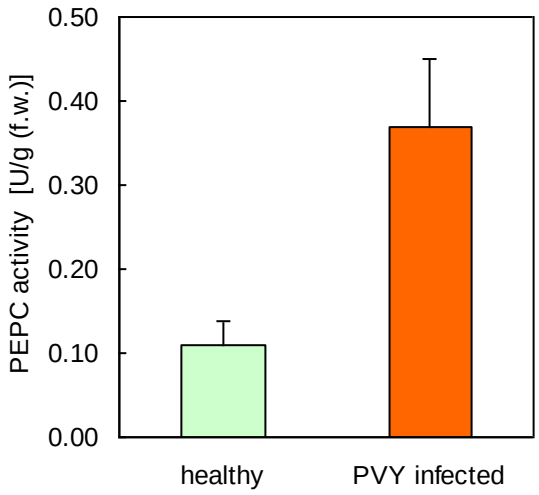

Figure 32: PEPC activity in tobacco leaves samples collected 17 days after PVY^{NTN} inoculation. Activity is calculated per fresh weight. Means +/- S.E. were calculated from 3 different set of plants and minimum 3 samples from each experiment were measured.

3.3.3. Detection of PEPC activity in gel of native electrophoresis

Native electrophoresis was performed to study PEPC isoforms in crude extracts from tobacco leaves. Approximately 200 μg protein was subjected to PAGE (6% gel) under non-denaturating conditions. The PEPC activity was detected in gel as dark bands on fluorescent background (see Material and methods). Single band was visible after the staining for PEPC activity (Figure 33). Band corresponding to sample from PVY^{NTN} infected leaves showed higher intensity compared to healthy control.

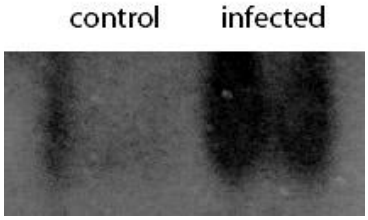

Figure 33: Native electrophoresis gel (6%) stained for PEPC activity. Approximately 200 μg protein of crude samples from healthy and PVY^{NTN} infected tobacco leaves were separated and staining for PEPC activity was performed according to Rivoal et al. (2002).

3.3.4. Changes in PEPC protein amount during PVY^{NTN} infection

The amount of PEPC protein in tobacco leaves was determined by Western blot analysis using anti-PEPC antibodies. 10 μg of protein from crude leaf extract were separated by SDS electrophoresis. Proteins were transferred to nitrocellulose membrane and the immunochemical detection of PEPC was carried out using polyclonal rabbit antiserum raised against maize seed PEPC. Bound antibodies were visualized using alkaline phosphatase conjugated mouse antirabbit IgG. Figure 34 shows no significant change in PEPC protein amount in PVY^{NTN} infected tobacco leaves compared to healthy control. However, the same infected tobacco samples provided more than 3 times higher PEPC activity (Figure 32).

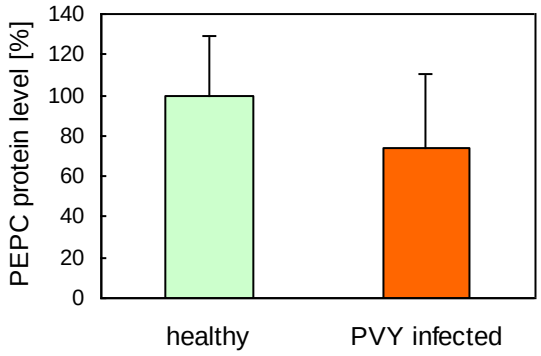

Figure 34: Amount of immunologically detected PEPC protein in control and infected tobacco leaves collected 17 days after PVY^{NTN} inoculation. Graph shows means +/- S.E. collected from 3 different sets of plants. 100% is equal to amount of PEPC protein in control samples.

3.3.5. Changes in PEPC transcription during PVY^{NTN} infection

Amount of PEPC mRNA was measured in tobacco leaves by real-time RT PCR. Specific primers for PEPC were designed by Tib Molbiol according to *N. tabacum* PEPC cDNA sequence (accession nr. X59016). *Actin9* was used as reference gene. Ratio of PEPC/actin9 transcripts was calculated from equation 4.

PCR efficiency (E) was calculated from equation 5, *slope* value was obtained from calibration curve of 4 different template concentrations. Efficiencies of PCR with PEPC and actin9 primers were 1.7 and 1.9, respectively.

Figure 35 shows increase of PEPC transcription 10-17 days after virus inoculation in infected tobacco leaves. The maximal PEPC transcription was observed 10 days after virus

inoculation and was twice higher as compared with control healthy plants. These results were measured in the second experimental set of plants.

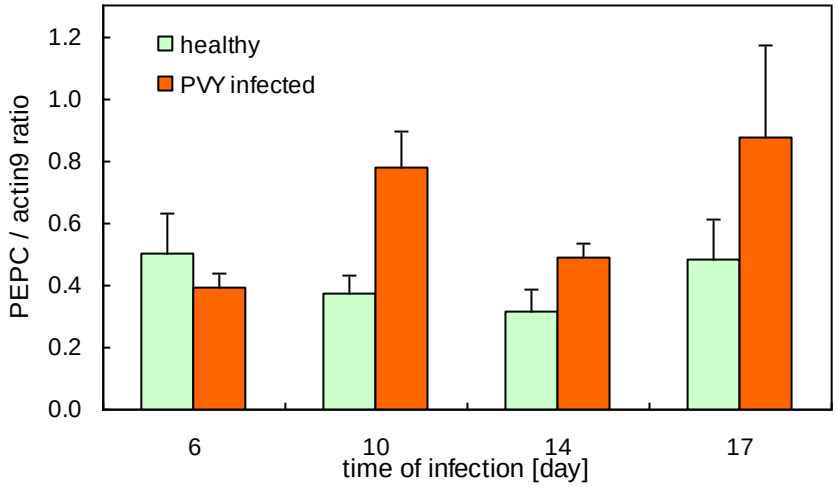

Figure 35: Amount of PEPC mRNA in tobacco leaves during PVY^{NTN} infection. Result corresponds to ratio of PEPC to actin9 mRNA. Means +/- S.E. were calculated from 3 different measurements.

Contrary, results from the third experiment showed no significant change in PEPC transcription in infected tobacco leaves 17 days after virus inoculation (Figure 36). This result corresponded well to no change in PEPC protein amount (Figure 34), however the same infected tobacco samples provided more than 3 times higher PEPC activity in samples collected from infected tobacco plants (Figure 32).

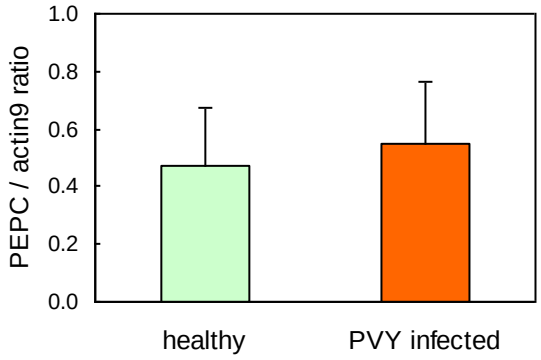

Figure 36: Amount of PEPC mRNA in infected tobacco leaves collected 17 days after PVY^{NTN} inoculation measured by real-time PCR method. Result corresponds to ratio of PEPC to actin9 mRNA. Means +/- S.E. were calculated from 3 different set of plants and minimally 3 samples from each experiment were measured.

3.3.6. Changes in PEPC phosphorylation during PVY^{NTN} infection

As there were no changes in PEPC expression or changes were not significant enough to cover 300% (and higher) increase in activity, we studied the post-translational modification of PEPC protein. Phosphorylation of serine residue near N terminus of plant type PEPC plays important role in its activity regulation. The PEPC, from crude extracts of both control and infected leaves collected 17th day after virus inoculation, was treated by alkaline phosphatase and decreasing PEPC activity was monitored. After 4 hours of treatment the PEPC activity reached the minimal value and remained stabile in both control and infected samples (Figure 37). Thus the enzyme probably becomes completely dephosphorylated.

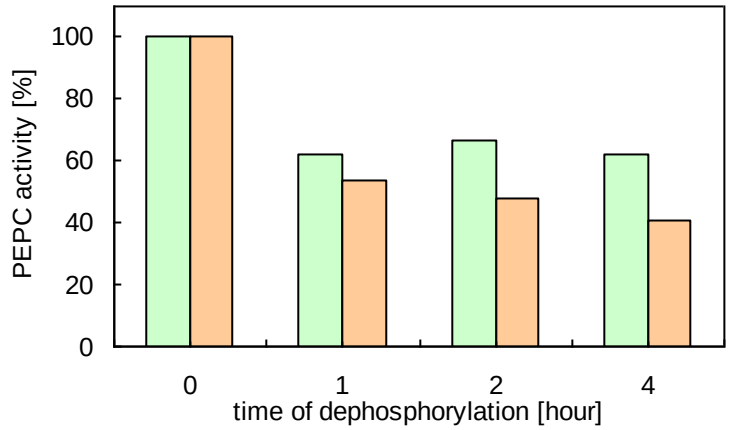

Figure 37: PEPC from tobacco leaves was dephosphorylated by alkaline phosphatase. Time course of PEPC activity of control (green line) and PVY^{NTN} infected (orange line) plants during dephosphorylating reaction. Activities are in percents, 100% is activity corresponds to native PEPC and is equal to 0.17 U/g [f.w.] and 0.44 U/g [f.w.] for healthy and PVY^{NTN} infected, respectively.

3.3.6.1. Different response of PEPC activity to dephosphorylation

Figure 38 shows different progress in total dephosphorylation in control and infected tobacco plants. PEPC activity in the dephosphorylated control sample was 60% when compared to native form. The difference was more evident in PVY^{NTN} infected samples where the value of dephosphorylated PEPC activity was 40% compared to native form (Figure 38). The higher sensitivity to phosphatase treatment indicates probably the higher phosphorylation level of PEPC in native form.

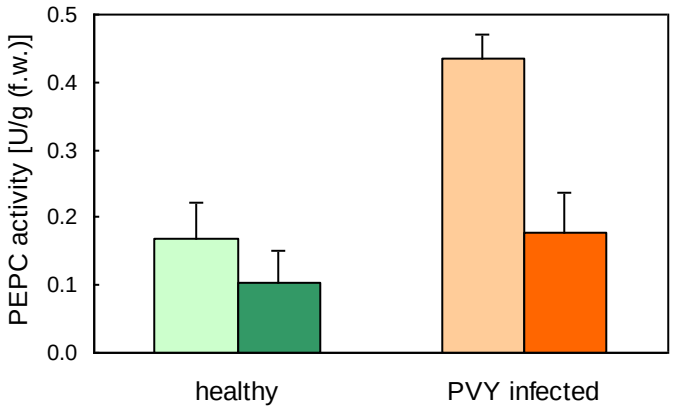

Figure 38: PEPC from tobacco leaves was dephosphorylated by alkaline phosphatase. Difference between native (light green and orange) and dephosphorylated (dark green and orange) PEPC in control and PVY^{NTN} infected leaves.

3.3.6.2. Measurement of free phosphate

Concentration of free phosphate was measured in crude extracts using Phosphate estimation assay kit. Phosphatase treated extracts (dark columns) exhibited higher phosphate concentration compared to non-treated extracts (Figure 39). Concentration of phosphate in dephosphorylated extracts was 145% and 185% in healthy and PVY^{NTN} samples, respectively, compared to non-treated extracts. Concentration of free phosphate was similar in samples from both control and PVY^{NTN} tobacco leaves.

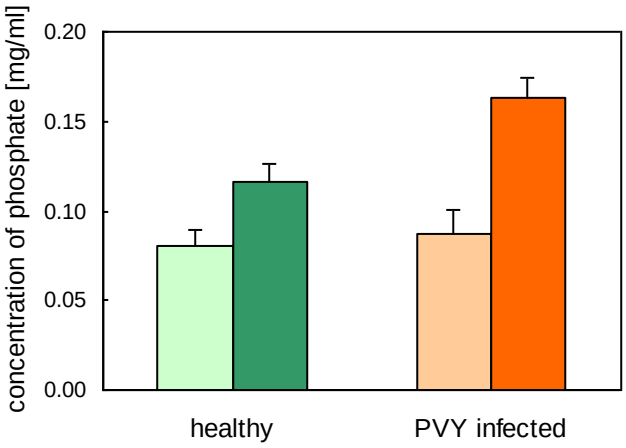

Figure 39: Concentration of free phosphate in native (light green and orange) and phosphatase treated (dark green and orange) extracts from healthy and PVY^{NTN} tobacco leaves.

3.3.6.3. Immunochemical detection of phosphoproteins

Western blot analysis using commercial antibodies against phosphoamino acids was performed for detection of phosphoproteins. 150 μg of proteins were separated by SDS electrophoresis and transferred to nitrocellulose membrane. Immunochemical detection of phosphoproteins was carried out using anti-phosphoamino acids (specific for phosphoserine, phosphothreonine, and phosphotyrosine; rabbit as a source organism). Bound antibodies were visualized by alkaline phosphatase conjugated mouse anti-rabbit IgG. CDP-Star (derivate of phenyl phosphate) was used as substrate for alkaline phosphatase.

Figure 40 shows higher intensity of band corresponding to PEPC in PVY^{NTN} infected sample in comparison with healthy control.

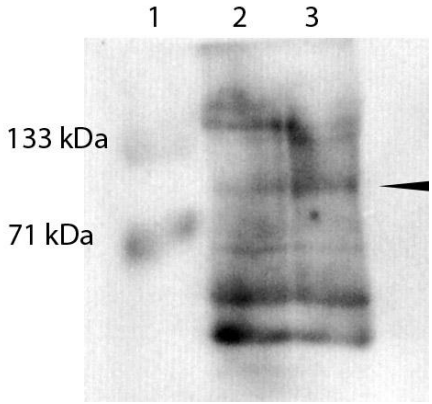

Figure 40: Detection of phosphoproteins by Western blot analysis using anti-phosphoamino acids antibodies. Arrow indicates PEPC band. 1 ... marker; 2 ... healthy sample; 3 ... PVY^{NTN} infected sample (17th day after virus inoculation).

3.3.7. Changes in metabolite concentration during PVY^{NTN} infection

The PEPC activity is in plants regulated by various cell metabolites. The most important regulatory mechanisms are the inhibitory effect of malate and the activating effect of glucose-6-phosphate. Concentrations of malate, glucose and glucose-6-phosphate were measured in tobacco leaves. Malate and glucose-6-P concentrations were 2- and 4-fold, respectively, higher in PVY^{NTN} infected tobacco leaves; concentration of glucose was similar in infected and healthy plants (Figure 41).

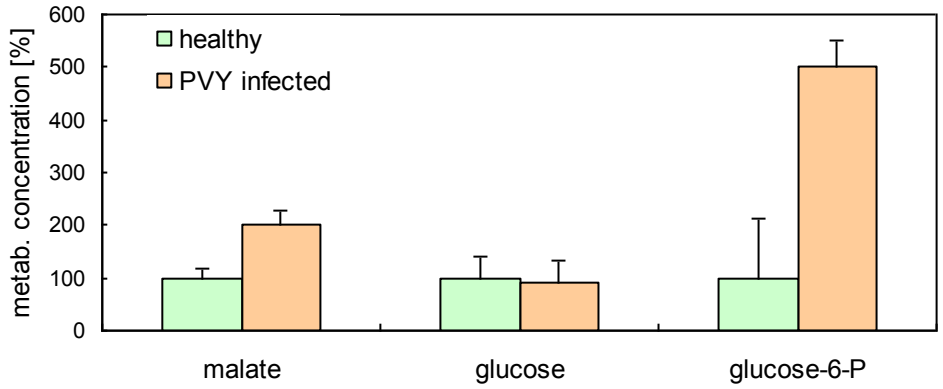

Figure 41: Concentrations of malate, glucose and glucose-6-P in tobacco leaves of healthy plants and those infected by PVY^{NTN}. Relative concentrations (expressed as % of healthy controls) are presented.

3.4. Effect of cytokinins on PEPC activity in tobacco leaves during stress

Transgenic plants over-expressing bacterial gene coding for isopentenyl transferase (*ipt*), a key enzyme of cytokinin biosynthesis, were used for study of the effect of cytokinins on tobacco response to the biotic stress. The *ipt* transgenic tobacco plants had increased concentration of endogenous cytokinins. Four types of plants were used for our experiments: control tobacco (*N. tabacum L.*, cv. Petit Havana SR1) from seeds (SR1) or grafted onto the control rootstock (SRG); *ipt* transgenic shoots grafted on control rootstock (G) and autogamic progeny of the transgenic grafts, which are able to form a small root system (SE).

3.4.1. Rubisco activity in *ipt* transgenic tobacco plants infected by PVY^{NTN}

Rubisco activity was studied after infection with PVY^{NTN} in control rooted plants (SR1), control grafts (SRG), *ipt* transgenic tobacco plants (SE) and *ipt* transgenic grafts (G). Leaf samples were kindly provided by Dr. H. Synková (IEB CAS). Healthy SR1 plants exhibited the highest Rubisco activity compared to other plant types (Figure 42). SRG and SE plants exhibited more than 70% reduction in Rubisco activity as compared with SR1 plants. Even lower activity was detected in samples from G. PVY infection caused the most significant decline in SR1 (ca. 20% of healthy control), while 0 or only 10 - 15% activity reduction in G and SRG + SE plants, respectively, was observed after infection.

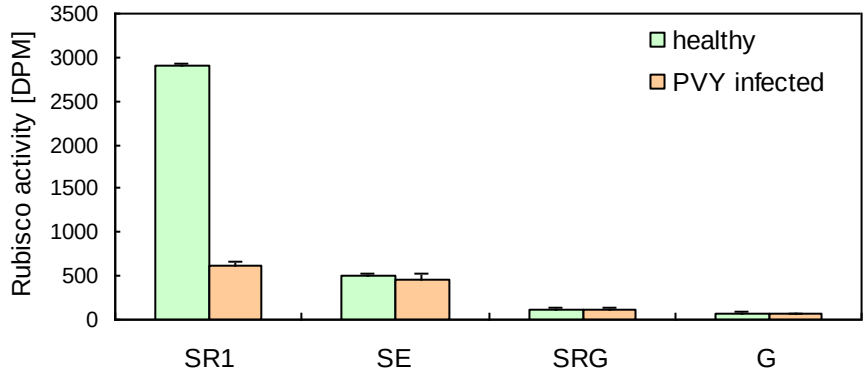

Figure 42: Rubisco activity in healthy (green columns) and PVY^{NTN} infected (orange columns) control, rooted tobacco (SR1), *ipt* transgenic rooted plants (SE), control grafts (SRG) and *ipt* transgenic grafts (G). Leaf samples were collected 15-18 days after virus inoculation. The values are means +/- S.E.

3.4.2. Activity of PEPC, NADP-ME and PPDK in ipt transgenic tobacco plants infected by PVY^{NTN}

Effect of PVY^{NTN} infection on PEPC, NADP-ME and PPDK activities were studied in control (SR1) and *ipt* transgenic rooted tobacco plants (SE). Leaf samples collected 4-17 days after inoculation were kindly provided by Dr. H. Synková (IEB CAS).

The activities of all three enzymes started increasing in control SR1 plants 7 days (PEPC) and 10 days (NADP-ME and PPDK), respectively, after the virus inoculation (Figure 43, Figure 44 and Figure 45). The maximal increase of activity was observed 13 days after virus inoculation and the activity was 3 times (PEPC) and 5 times (NADP-ME and PPDK), respectively, higher compared to control healthy plants. The progress of enzymes activities was similar to that in previous experiment (Figure 30). SE transgenic tobacco plants embodied delay in elevation of enzyme activities. In these plants activity of PEPC started increasing 13 days after virus inoculation and the maximum reached value 2.3 times higher than healthy controls. Activities of NADP-ME and PPDK were both increased 17 days after inoculation and were only 2.5-fold higher as compared with healthy controls (Figure 43, Figure 44 and Figure 45).

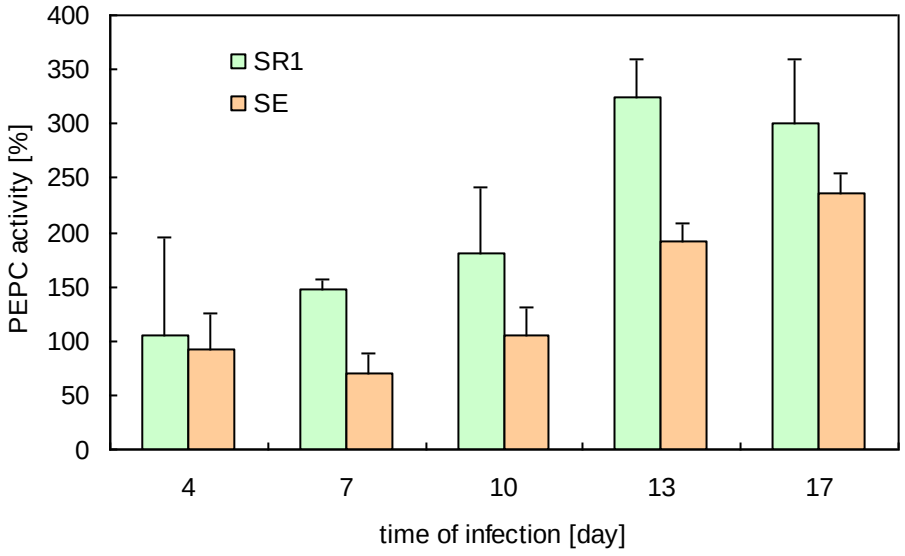

Figure 43: PEPC activity in control (SR1) and *ipt* transgenic rooted tobacco plants (SE) during PVY^{NTN} infection. Relative values (% of healthy control) are shown.

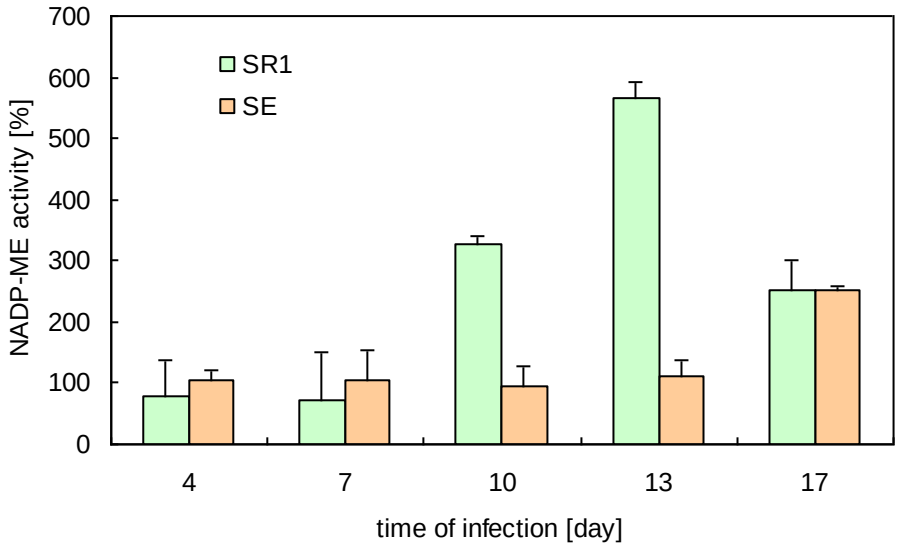

Figure 44: NADP-ME activity in control (SR1) and *ipt* transgenic rooted tobacco plants (SE) during PVY^{NTN} infection. Relative values (% of healthy control) are shown.

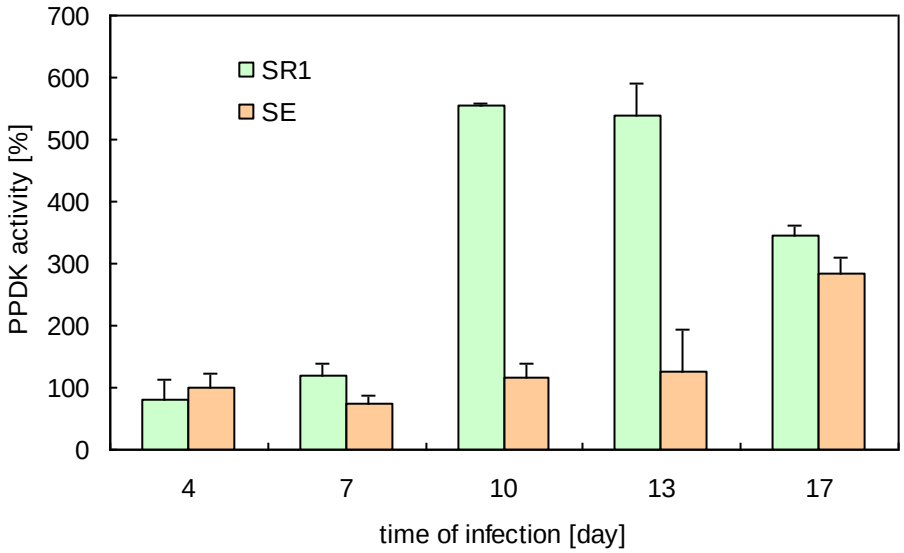

Figure 45: PPDK activity in control (SR1) and *ipt* transgenic rooted tobacco plants (SE) during PVY^{NTN} infection. Relative values (% of healthy control) are shown.

4. Discussion

Plants frequently encounter stresses, external conditions that adversely affect growth, development, or productivity. Stresses can be biotic, imposed by other organisms, or abiotic, arising from an excess or deficit in the physical or chemical environment. Among the environmental conditions that cause damage is water-logging, drought, high or low temperatures, excessive soil salinity, inadequate mineral nutrients in the soil, and too much or too little light. Phytotoxic compounds such as ozone can also damage plant tissues. Plants must continuously defend themselves against attack from bacteria, viruses, fungi, invertebrates, and even other plants. Because of their immobility, which precludes escape, plants evolved various defense mechanisms during their evolution. These can either prevent invasion of specific pathogen or they are of general character, e.g. strong cell walls and cuticula, which make the whole plant more difficult to penetrate for most organisms (Hammond-Kosack and Jones, 2000).

The level of adverse conditions should be specified in stress studies. In case of abiotic stress we can measure concentration of chemical compounds, light intensity or duration of certain treatment, e.g. drought. However this is only approximation of the real status, as plants are *in vivo* exposed to many factors simultaneously and thus the situation becomes more complex.

Study of biotic stress is more difficult. Plants are usually resistant to most pathogens due to their thick cell walls, periphery cuticula layer, secondary metabolites with various anti-pathogen functions and many others. Even pathogens, which are able to overcome plant defense system, cause the disease with variable severity, depending on factors like age of the plant, environmental conditions, presence of other pathogens etc. ELISA is classic method to detect presence of virus in plant (Clark and Adams, 1977; Čeřovská, 1998). Antibodies raised against certain viral protein (usually coat protein) bind to the antigen and can be used for semi-quantitative measurement of the amount of virus protein in plant material. The drawback of this method is the lower specifity of polyclonal antibodies and complicated and expensive process of preparation of high quality antigen. Furthermore, ELISA allows detection of the presence of certain viral protein, but virus can spread through the host plant in a low concentration. The detection of viral nucleic acid by polymerase chain reaction and mainly by the quantitative RT PCR seems to be more sensitive method for measurement of severity of virus invasion (Canning et al., 1996).

Two types of viruses from the same genus, which differ in the severity of their symptoms under the same conditions, were used in present work. *Nicotiana tabacum* L. cv. Petit Havana was chosen as host organism. Both viruses are able to infect tobacco systemically, which means that they can expand in the plant from the site of inoculation to the whole organism. Tobacco plants were inoculated at age of 3 - 4 weeks. Presence of virus was monitored by TAS ELISA. Figure 28 shows typical progress of PVA and PVY^{NTN} infection. Samples from both PVA and PVY^{NTN} infected plants gave positive reaction with antiviral antibodies, however they differed in intensity of signal measured as absorbance at 405 nm. PVY^{NTN} infection, which causes much more severe symptoms than PVA infection, gave ten times higher absorbance at 405 nm. Thus, PVY^{NTN} with its massive accumulation in tobacco cells seemed to be a better candidate for its stronger response than PVA under conditions of our experiment.

Figure 29 shows amount of PVY^{NTN} RNA in tobacco leaves 6, 10, 14 and 17 days after inoculation. The results have been obtained by reverse transcription followed by quantitative RT PCR, the expression values were related to expression of standard gene *Actin9*, which is not induced by viral infection (Rizhsky et al., 2002). PVY^{NTN} RNA was detected only in inoculated tobacco leaves at very high level. The ratio PVY^{NTN}/Actin9 was 200 - 500 in leaf samples collected 10 - 17 days after the inoculation.

Figure 28 and Figure 29 cannot be directly compared, since they were obtained by different methods and samples originated from different experiments. Maximal viral content was observed 6^{th} day after the inoculation at the first experiment. The presence of virus at the second experiment became distinguishable in sample collected 10 days after inoculation.
Direct impact on plant specific defence mechanisms is usually studied during biotic stress. In case of viral infection, gene silencing and hyper-sensitive reaction manifested as oxidative burst followed by activation of ROS scavenging system are main defence mechanisms (Doke, 1983; Waterhouse et al., 2001; Mahalingam and Fedoroff, 2003).

Studies of the effect of viral infection on plant primary metabolism are less common. Reduced photosynthesis and increased susceptibility to photoinhibition caused by plant viruses was observed by Rahutai et al. (2000). Balachandran at al. (1994) reported decrease of Rubisco activity in leaves infected by tobacco mosaic virus. Our results also showed that PVY^{NTN} infection affected Rubisco activity (Figure 42)(Synková et al., 2006). In tobacco mosaic virus infected plants, viral coat protein was essentially bound to photosystem 2 complex and was considered responsible for decreased photosystem 2 electron transport

(Banerjee et al, 1995). Similar result was reported by our group; net photosynthetic rate was affected by PVY^{NTN} and PVA infection, the more severely in case of PVY^{NTN} infection. We proposed that the decline in net photosynthetic rate was caused by stomata closure and also by inhibition of photosystem 2 function (Ryšlavá et al., 2003).

Beside influence on photosynthetic apparatus we also studied effect of potyviral infection on activities of anaplerotic enzymes, namely phosphoenolpyruvate carboxylase (PEPC), NADP dependent malic enzyme (NADP-ME) and pyruvate, phosphate dikinase (PPDK). Activities of all studied enzymes increased during PVY^{NTN} infection; activities of the PEPC and PPDK were 2 and 2.5, respectively, higher compared to healthy controls, while activity of NADP-ME was even 4 times higher (Figure 30). Increase of PEPC activity during PVY^{NTN} infection was proved in later experiments (Figure 32 and Figure 43). Effect of PVA infection on enzyme activities was not as profound as PVY^{NTN} infection (Figure 31). Only activity of NADP-ME was significantly increased (2-fold compared to healthy control). We could see that PVA, as a virus exhibiting lower accumulation in infected tobacco plants (Figure 28), caused lower response of studied anaplerotic enzymes.

This is, according to our knowledge, the first report on the effect of biotic stress on activities of presented enzymes. There have been only a few studies describing effect of abiotic stresses on the PEPC activity. Several groups studied water stress (drought, high concentration of salts) and its effect on PEPC activity. Water stress induced PEPC activity in pea leaves and wheat seedlings (Fedina and Popova, 1996; Thind and Malik, 1988). Asai et al. (2000) reported increase of the PEPC activity in *Vicia faba* at high concentrations of mannitol. Water deficit and low-oxygen stress induced activity of the PEPC together with pyruvate, phosphate dikinase and malate dehydrogenase in roots of rice (Moons et al., 1998). Detailed study of wheat at high concentration of salts was performed by Gonzales et al. (2003) and Sanchez et al. (2003). They found increased activity of PEPC in roots, caused by higher expression of one of the PEPC gene. PEPC protein level increased in *Mesembryanthemum crystallinum* suspension culture at high concentration of NaCl (Thomas et al. 1992). The expression of CAM-specific PEPC gene was found to be induced by salt stress, which promoted the C_3 to CAM switch (Cushman and Bonhert, 1999).

Nutrition stress has also been reported to affect PEPC activity. Phosphorus and iron deficiency induced PEPC activity in plant roots (De Nisi and Zocchi, 2000; Johnson et al. 1996). Higher expression of the enzyme mRNA was found in both studies. Different kinetic parameters of PEPC were monitored in cucumber roots under iron deficient compared to

control roots. This effect was caused either by expression of different PEPC isoforms or by change in PEPC phosphorylation state (De Nisi and Zocchi, 2000).

Higher PEPC activity was reported in needles of *Pinus halepensis* and *Picea abies* exposed to ozone (Sehmer et al., 1998; Fontaine et al., 2003). Apart increased expression of the enzyme was measured by Fontaine et al. (2003), also shift in malate sensitivity was observed, which indicated different post-translational regulation of PEPC by phosphorylation.

Plant cell can induce activity of enzymes in several ways. The most common is elevation of the expression of the corresponding gene. In case of PEPC, its activity can be also regulated at post-translational level, namely by phosphorylation of the serine residue on the N-terminus of PEPC protein. According to published works it is apparent that the most common mechanism of the increase of PEPC activity is the synthesis *de-novo*. We followed this idea and focused on the study of PEPC transcription profile in tobacco during infection by PVY^{NTN}. PEPC primers for real-time PCR were designed from the only one known tobacco PEPC sequence. After reverse transcription followed by quantitative real-time PCR, we measured the amount of PEPC mRNA compared to mRNA of *Actin9*. Expression of *Actin9* gene was found not to be affected by virus infection (Rihzsky et al., 2002). Figure 35 and Figure 36 show only minor increase (1.5-fold) or no increase at all of *PEPC* transcription in tobacco leaves during the PVY^{NTN} infection. The result of immunochemical detection of PEPC (Figure 34) showed no change in PEPC protein level.

Since our results did not support the hypothesis that synthesis *de-novo* would be a source of higher PEPC activity in leaves of infected tobacco plants, we examined the possibility of its regulation on post-translational level. As stated above, plant PEPC can be phosphorylated on serine residue near N-terminus of the protein. We examined whether this phosphorylation could cause the difference in specific PEPC activity in control and infected tobacco leaves. Possibility of this type of regulation in plants has been reported by research of Fontaine et al. (2003) and Duff and Chollet (1995). Besides, PEPC activity can be regulated by certain cell metabolites acting as activators or inhibitors. Detailed studies of PEPC kinetics have been performed mostly on photosynthetic C_4 or CAM isoforms. The understanding of C_3 one has been still at lower level. Therefore, we purified PEPC from leaves of tobacco (*Nicotiana tabacum* L. cv. Petit Havana), typical C_3 plant and determined kinetic parameters.

PEPC was purified from tobacco leaves to the final specific activity 0.8 U/mg. This low value corresponds to other reports on PEPC isolated from C_3 plant (e.g. 0.137 U/mg from *Cicer arietinum*, Singhal and Singh, 1986). Higher activity can be found in photosynthetic organs of C_4 plants (21 U/mg from *Zea mays*, Ogawa et al., 1997), or in seeds or roots of C_3 plants (24.2 U/mg from *Ricinus communis*, Tripodi et al. 2005).

We obtained dephosphorylated form of PEPC by treatment of native isolated enzyme with alkaline phosphatase. PEPC activity was dropping during the dephosphorylation (Figure 19) and after 3 hours of reaction it reached its minimum. Inhibitors of plant proteases were present in reaction, thus the degradation of proteins was not the reason for the drop of PEPC activity. We presume that PEPC is completely dephosphorylated after 4 hours of phosphatase treatment. Control reaction at presence of phosphatase inhibitors showed no change in PEPC activity during whole experiment.

Activity of the dephosphorylated PEPC was 60% compared to the native one. Similar results have been shown in case of the light and dark (phosphorylated and dephosphorylated) forms of the enzyme isolated from wheat and castor oil seeds (Tripodi et al., 2005; Duff and Chollet, 1995).

We tried to phosphorylate PEPC by treatment with protein kinase. Native PEPC isolated from tobacco leaves was incubated with protein kinase A for 3 hours at 25^{o}C. Activity of PEPC did not change during the whole experiment. The same result was obtained when previously dephosphorylated PEPC was used as a substrate of protein kinase A at the presence of phosphatase inhibitors. We used conditions for the kinase reaction reported for successful phosphorylation of PEPCs isolated from maize seeds (Černý, 2007). We suppose that the tobacco leaf PEPC is not substrate for protein kinase A used in the experiment.

We determined several kinetic parameters of native and dephosphorylated tobacco PEPC. Affinity of the native and dephosphorylated PEPC to substrate PEP was measured at optimal pH 8.1 and sub-optimal pH 7.3. Tobacco leaf PEPC showed typical hyperbolic character described by Michaelis-Menten equation (equation 1) with values of K_m 0.25 mM and 0.45 mM at pH 8.1 and 7.3, respectively. Values of K_m of dephosphorylated enzyme were 0.21 mM and 0.47 mM at pH 8.1 and 7.3, respectively. Both native and dephosphorylated tobacco PEPC showed the same affinity to PEP. This seems to be a usual attribut of plant PEPC; however, even different affinity to PEP of phosphorylated and dephosphorylated PEPC has been reported in castor oil seeds (Tripodi et al., 2005). Low value of K_m and thus high affinity to the substrate correspond to non-photosynthetic PEPC isoform (Svensson et al., 2003). Result of Černý (2007) indicated high affinity of maize seed

form of PEPC to PEP as well. On the contrary, C_4 photosynthetic isoform usually showed lower affinity to substrate (e.g. maize PEPC K_m 1.1 mM and 8.7 mM at pH 8.1 and 7.3, respectively; Frank et al., 1999). K_m of PEPC isolated from another C_4 plant, *Setaria verticillata*, was 1.43 mM at pH 7.8 (Karabourniotis et al., 1985). The low affinity enables another possible regulation of PEPC activity, which evolved only in photosynthetic forms of the enzyme.

Effect of several cell metabolites and potential PEPC effectors on dependence of reaction rate of PEPC on substrate concentration was studied. Malate proved to be a potent inhibitor of tobacco PEPC. Lineweaver-Burke and Dixon plot together with the best fit of measured data into equation 2 revealed that the inhibition is of a mixed type described by 2 inhibition constants (K_{IU} and K_{IC}). Values of both constants for native and dephosphorylated PEPC are shown in Table 6. It is evident that there is no significant difference in malate sensitivity between phosphorylated and dephosphorylated PEPC form. Most kinetic studies of PEPC in C_4 plants were performed using the photosynthetic form which in dephosphorylated state showed higher sensitivity to malate inhibition than in the phosphorylated one (Chollet et al., 1996). Our group demonstrated that PEPC isolated from maize seeds, thus non-photosynthetic form, shows also different response to malate inhibition in dependence on the phosphorylation state (Černý, 2007). Different kinetic properties of dephosphorylated and phosphorylated PEPC in C_3 plants were reported also by Tripodi et al. (2005) and Duff and Chollet (1995). Tripodi et al. (2005) found PEPC isoform in castor bean (PEPC2), which exhibited considerably lower sensitivity to malate inhibition in its dephosphorylated state. However, other attributes of this isoform differed from standard PEPCs (i.e. heterooctameric structure of the protein, lower specific activity in phosphorylated state). PEPC isoform similar to that in castor beans has been found in green algae *S. minutum* (Rivoal et al., 2002).

Effect of aspartate, another potential PEPC inhibitor, on PEPC activity was studied as well. In comparison with malate, aspartate was less potent inhibitor of PEPC activity. Inhibition constants were calculated and are shown in Table 6. Values of inhibition constants indicate very weak competitive inhibition. There has been no difference in sensitivity to aspartate between phosphorylated and dephosphorylated PEPC. Aspartate binding site has been found by X-ray crystallographic analysis in maize photosynthetic form of PEPC (Kai et al., 2003). It has been shown that aspartate is a potent inhibitor of PEPC in C_4 plants, with inhibition effect 20-70% of an initial activity at 1 mM concentration (Huber and Edwards, 1975). Two PEPC isoforms from developing castor oil seeds showed different sensitivity to

aspartate. PEPC1 exhibited 10 times higher sensitivity to aspartate compared to PEPC2. Phosphorylation state did not affect the sensitivity to aspartate in either PEPC isoform (Tripodi et al., 2005).

Table 6: Kinetic parameters of the native and dephosphorylated tobacco leaf PEPC at pH 7.3. Values of inhibition constants were estimated by the best fit to equation 2.

	Native form		Dephosphorylated form	
	K_{IC} [mM]	K_{IU} [mM]	K_{IC} [mM]	K_{IU} [mM]
Malate	0.2	1.3	0.5	1.7
Aspartat	3	$> 10^5$	3	$> 10^5$

Table 7 summarizes studies on inhibition of PEPC by malate and differences in sensitivity of phosphorylated and dephosphorylated forms. Unfortunately these values were obtained under different conditions. Variance in method of I_{50} calculation should be taken in account as well. Some older works, but also a few of the recent ones, were performed using inappropriate buffers with low buffering capacity. These buffer systems (e.g. 50 mM Tris buffer) cannot be sufficient for precise measurements at malate concentration range 1 mM and above. Results obtained in this way may suffer by considerable inaccuracy. In any case, more kinetic data on non-photosynthetic PEPCs are necessary to evaluate the character of PEPC isolated from tobacco leaves. Enzyme isolated from leaves of other C_3 tobacco related plants and of also plants evolutionary distinct from tobacco would be an interesting material for comparison of character of phosphorylated and non-phosphorylated form.

Table 7: Sensitivity of different PEPC isoforms to malate. I_{50} values were calculated according to cited references.

source	Phosphorylated	Dephosphorylated	Literature
Maize seed	4 mM	1.5 mM	Černý, 2007
Maize leaf	0.72 mM	0.27 mM	Mendez et al., 2000
Wheat	1.23 mM	0.26 mM	Duff, 1995
Ricinus 1	0.075 mM	0.029 mM	Tripodi et al., 2005
Ricinus 2	0.57 mM	1.47 mM	Tripodi et al., 2005

Several metabolites were studied for their potential activating effect on PEPC reaction rate. Glycine and 3-phosphoglycerate did not exhibit any effect in our experiments. Glycine was found to activate PEPC isolated from maize (Mareš et al., 1979; Stiborová, 1988). Stimulatory effect of 3-PG was described in *Cicer arietinum* and some bacteria (Singal and Singh, 1986).

Glucose-6-phosphate has been potent activator of tobacco leaf PEPC. 1 mM glucose-6-P caused 100% increase of the reaction rate of native PEPC at pH 7.3 and unsaturated concentration of PEP. Dephosphorylated PEPC was also activated but to a lower extent. 1 mM glucose-6-P caused 40% increase of the reaction rate of dephosphorylated PEPC at pH 7.3 and unsaturated concentration of PEP. Activation was lower at pH 8.1 and at high concentrations of PEP. This characteristic is in accordance with other studies of PEPC. Both C_3 and C_4 PEPC isoforms were found to be activated by glucose-6-P. Activating effect is generally more evident at lower pH and in case of phosphorylated PEPC form.

Dephosphorylated tobacco PEPC is apparently similarly sensitive to malate inhibition to phosphorylated form. This conclusion differs from most previously described plant PEPC enzymes. Tobacco PEPC isoform could be more resistant to malate inhibition in dephosphorylated state similarly to the PEPC 2 in *Ricinus communis*, however, the difference in K_{IC} and K_{IU} of phosphorylated and dephosphorylated enzyme obtained by our measurements did not reach statistical significance.

Similar sensitivity of phosphorylated and dephosphorylated PEPC to malate inhibition did not allow us using this method to distinguish phosphorylation state of PEPC in healthy and PVY^{NTN} infected tobacco plants. Thus we chose different ways to monitor phosphorylation state of the enzyme. First, we exploited the fact that dephosphorylated PEPC has lower specific activity. By complete dephosphorylation of the sample with more phosphorylated PEPC, the decrease of activity should be bigger than in sample with less phosphorylated PEPC. Figure 37 and Figure 38 show changes in PEPC activity of native and dephosphorylated PEPC in healthy and PVY^{NTN} infected sample. Complete dephosphorylation of sample collected from PVY^{NTN} infected tobacco leaves caused higher (60%) decline of the PEPC activity compared to the healthy one (40%). Second, we measured the concentration of free phosphate in crude extracts and extracts treated by alkaline phosphatase. While phosphate concentration was similar in healthy and PVY^{NTN} samples, after dephosphorylation there was higher concentration of free phosphate in infected sample (Figure 39). Thus, the dephosphorylation revealed elevated phosphate content in those samples which led to assumption that the phosphorylation level must be higher in samples from PVY^{NTN} infected plants. Third, phosphoproteins were detected immunochemically by Western blot analysis using anti-phosphoamino acids antibodies. Figure 40 shows stronger band which possibly corresponds to PEPC in infected sample compared to control one. Assuming the same concentration of protein, we conclude that the PEPC phosphorylation is more distinct in PVY^{NTN} samples. All these results indicate that our

hypothesis of post-translational regulation of PEPC activity during PVY^{NTN} infection in tobacco leaves is correct.

Higher phosphorylation of PEPC in PVY^{NTN} infected leaves is not probably the only source of higher measured activity. Other factors seem to play a role too. The expression of the PEPC can be altered at non-detectable level. Further on, cell metabolites can function as modulators of PEPC activity *in vivo*. We found increase of glucose-6-phosphate in infected tobacco leaves (Figure 41). Four times higher concentration of malate has been found in infected tobacco leaves. Glucose-6-P is potent PEPC activator and can act as a component of glycolysis in replenishing of phosphoenolpyruvate. Malate in return inhibits PEPC activity and lowers cell pH. It is also substrate of NADP-malic enzyme, which activity is also induced by PVY infection. NADP-ME catalyzes reaction of malate and NADP to yield pyruvate, NADPH and CO_2. NADPH is an important compound in biosynthetic pathways and substrate of many detoxification enzymes. CO_2 can be utilized directly in chloroplast by Rubisco in photosynthesis. It is possible to alter the ratio of carboxylation and oxidation in favor of the former one by accumulation of CO_2 in the vicinity of Rubisco, which may result in elevation of the photosynthetic activity of the enzyme (Spreitzer and Salvucci, 2002).

What could be the meaning of induced PEPC activity in tobacco leaves during virus infection? I propose 3 main functions. 1) Production of oxaloacetate and replenishment of substrates of tricarboxylic acid cycle. Substrates of TCA can be used for synthesis of amino acids needed in formation of specific defense proteins. 2) PEPC together with NADP-ME, malate dehydrogenase and pyruvate, phosphate dikinase form reaction cycle which converts NADH to NADPH at the cost of ATP. Activities of PEPC, NADP-Me and PPDK are all induced by PVY infection. Malate dehydrogenase is in plants present at very high level by itself. NADPH is utilized in biosynthetic pathways and as a substrate for several antioxidant and detoxification enzymes. Higher demand of both could be expected during the biotic stress conditions. 3) PEPC fixes bicarbonate into C_4 compound, malate. CO_2 can be released for the photosynthetic function. This is a key step in C_4 and CAM metabolisms, which probably evolved under stress conditions (e.g. higher temperature, insufficient water supply or high concentration of salts). Shift from C_3 to CAM metabolism has been reported in several plants exposed to salt stress (Lepiniec et al., 1994; Herppich et al., 1992). Originally, C_4 metabolism was considered as complicated morphologically differentiated system, in which fixation and release of CO_2 happens in different cell types (Kranz-type anatomy). Recently, a new type of C_4 metabolism was found, in which both fixation and release of CO_2

proceed in the same cell. Inbound CO_2 is fixed at the cell periphery or one end of the cell, while release proceeds in chloroplasts in the center of the cell or at the other end. This process is also known as single-cell type C_4 metabolism (Edwards et al., 2004). Hypothetically, this effect could happen in C_3 plants, too. In our experiments, plants infected by PVY^{NTN} closed their stomata and lowered photosynthesis (Ryšlavá et al., 2003). The drop of inbound CO_2 could be compensated by its more effective disposal. Higher activity of PEPC and related enzymes can provide such advantage.

How plants increase PEPC activity? According to studies mentioned above the main source of increased PEPC activity is synthesis *de novo* and modulated expression. Altering of the phosphorylation state by stress has been discussed in few publications. Protein synthesis apparatus should not be damaged during abiotic stress and thus the synthesis of new proteins appears to be the simplest solution to increase activity of the enzyme. The situation is different during biotic stress caused by virus infection. Translational apparatus of the infected plant is used for the production of defense proteins and competes with the virus tendency to multiply itself in the host cells. Thus, the expression of PEPC remains non-altered and post-translational changes may play more important regulatory role. However, the way used by plant cells to induce the phosphorylation of PEPC still remains to be elucidated.

PEPC is in plants phosphorylated by specific PEPC kinase. This is the smallest kinase found so far, Ca^{2+} independent, coded in plants by a small gene family. Garcia-Maurino et al. (2003) reports the induction of PEPC-kinase activity during salt stress in leaves of *Sorghum vulgare*. Activity of PEPC-kinase is regulated by light (C_4 and C_3 plants) or circadian mechanism (CAM plants). Recently, further studies suggest that phosphorylation is also regulated and over-ridden by some compensatory mechanisms and by oxidative or salt stress (Izui et al., 2004). Originally, PEPC-kinase was thought to be regulated by the rate of synthesis *de novo* in a view of its constantly rapid degradation. Recently, another possibility of regulation at the level of enzyme activity was proposed; Nimmo et al. (2001) detected a 55-kDa inhibitor protein in maize extracts, and proposed its function in masking of the basal level of the kinase activity. Saze et al. (2001) reported possible redox regulation of purified maize PEPC-kinase. The PEPC-kinase could be readily inactivated under mild-oxidative conditions and reactivated efficiently by thioredoxin-mediated reduction. Which of the potential ways of regulation take place during biotic stress cannot be unequivocally concluded from our results.

Role of plant hormones in plants during stress has been studied in several works. Our experiments examined the reaction of *ipt* transgenic tobacco plants to PVY^{NTN} infection. Gene for isopentenyl transferase (*ipt*), the key enzyme in cytokinins biosynthesis, was introduced into tobacco plants (Faiss et al., 1997). We compared control tobacco (SR1) and control grafted plants (SRG), transgenic grafts (G) and autogamic progeny of the transgenic grafts, which were able to form only a small root system (SE). Rubisco activity, one of the photosynthetic markers, has been monitored in leaves of studied plants (Figure 42). PVY^{NTN} infection caused 80% decline of Rubisco activity in control SR1 plants. Rubisco activity was significantly lower even in healthy SE, G and SRG plants compared to SR1. PVY^{NTN} infection caused only 10-15 % reduction. This result indicates that photosynthetic activity is affected even in control grafts as well as by higher cytokinin concentrations, both factors acting as stress. Infection in this case caused no additional changes in this parameter. Unfortunately, based on this result we cannot decide whether the transgenic plants are more resistant to the infection.

Next, we studied effect of PVY^{NTN} infection on PEPC, NADP-ME and PPDK in control SR1 and rooted *ipt* transgenic (SE) tobacco plants (Figure 43, Figure 44 and Figure 45). Plants were grown under the same conditions, were at about the same age and the infection was carried out the same way. Activities of all three enzymes were induced in both plant types upon infection. SR1 plants embodied the induction 7 - 10 days after the inoculation of the virus. SE plants showed this increase 7 days later, 13 - 17 days after the inoculation. The symptoms of the infection were milder in SE plants. Thus it seems that transgenic plants were more resistant to the infection. This is in accordance with the result of Dermastia and Ravnikar (1995) who postulated that higher cytokinin levels prior to virus infection could help alleviate the impact of infection and retard the virus replication and development. Similar result has been published by Pogány et al. (2004). In their work, cytokinin overproducing tobacco line was less susceptible to *tobacco necrosis virus*. Besides restriction of the virus-induced necrosis, the transgenic tobacco plants were also able to suppress partly the accumulation of virus coat protein in the infected tissues. This possibility indicates an interesting potential of commercial utilization of the described phenomenon.

5. Conclusions

- ✓ *Nicotiana tabacum* L. plants were subjected to biotic stress caused by potyviral infection, namely by potato virus A and potato virus Y, strain NTN. Presence of viruses was monitored immunochemically by ELISA and by real time PCR. PVY^{NTN} caused more severe symptoms, provided stronger signal during ELISA detection and activities of studied enzymes (PEPC, NADP-ME, PPDK) were significantly higher than in case of PVA infection. PVY^{NTN} was used for further physiologic studies.
- ✓ PEPC activity was approximately three times higher in PVY^{NTN} infected tobacco leaves compared to healthy control. Native electrophoresis with specific staining for PEPC activity showed only 1 band in both control and infected plant samples.
- ✓ The mechanism of the increase of PEPC activity during PVY^{NTN} infection was studied. No difference in the amount of PEPC protein was detected immunochemically. Amount of PEPC mRNA was not also significantly altered in infected tobacco leaves.
- ✓ PEPC was purified from tobacco leaves and several kinetic parameters were determined. Only one isoform was found in leaves of tobacco. The enzyme showed Michaelis-Menten reaction rate dependency on the concentration of the substrate phosphoenolpyruvate. Effects of possible allosteric activators and inhibitors were monitored. L-malate proved to be a potent inhibitor, L-aspartate was very weak inhibitor. Glucose-6-P caused activation of the enzyme. All these effects were observed at sub-optimal pH 7.5, while optimal pH 8.1 gave no or very little inhibition/activation. Glycine and 3-phosphoglycerate had no effect on PEPC activity at either pH.
- ✓ PEPC isolated from tobacco leaves was dephosphorylated with alkaline phosphatase. The maximal reaction rate of dephosphorylated enzyme was lower compared to native form. However the hyperbolic profile of dependence of reaction rate on concentration of phosphoenolpyruvate was maintained and no difference in K_m was detected. While sensitivity to malate and aspartate of native and dephosphorylated forms of PEPC was similar, glucose-6-P caused lower activation of dephosphorylated PEPC compared to the native form.
- ✓ Role of phosphorylation in regulation of PEPC activity during PVY^{NTN} infection was studied. Changes in PEPC activity and free phosphate concentration were compared

in native and dephosphorylated samples of control and infected tobacco leaves. The result shows higher concentration of phosphate released by alkaline phosphatase treatment in infected samples. The drop in PEPC activity caused by dephosphorylation was also more severe in infected samples. Western blot analysis using anti-phosphoamino acids antibodies showed more intensive band corresponding to PEPC in infected samples. All these results indicate that the phosphorylation of PEPC in tobacco leaves is induced during potyviral infection.

- ✓ Transgenic tobacco plants with higher concentration of endogenous cytokinins were tested for sensitivity to PVY^{NTN}. Significant delay (5 – 7 days) in the stimulation of the activities of selected enzymes (PEPC, NADP-ME and PPDK) was observed after infection in transgenic plants in comparison with wild-type. Virus infection did not cause any drop in Rubisco activity in transgenic plants, which was very distinct in wild-type plants. These results together with other observations indicate higher resistance of plants with elevated concentration of cytokinins to viral infection.

6. Literature

6.1. Books

Bray,E.A., Bailey-Serres,J. & Weretilnyk,E.: Responses to Abiotic Stresses. In: Biochemistry & molecular biology of plants (Buchanan,B.B., Gruissem,W. & Jones,R.L., eds) American Society of Plant Physiologists, Rockville, Maryland (2000)

Clarke,S.F.: Physiological and molecular interactions between plant hormones on white clover mosaic virus infection of *Phaseolus vulgaris L.*, PhD Thesis, Dunedin, Univeristy of Otago, New Zaeland, (1996)

Hammond-Kosack,K. & Jones,J.D.G.: Responses to Plant Pathogens. In: In: Biochemistry & molecular biology of plants (Buchanan,B.B., Gruissem,W. & Jones,R.L., eds) American Society of Plant Physiologists, Rockville, Maryland (2000)

Ho,L.C.: Tomato. In: Photoassimilate distribution in plants (Zamski,E., Schaffer,A.A., eds) Dekker, New York, pp 709-728 (1996)

MacRobbie,E.A.C.: Ionic relation of guard cell. In: Stomatal function (Zeiger,E., Farquhar,G.D. & Cowan,I.R., eds.) Stanford, CA: Stanford University Press (1987)

Shukla,D., Ward,C.W. & Brunt,A.A.: The Potyviridae, CAB International, Wallingford, pp. 32-51 (1994)

Simpson,P.G. & Withman,W.B.: Anabolic pathways in methanogens. In Methanogenesis: ecology, physiology, biochemistry, and genetics. (Ferry,J.G., eds) Chapman and Hall, New York, N.Y. (1993)

6.2. Journals

Agrawal,G.K., Rakwal,R., Jwa,N.S., & Agrawal,V.P. Signalling molecules and blast pathogen attack activates rice OsPR1a and OsPR1b genes: A model illustrating components participating during defence/stress response. *Plant Physiol. Biochem.* **39**, 1095-1103 (2001).

Akiyoshi,D.E., Klee,H., Amasino,R.M., Nester,E.W. & Gordon,M.P. T-DNA of Agrobacterium tumefaciens encodes an enzyme of cytokinin biosynthesis. *Proc. Natl. Acad. Sci. USA* **81**, 5994-5998 (1984)

Akhani,H., Barroca,J., Koteeva,N., Voznesenskaya,E., Franceschi,V., Edwards,G., Ghaffari,S.M. & Ziegler,H. Bienertia sinuspersici (Chenopodiaceae): A new species from southwest Asia and discovery of a third terrestrial C4 plant without Kranz anatomy. *Systematic Botany* **30**, 290-301 (2005).

Andreo,C.S., Gonzalez,D.H., & Iglesias,A.A. Higher-plant phosphoenolpyruvate carboxylase – Structure and regulation. *FEBS Lett.* **213**, 1-8 (1987).

Asada,K. The water-water cycle in chloroplasts: Scavenging of active oxygens and dissipation of excess photons. *Annu. Rev. Plant Physiol. Plant Molec. Biol.* **50**, 601-639 (1999).

Asai,N., Nakajima,N., Tamaoki,M., Kamada,H., & Kondo,N. Role of malate synthesis mediated by phosphoenolpyruvate carboxylase in guard cells in the regulation of stomatal movement. *Plant Cell Physiol.* **41**, 10-15 (2000).

Astot,C. Dolezal,K., Nordstrom,A., Wang,Q., Kunkel,T., Moritz,T., Chua,N.H. & Sandberg,G. An alternative cytokinin biosynthesis pathway. *Proc. Natl. Acad. Sci. U. S. A.* **97**, 14778-14783 (2000).

Bakrim,N., Brulfert,J., Vidal,J., & Chollet,R. Phosphoenolpyruvate carboxylase kinase is controlled by a similar signaling cascade in CAM and C-4 plants. *Biochem. Biophys. Res. Commun.* **286**, 1158-1162 (2001).

Balachandran,S., Osmond,C.B., & Daley,P.F. Diagnosis of the earliest strain specific interactions between tobacco mosaic virus and chloroplasts of tobacco leaves in-vivo by mean of chlorophyl fluorescence imaging. *Plant Physiol.* **104**, 1059-1065 (1994).

Bandurski,R.S. & Greiner,C.M. The enzymatic synthesis of oxalacetate from phosphoryl-enolpyruvate and carbon dioxide. *J. Biol. Chem.* **204**, 781-786 (1953).

Banerjee,N., Wang,J.Y., & Zaitlin,M. A single nucleotide change in the coat protein gene of tobacco mosaic virus is involved in the induction of severe chlorosis. *Virology* **207**, 234-239 (1995).

Beczner,L., Horvath,J., Romhanyi,I., & Forster,H. Studies on the etiology of tuber necrotic ringspot disease in potato. *Potato Res.* **27**, 339-352 (1984).

Blasing,O.E., Westhoff,P., & Svensson,P. Evolution of C4 phosphoenolpyruvate carboxylase in Flaveria, a conserved serine residue in the carboxyl-terminal part of the enzyme is a major determinant for C4-specific characteristics. *J. Biol. Chem.* **275**, 27917-27923 (2000).

Blasing,O.E., Ernst,K., Streubel,M., Westhoff,P., & Svensson,P. The non-photosynthetic phosphoenolpyruvate carboxylases of the C4 dicot Flaveria trinervia - implications for the evolution of C4 photosynthesis. *Planta* **215**, 448-456 (2002).

Blokhina,O., Virolainen,E., & Fagerstedt,K.V. Antioxidants, oxidative damage and oxygen deprivation stress: a review. *Ann. Bot.* **91**, 179-194 (2003).

Bolwell,G.P. & Wojtaszek,P. Mechanisms for the generation of reactive oxygen species in plant defence - a broad perspective. *Physiol. Mol. Plant Pathol.* **51**, 347-366 (1997).

Bradford,M.M. Rapid and sensitive method for quantification of microgram quantities of protein utilizing principle of protein-dye binding. *Anal. Biochem.* **72**, 248-254 (1976).

Braidot,E., Petrussa,E., Vianello,A., & Macri,F. Hydrogen peroxide generation by higher plant mitochondria oxidizing complex I or complex II substrates. *FEBS Lett.* **451**, 347-350 (1999).

Broglie,K., Chet,I., Holliday,M., Cressman.R., Biddle,P., Knowlton,S., Mauvais,C.J. & Broglie,R. Transgenic plants with enhanced resistance to the fungal pathogen Rhizoctonia solani. *Science* **254**, 1194-1197 (1991).

Brzobohatý,B., Moore,I., Kristoffersen,P., Bako,L., Campos,N., Schell,J. & Palme,K. Release of active cytokinin by a beta-glucosidase localized to the maize root-meristem. *Science* **262**, 1051-1054 (1993).

Canning,E.S.G., Penrose,M.J., Barker,I., Coates,D., & Ub Improved detection of barley yellow dwarf virus in single aphids using RT-PCR. *J. Virol. Methods* **56**, 191-197 (1996).

Černý,M.: Izolace a charakterizace fosfoenolpyruvátkarboxylasy ze semen *Zea mays*, Diploma thesis, Faculty of Sciences, Charles University in Prague, Department of biochemistry (2007)

Čeřovská,N. Production of monoclonal antibodies to potato virus Y-NTN strain and their use for strain differentiation. *Plant Pathol.* **47**, 505-509 (1998).

Champigny,M.L. & Foyer,C. Nitrate Activation of Cytosolic Protein-Kinases Diverts Photosynthetic Carbon from Sucrose to Amino-Acid Biosynthesis - Basis for a New Concept. *Plant Physiol.* **100**, 7-12 (1992).

Chardot,T.P. & Wedding,R.T. Role of cysteine in activation and allosteric regulation of maize phosphoenolpyruvate carboxylase. *Plant Physiol.* **98**, 780-783 (1992).

Chen,W.Q.J. & Zhu,T. Networks of transcription factors with roles in environmental stress response. *Trends Plant Sci.* **9**, 591-596 (2004).

Chollet,R., Vidal,J., & Oleary,M.H. Phosphoenolpyruvate carboxylase: A ubiquitous, highly regulated enzyme in plants. *Annu. Rev. Plant Physiol. Plant Molec. Biol.* **47**, 273-298 (1996).

Clark,M.F. & Adams,A.N. Characteristics of microplate method of enzyme-linked immunosorbent assay for detection of plant-viruses. *J. Gen. Virol.* **34**, 475-483 (1977).

Clarke,S.F., McKenzie,M.J., Burritt,D.J., Guy,P.L., & Jameson,P.E. Influence of white clover mosaic potexvirus infection on the endogenous cytokinin content of bean. *Plant Physiol.* **120**, 547-552 (1999).

Clarke,S.F., Burritt,D.J., Jameson,P.E., & Guy,P.L. Effects of plant hormones on white clover mosaic potexvirus double-stranded RNA. *Plant Pathol.* **49**, 428-434 (2000).

Collinge,D.B., Kragh,K.M., Mikkelsen,J.D., Nielsen,K.K., Rasmussen,U. & Vad,K. Plant chitinases. *Plant J.* **3**, 31-40 (1993).

Coursol,S., Giglioli-Guivarc'h,N., Vidal,J., & Pierre,J.N. An increase in phosphoinositide-specific phospholipase C activity precedes induction of C-4 phosphoenolpyruvate carboxylase phosphorylation in illuminated and NH4Cl-treated protoplasts from Digitaria sanguinalis. *Plant J.* **23**, 497-506 (2000).

Cushman,J.C. & Bohnert,H.J. Crassulacean acid metabolism: Molecular genetics. *Annu. Rev. Plant Physiol. Plant Molec. Biol.* **50**, 305-332 (1999).

De Nisi,P. & Zocchi,G. Phosphoenolpyruvate carboxylase in cucumber (Cucumis sativus L.) roots under iron deficiency: activity and kinetic characterization. *J. Exp. Bot.* **51**, 1903-1909 (2000).

Dermastia,M. & Ravnikar,M. Altered cytokinin pattern and enhanced tolerance to potato virus Y-NTN in the susceptible potato cultivar (Solanum tuberosum cv Igor) grown in vitro. *Physiol. Mol. Plant Pathol.* **48**, 65-71 (1996).

Dixon,M. The determination of enzyme inhibitor constants. *Biochem. J.* **55**, 170-171 (1953).

Dixon,R.A. Natural products and plant disease resistance. *Nature* **411**, 843-847 (2001).

Doke,N. Involvement of superoxide anion generation in the hypersensitive response of potato-tuber tissues to infection with an incompatible race of Phytophthora infestans and to the hyphal wall components. *Physiological Plant Pathology* **23**, 345-357 (1983).

Dong,L.Y., Masuda,T., Kawamura,T., Hata,S., & Izui,K. Cloning, expression, and characterization of a root-form phosphoenolpyruvate carboxylase from Zea mays: Comparison with the C-4-form enzyme. *Plant Cell Physiol.* **39**, 865-873 (1998).

Duan,X.L., Li,X.G., Xue,Q.Z., AboElSaad,M., Xu, D.P. & Wu,R. Transgenic rice plants harboring an introduced potato proteinase inhibitor II gene are insect resistant. *Nat. Biotechnol.* **14**, 494-498 (1996).

Duff,S.M.G. & Chollet,R. In-vivo regulation of wheat-leaf phosphoenolpyruvate carboxylase from by reversible phosphorylation. *Plant Physiol.* **107**, 775-782 (1995).

Echevarria,C., Pacquit,V., Barkim,N., Osuna,L., Delgado,B., Arriodupont,M. & Vidal,J. The effect of pH on the covalent and metabolic control of C-4 phosphoenolpyruvate carboxylase from sorghum leaf. *Arch. Biochem. Biophys.* **315**, 425-430 (1994).

Edwards,G.E., Franceschi,V.R., & Voznesenskaya,E.V. Single-cell C-4 photosynthesis versus the dual-cell (Kranz) paradigm. *Annu. Rev. Plant Biol.* **55**, 173-196 (2004).

Ettema,T.J.G., Makarova,K.S., Jellema,G.L., Gierman,H.J., Koonin,E.V., Huynen,M.A., de Vos,W.A. & van der Oost,J. Identification and functional verification of archaeal-type phosphoenolpyruvate carboxylase, a missing link in archaeal central carbohydrate metabolism. *Journal of Bacteriology* **186**, 7754-7762 (2004).

Faiss,M., Zalubilova,J., Strnad,M., Schmulling,T., & Xw Conditional transgenic expression of the ipt gene indicates a function for cytokinins in paracrine signaling in whole tobacco plants. *Plant J.* **12**, 401-415 (1997).

Fedina,I.S. & Popova,A.V. Photosynthesis, photorespiration and proline accumulation in water-stressed pea leaves. *Photosynthetica* **32**, 213-220 (1996).

Ferreira,F.J. & Kieber,J.J. Cytokinin signaling. *Curr. Opin. Plant Biol.* **8**, 518-525 (2005)

Fontaine,V., Pelloux,J., Podor,M., Afif,D., Gerant,D., Grieu,P. & Dizengremel,P. Carbon fixation in Pinus halepensis submitted to ozone. Opposite response of ribulose-1,5-bisphosphate carboxylase/oxygenase and phosphoenolpyruvate carboxylase. *Physiol. Plant.* **105**, 187-192 (1999).

Fontaine,V., Cabane,M., & Dizengremel,P. Regulation of phosphoenolpyruvate carboxylase in Pinus halepensis needles submitted to ozone and water stress. *Physiol. Plant.* **117**, 445-452 (2003).

Fujita,N., Izui,K., Nishino,T., & Katsuki,H. Reaction-Mechanism of Phosphoenolpyruvate Carboxylase - Bicarbonate-Dependent Dephosphorylation of Phosphoenol-Alpha-Ketobutyrate. *Biochemistry* **23**, 1774-1779 (1984).

Fujita,N., Miwa,T., Ishijima,S., Izui,K., & Katsuki,H. The Primary Structure of Phosphoenolpyruvate Carboxylase of Escherichia-Coli - Nucleotide-Sequence of the Ppc Gene and Deduced Amino-Acid-Sequence. *Journal of Biochemistry* **95**, 909-916 (1984).

Gao,Y. & Woo,K.C. Regulation of phosphoenolpyruvate carboxylase in Zea mays by protein phosphorylation and metabolites and their roles in photosynthesis. *Aust. J. Plant Physiol.* **23**, 25-32 (1996).

Garcia-Maurino,S., Monreal,J.A., Alvarez,R., Vidal,J. & Echevarria,C. Characterization of salt stress-enhanced phosphoenolpyruvate carboxylase kinase activity in leaves of Sorghum vulgare: independence from osmotic stress, involvement of ion toxicity and significance of dark phosphorylation. *Planta* **216**, 648-655 (2003).

Gillissen,B., Burkle,L., Andre,B., Kuhn,C., Rentsch,D., Brandl,B. & Frommer,W.B. A new family of high-affinity transporters for adenine, cytosine, and purine derivatives in arabidopsis. *Plant Cell* **12**, 291-300 (2000).

Gonzalez,M.C., Sanchez,R., & Cejudo,F.J. Abiotic stresses affecting water balance induce phosphoenolpyruvate carboxylase expression in roots of wheat seedlings. *Planta* **216**, 985-992 (2003).

Grant,J.J. & Loake,G.J. Role of reactive oxygen intermediates and cognate redox signaling in disease resistance. *Plant Physiol.* **124**, 21-29 (2000).

Grayer,R.J. & Kokubun,T. Plant-fungal interactions: the search for phytoalexins and other antifungal compounds from higher plants. *Phytochemistry* **56**, 253-263 (2001).

Guillet,C., Just,D., Benard,N., Destrac-Irvine,A., Baldet,P., Hernould,M., Causse,M., Raymond,P. & Rothan,C. A fruit-specific phosphoenolpyruvate carboxylase is related to rapid growth of tomato fruit. *Planta* **214**, 717-726 (2002).

Haberer,G. & Kieber,J.J. Cytokinins. New insights into a classic phytohormone. *Plant Physiol.* **128**, 354-362 (2002).

Hata,S., Izui,K., & Kouchi,H. Expression of a soybean nodule-enhanced phosphoenolpyruvate carboxylase gene that shows striking similarity to another gene for a house-keeping isoform. *Plant J.* **13**, 267-273 (1998).

Herppich,W., Herppich,M., & Vonwillert,D.J. The irreversible C3 to CAM shift in well-watered and salt-stresses plants of Mesembryanthemum crystallinum is under strict ontogenic control. *Bot. Acta* **105**, 34-40 (1992).

Huber,S. & Edwards,G. Effect of oxygen on CO2 fixation by mesophyll protoplast extracts of C3 and C4 plants. *Biochem. Biophys. Res. Commun.* **67**, 28-34 (1975).

Iwai,T., Kaku,H., Honkura,R., Nakamura,S., Ochiai,H., Sasaki,T. & Ohashi,Y. Enhanced resistance to seed-transmitted bacterial diseases in transgenic rice plants overproducing an oat cell-wall-bound thionin. *Mol. Plant-Microbe Interact.* **15**, 515-521 (2002).

Izui,K., Matsumura,H., Furumoto,T., & Kai,Y. Phosphoenolpyruvate carboxylase: A new era of structural biology. *Annu. Rev. Plant Biol.* **55**, 69-84 (2004).

Jeanneau,M., Vidal,J., Gousset-Dupont,A., Lebouteiller,B., Hodges,M., Gerentes,D. & Perez,P. Manipulating PEPC levels in plants. *J. Exp. Bot.* **53**, 1837-1845 (2002).

Johnson,J.F., Vance,C.P., & Allan,D.L. Phosphorus deficiency in Lupinus albus - Altered lateral root development and enhanced expression of phosphoenolpyruvate carboxylase. *Plant Physiol.* **112**, 31-41 (1996).

Jones,R.J. & Schreiber,B.M.N. Role and function of cytokinin oxidase in plants. *Plant Growth Regul.* **23**, 123-134 (1997).

Jwa,N.S., Agrawal,G.K., Tamogami,S., Yonekura,M., Han,O., Iwahashi,H. & Rakwal,R. Role of defense/stress-related marker genes, proteins and secondary metabolites in defining rice self-defense mechanisms. *Plant Physiol. Biochem.* **44**, 261-273 (2006).

Kai,Y., Matsumura,H., Inoue,T., Terada,K., Nagara,Y., Yoshinaga,T., Kihara,A., Tsumura,A. & Izui,K. Three-dimensional structure of phosphoenolpyruvate carboxylase: A proposed mechanism for allosteric inhibition. *Proc. Natl. Acad. Sci. U. S. A.* **96**, 823-828 (1999).

Kai,Y., Matsumura,H., & Izui,K. Phosphoenolpyruvate carboxylase: three-dimensional structure and molecular mechanisms. *Arch. Biochem. Biophys.* **414**, 170-179 (2003).

Kakimoto,T. Identification of plant cytokinin biosynthetic enzymes as dimethylallyl diphosphate : ATP/ADP isopentenyltransferases. *Plant Cell Physiol.* **42**, 677-685 (2001).

Kamínek,M., Motyka,V. & Vaňková,R. Regulation of cytokinin content in plant cells. *Phys. Plant*. **101**, 689-700 (1997)

Karabourniotis,G., Manetas,Y., & Gavalas,N.A. Detecting photoactivation of phosphoenolpyruvate carboxylase in C-4 plants – An effect oh pH. *Plant Physiol.* **77**, 300-302 (1985).

Klee,H.J. & Romano,C.P. The roles of phytohormones in development as studied in transgenic plants. *Crit. Rev. Plant Sci*. **13**, 311-324 (1994)

Kopka,J., Provart,N.J., & MullerRober,B. Potato guard cells respond to drying soil by a complex change in the expression of genes related to carbon metabolism and turgor regulation. *Plant J.* **11**, 871-882 (1997).

Laemmli,U.K. Cleavage of structural proteins during assembly of head of bacteriophage-T4. *Nature* **227**, 680 (1970).

Lamb,C. & Dixon,R.A. The oxidative burst in plant disease resistance. *Annu. Rev. Plant Physiol. Plant Molec. Biol.* **48**, 251-275 (1997).

Lara,M.V., Chuong,S.D.X., Akhani,H., Andreo,C.S., & Edwards,G.E. Species having C-4 single-cell-type photosynthesis in the Chenopodiaceae family evolved a photosynthetic phosphoenolpyruvate carboxylase like that of Kranz-type C-4 species. *Plant Physiol.* **142**, 673-684 (2006).

Latzko,E. & Kelly,G.J. The many-faceted function of phosphoenolpyruvate carboxylase in C-3 plants. *Physiologie Vegetale* **21**, 805-815 (1983).

Lee,D.H. & Lee,C.B. Chilling stress-induced changes of antioxidant enzymes in the leaves of cucumber: in gel enzyme activity assays. *Plant Sci.* **159**, 75-85 (2000).

Lee,J.H., Hubel,A., & Schoffl,F. Derepression of the activity of genetically engineered heat-shock factor causes constitutive synthesis of heat-shock proteins and increased thermotolerance in transgenic Arabidopsis. *Plant J.* **8**, 603-612 (1995).

Lepiniec,L., Vidal,J., Chollet,R., Gadal,P., & Cretin,C. Phosphoenolpyruvate Carboxylase - Structure, Regulation and Evolution. *Plant Sci.* **99**, 111-124 (1994).

Linthorst,H.J.M. Pathogenesis-related proteins of plants. *Crit. Rev. Plant Sci.* **10**, 123-150 (1991).

Lusso,M. & Kuc,J. The effect of sense and antisense expression of the PR-N gene for beta-1,3-glucanase on disease resistance of tobacco to fungi and viruses. *Physiol. Mol. Plant Pathol.* **49**, 267-283 (1996).

Mahalingam,R., Fedoroff,N., & Fx Stress response, cell death and signalling: the many faces of reactive oxygen species. *Physiol. Plant.* **119**, 56-68 (2003).

Mareš,J., Bárthová,J., & Léblová,S. Purification and the properties of phosphoenolpyruvate carboxylase from green leaves of maize. *Collect. Czech. Chem. Commun.* **44**, 1835-1840 (1979).

Matsumura,H., Terada,M., Shirakata,S., Inoue,T., Yoshinaga,T., Izui,K. & Kai,Y. Plausible phosphoenolpyruvate binding site revealed by 2.6 angstrom structure of Mn2+-bound phospoenolpyruvate carboxylase from Escherichia coli. *FEBS Lett.* **458**, 93-96 (1999).

Matsumura,H., Xie,Y., Shirakata,S., Inoue,T., Yoshinaga,T., Ueno,Y., Izui,K. & Kai,Y. Crystal structures of C-4 form maize and quaternary complex of E-coli phosphoenolpyruvate carboxylases. *Structure* **10**, 1721-1730 (2002).

Mok,D.W.S. & Mok,M.C. Cytokinin metabolism and action. *Annu. Rev. Plant Physiol. Plant Molec. Biol.* **52**, 89-118 (2001).

Moons,A., Valcke,R., & Van Montagu,M. Low-oxygen stress and water deficit induce cytosolic pyruvate orthophosphate dikinase (PPDK) expression in roots of rice, a C-3 plant. *Plant J.* **15**, 89-98 (1998).

Moravec,T., Čeřovská,N. & Boonham,N. The detection of recombinant, tuber necrosing isolates of Potato virus Y (PVYNTN) using a three-primer PCR based in the coat protein gene. *J. Virol. Methods* **109**, 63-68 (2003).

Munns,R. Genes and salt tolerance: bringing them together. *New Phytol.* **167**, 645-663 (2005).

Nakamura,T., Yoshioka,I., Takahashi,M., Toh,H., & Izui,K. Cloning and sequence-analysis of the gene for phosphoenolpyruvate carboxylase from an extreme thermophile, Thermus Sp. *Journal of Biochemistry* **118**, 319-324 (1995).

Nimmo,G.A., Nimmo,H.G., Hamilton,I.D., Fewson,C.A., & Wilkins,M.B. Purification of the phosphorylated night form and dephosphorylated day form of phosphoenolpyruvate carboxylase from Bryophyllum fedtschenkoi. *Biochem. J.* **239**, 213-220 (1986).

Nimmo,G.A., Wilkins,M.B., & Nimmo,H.G. Partial purification and characterization of a protein inhibitor of phosphoenolpyruvate carboxylase kinase. *Planta* **213**, 250-257 (2001).

Nimmo,H.G. The regulation of phosphoenolpyruvate carboxylase in CAM plants. *Trends Plant Sci.* **5**, 75-80 (2000).

Oaks,A. Efficiency of Nitrogen-Utilization in C-3 and C-4 Cereals. *Plant Physiol.* **106**, 407-414 (1994).

Ogawa,N., Kai,T., Yabuta,N., & Izui,K. Phosphoenolpyruvate carboxylase of maize leaves: An improved method for purification and reduction of the inhibitory effect of malate by ethylene glycol and bicarbonate. *Plant Cell Physiol.* **38**, 76-80 (1997).

Passardi,F., Cosio,C., Penel,C., & Dunand,C. Peroxidases have more functions than a Swiss army knife. *Plant Cell Reports* **24**, 255-265 (2005).

Patel,H.M., Kraszewski,J.L., & Mukhopadhyay,B. The phosphoenolpyruvate carboxylase from Methanothermobacter thermautotrophicus has a novel structure. *Journal of Bacteriology* **186**, 5129-5137 (2004).

Perata,P. & Alpi,A. Plant-responses to anaerobiosis. *Plant Sci.* **93**, 1-17 (1993).

Pogany,M., Koehl,J., Heiser,I., Elstner,E.F. & Barna,B. Juvenility of tobacco induced by cytokinin gene introduction decreases susceptibility to Tobacco necrosis virus and confers tolerance to oxidative stress. *Physiol. Mol. Plant Pathol.* **65**, 39-47 (2004).

Rahoutei,J., Garcia-Luque,I., & Baron,M. Inhibition of photosynthesis by viral infection: Effect on PSII structure and function. *Physiol. Plant.* **110**, 286-292 (2000).

Rivoal,J., Smith,C.R., Moraes,T.F., Turpin,D.H. & Plaxton,W.C. Method for activity staining after native polyacrylamide gel electrophoresis using a coupled enzyme assay and fluorescence detection: Application to the analysis of several glycolytic enzymes. *Anal. Biochem.* **300**, 94-99 (2002).

Rivoal,J., Turpin,D.H. & Plaxton,W.C. In vitro phosphorylation of phosphoenolpyruvate carboxylase from the green alga Selenastrum minutum. *Plant Cell Physiol.* **43**, 785-792 (2002).

Rizhsky,L., Liang,H.J., & Mittler,R. The combined effect of drought stress and heat shock on gene expression in tobacco. *Plant Physiol.* **130**, 1143-1151 (2002).

Rosahl,S. Lipoxygenases in plants - Their role in development and stress response. *Z. Naturforsch. (C)* **51**, 123-138 (1996).

Ryan,C.A. Proteolytic-enzymes and their inhibitors in plants. *Annu. Rev. Plant Physiol. Plant Molec. Biol.* **24**, 173-196 (1973).

Ryan,C.A. Protease inhibitors in plants – Genes for improving defenses against insects and pathogens. *Annu. Rev. Phytopathol.* **28**, 425-449 (1990).

Ryšlavá,H., Müller,K., Semorádová,S., Synková,H. & Čeřovská,N. Photosynthesis and activity of phosphoenolpyruvate carboxylase in Nicotiana tabacum L. leaves infected by Potato virus A and Potato virus Y. *Photosynthetica* **41**, 357-363 (2003).

Sachs,M.M., Subbaiah,C.C., & Saab,I.N. Anaerobic gene expression and flooding tolerance in maize. *J. Exp. Bot.* **47**, 1-15 (1996).

Sakano,K. Revision of biochemical pH-Stat: Involvement of alternative pathway metabolisms. *Plant Cell Physiol.* **39**, 467-473 (1998).

Sanchez,R. & Cejudo,F.J. Identification and expression analysis of a gene encoding a bacterial-type phosphoenolpyruvate carboxylase from Arabidopsis and rice. *Plant Physiol.* **132**, 949-957 (2003).

Sanchez,R., Flores,A., & Cejudo,F. Arabidopsis phosphoenolpyruvate carboxylase genes encode immunologically unrelated polypeptides and are differentially expressed in response to drought and salt stress. *Planta* **223**, 901-909 (2006).

Sano,H., Seo,S., Koizumi,N., Niki,T., Iwamura,H. & Ohashi,Y. Regulation by cytokinins of endogenous levels of jasmonic and salicylic acids in mechanically wounded tobacco plants. *Plant Cell Physiol.* **37**, 762-769 (1996).

Sarowar,S., Kim,E.N., Kim, Y.J., Ok,S.H., Kim,K.D., Hwang,B.K. & Shin,J.S. Overexpression of a pepper ascorbate peroxidase-like 1 gene in tobacco plants enhances tolerance to oxidative stress and pathogens. *Plant Sci.* **169**, 55-63 (2005).

Sauer,U. & Eikmanns,B.J. The PEP-pyruvate-oxaloacetate node as the switch point for carbon flux distribution in bacteria. *Fems Microbiol. Rev.* **29**, 765-794 (2005).

Saurer,M., Maurer,S., Matyssek,R., Landolt,W., Gunthardtgoerg,M.S. & Siegenthaler,U. The influence of ozone and nutrition on delta-C-13 in Betula pendula. *Oecologia* **103**, 397-406 (1995).

Saze,H., Ueno,Y., Hisabori,T., Hayashi,H., & Izui,K. Thioredoxin-mediated reductive activation of a protein kinase for the regulatory phosphorylation of C4-form phosphoenolpyruvate carboxylase from maize. *Plant Cell Physiol.* **42**, 1295-1302 (2001).

Schuller,K.A., Turpin,D.H., & Plaxton,W.C. Metabolite regulation of partially purified soybean nodule phosphoenolpyruvate carboxylase. *Plant Physiol.* **94**, 1429-1435 (1990).

Schuller,K.A. & Werner,D. Phosphorylation of soybean (glycine-max L) nodule phosphoenolpyruvate carboxylase in vitro decreases sensitivity to inhibition by L-malate. *Plant Physiol.* **101**, 1267-1273 (1993).

Sehmer,L., Fontaine,V., Antoni,F., & Dizengremel,P. Effects of ozone and elevated atmospheric carbon dioxide on carbohydrate metabolism of spruce needles. Catabolic and detoxification pathways. *Physiol. Plant.* **102**, 605-611 (1998).

Shao,H.B., Jiang,S.Y., Li,F.M., Chu, L.Y., Zhao,C.X., Shao,M.A., Zhao,X.N. & Li,F. Some advances in plant stress physiology and their implications in the systems biology era. *Colloid Surf. B-Biointerfaces* **54**, 33-36 (2007).

Shinozaki,K., Yamaguchi-Shinozaki,K., & Seki,M. Regulatory network of gene expression in the drought and cold stress responses. *Curr. Opin. Plant Biol.* **6**, 410-417 (2003).

Shinozaki,K. & Yamaguchi-Shinozaki,K. Gene networks involved in drought stress response and tolerance. *J. Exp. Bot.* **58**, 221-227 (2007).

Skoog,F. & Miller,C.O. Chemical regulation of growth and organ formation in plant tissues cultured in vitro. *Symp. Soc. Exp. Biol.* **11**: 118-131 (1957).

Skulachev,V.P. Membrane-linked systems preventing superoxide formation. *Biosci. Rep.* **17**, 347-366 (1997).

Slack,C.R. & Hatch, M.D. Comparative studies on the activity of carboxylases and other enzymes in relation to the new pathway of photosynthetic carbon dioxide fixation in tropical grasses, *Biochem. J.* **103,** 660-665 (1967).

Slesarev,A.I. *et al.* The complete genome of hyperthermophile Methanopyrus kandleri AV19 and monophyly of archaeal methanogens. *Proc. Natl. Acad. Sci. U. S. A.* **99**, 4644-4649 (2002).

Smart,L.B., Vojdani,F., Maeshima,M., & Wilkins,T.A. Genes involved in osmoregulation during turgor-driven cell expansion of developing cotton fibers are differentially regulated. *Plant Physiol.* **116**, 1539-1549 (1998).

Smith,R.G., Gauthier,D.A., Dennis,D.T., & Turpin,D.H. Malate-dependent and pyruvate-dependent fatty-acid synthesis in leukoplastids from developing castor endosperm. *Plant Physiol.* **98**, 1233-1238 (1992).

Spreitzer,R.J. & Salvucci,M.E. Rubisco: Structure, regulatory interactions, and possibilities for a better enzyme. *Annu. Rev. Plant Biol.* **53**, 449-475 (2002).

Stiborová,M. Phosphoenolpyruvate Carboxylase - the Key Enzyme of C-4-Photosynthesis. *Photosynthetica* **22**, 240-263 (1988).

Steinbuc,M. & Audran,R. Isolation of IgG from mammalian sera with aid of caprylic acid. *Arch. Biochem. Biophys.* **134** (2), 279 (1969)

Stitt,M., Lilley,R.M., Gerhardt,R., & Heldt,H.W. Metabolite levels in specific cells and subcellular compartments of plant-leaves. *Method Enzymol.* **174**, 518-552 (1989).

Stitt,M. Nitrate regulation of metabolism and growth. *Curr. Opin. Plant Biol.* **2**, 178-186 (1999).

Synková,H., Semorádová,Š., Schnablová,R., Müller,K., Pospíšilová,J., Ryšlavá,H., Malbeck,J. & Čeřovská,N. Effects of biotic stress caused by Potato virus Y on photosynthesis in ipt transgenic and control Nicotiana tabacum L. *Plant Sci.* **171**, 607-616 (2006).

Takei,K., Sakakibara,H., & Sugiyama,T. Identification of genes encoding adenylate isopentenyltransferase, a cytokinin biosynthesis enzyme, in Arabidopsis thaliana. *J. Biol. Chem.* **276**, 26405-26410 (2001).

Takei,K., Sakakibara,H., Taniguchi,M., & Sugiyama,T. Nitrogen-dependent accumulation of cytokinins in root and the translocation to leaf: Implication of cytokinin species that induces gene expression of maize response regulator. *Plant Cell Physiol.* **42**, 85-93 (2001).

Taya,Y., Tanaka,Y., & Nishimura,S. 5'-AMP is a direct precursor of cytokinin in *Dictyostelium discoideum*. *Nature* **271**, 545-547 (1978).

Taybi,T., Patil,S., Chollet,R., & Cushman,J.C. A minimal serine/threonine protein kinase circadianly regulates phosphoenolpyruvate carboxylase activity in crassulacean acid metabolism-induced leaves of the common ice plant. *Plant Physiol.* **123**, 1471-1481 (2000).

Thind,S.K. & Malik,C.P. Correlated changes of some amino-acids and protease in seedlings subjected to water and temperature stresses. *Phyton-Ann. REI Bot.* **28**, 261-269 (1988).

Thomas,J.C., Dearmond,R.L., & Bohnert,H.J. Influence of NaCl on growth, proline, and phosphoenolpyruvate carboxylase levels in Mesembryanthemum crystallinum suspension-cultures. *Plant Physiol.* **98**, 626-631 (1992).

Toh,H., Kawamura,T., & Izui,K. Molecular Evolution of Phosphoenolpyruvate Carboxylase. *Plant Cell and Environment* **17**, 31-43 (1994).

Tripodi,K.E., Turner,W.L., Gennidakis,S., & Plaxton,W.C. In vivo regulatory phosphorylation of novel phosphoenolpyruvate carboxylase isoforms in endosperm of developing castor oil seeds. *Plant Physiol.* **139**, 969-978 (2005).

Tsuchida,Y., Furumoto,T., Izumida,A., Hata,S., & Izui,K. Phosphoenolpyruvate carboxylase kinase involved in C-4 photosynthesis in Flaveria trinervia: cDNA cloning and characterization. *FEBS Lett.* **507**, 318-322 (2001).

Van Loon,L.C. & Van Strien,E.A. The families of pathogenesis-related proteins, their activities, and comparative analysis of PR-1 type proteins. *Physiol. Mol. Plant Pathol.* **55**, 85-97 (1999).

Vanloon,L.C. Pathogenesis-related proteins. *Plant Mol. Biol.* **4**, 111-116 (1985).

Vidal,J. & Chollet,R. Regulatory phosphorylation of C-4 PEP carboxylase. *Trends Plant Sci.* **2**, 230-237 (1997).

Voesenek,L., Colmer,T.D., Pierik,R., Millenaar,F.F., & Peeters,A.J.M. How plants cope with complete submergence. *New Phytol.* **170**, 213-226 (2006).

Voznesenskaya,E.V., Edwards,G.E., Kiirats,O., Artyusheva,E.G., & Franceschi,V.R. Development of biochemical specialization and organelle partitioning in the single-cell C-4 system in leaves of Borszczowia aralocaspica (Chenopodiaceae). *American Journal of Botany* **90**, 1669-1680 (2003).

Vremarr,H.J., Skoog,F., Frihart,C.R. & Leonard,N.J. Cytokinins in Pisum transfer ribonucleic acid. *Plant Physiol*. **49**, 848–851 (1972).

Wang,Y.H. & Chollet,R. In-vitra phosphorylation of purified tobacco-leaf phosphoenolpyruvate carboxylase. *FEBS Lett.* **328**, 215-218 (1993).

Waterhouse,P.M., Wang,M.B., & Lough,T. Gene silencing as an adaptive defence against viruses. *Nature* **411**, 834-842 (2001).

Willeford,K.O. & Wedding,R.T. Oligomerization and regulation of higher-plant phosphoenolpyruvate carboxylase. *Plant Physiol.* **99**, 755-758 (1992).

Wu,M.X. & Wedding,R.T. Regulation of phosphoenolpyruvate carboxylase from Crassula argentea – Further evidence on the dimer-tetramer interconversion. *Plant Physiol.* **84**, 1080-1083 (1987).

Yamaguchi-Shinozaki,K. & Shinozaki,K. Organization of cis-acting regulatory elements in osmotic- and cold-stress-responsive promoters. *Trends Plant Sci.* **10**, 88-94 (2005).